An Analytical Form of the Boscovich Curve with Applications

AUGUSTUS PRINCE

Palm Coast, FL

Using an analysis from a physical and phenomenological viewpoint employing the renowned and recognized continuity of Boscovich's force curve, a new paradigm is formulated to explicate various physical phenomena in both the micro-world and the macro-world. Within this paradigm, an algorithm is established which produced a functional representation of the atomic spectra of hydrogen and a temperature dependent blackbody energy distribution of radiation which compares very favorably with the experimental data. Further representations afford suggestions for the predictions of the specific heat of solids, photoelectric effect, etc. The Boscovichian points are assumed to move under the action of a force (acceleration) that varies inversely proportional to the cube of the radius from the point center, which leads to an orbit described by an equiangular (logarithmic) spiral. This spiral is subsequently used to simulate the concepts used in phyllotaxis (a constituent of plant morphology) and the gnomonic growth of mollusk shells (e.g. nautilus). The intercepts for the stable and unstable points on the Boscovich curve, which are the roots of the equation used, are calculated via the application of Fibonacci-type sequence of integers. In addition, utilizing the shape of Boscovich's "extended" curve of force (acceleration), the prospect of interpreting the mysterious attractive force beyond the visible Newtonian region of space (e.g. black holes, dark energy, etc.) is proposed. It is hoped that this phenomenological approach will serve as a beginning for description of both the micro-universe and the macro-universe.

Introduction

In any discussion, verbal or written, of Boscovich's (1922) magnum opus *Philosophiae Naturalis Theoria reducta ad unicam Legem Virium in Natura Existentium*. "Theory of Natural Philosophy reduced to a single law of the forces which exist in nature" (Boscovich, 1922), there usually always is a mention or reference made to his "curve of forces". These citations frequently are applied to its qualitative features and, to my knowledge, never to its quantitative features. It is the purpose of this paper to address the quantitative features of the curve leading to an analysis for empirical applications. Ivanovic (1988) provides another recent overview of some of the features of Boscovich's curve. Boscovich (1922), in *Theoria* notes 10–11, presents his curve of forces as a single, continuous curve shown in Fig. 1.

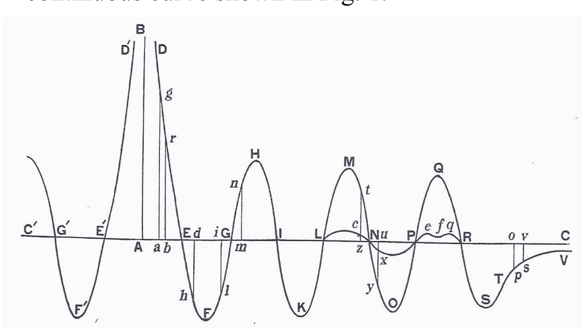

Fig 1. From *Theoria* (Boscovich, 1922)

Note 1 – Hereafter referred to as *Theoria*. This paper uses the Latin-English edition, prepared by J. M. Child (1922). Boscovich (1922) states that this graphical representation does not require knowledge of geometry to set it forth (note 11 ibid) but only to glance at it as a portrait.

Description

A detailed description is presented in *Theoria* with the following six conditions:

117. The investigation of the equation, by which a curve of the form that will represent my law of forces can be expressed, requires a deeper knowledge of analysis itself. Wherefore I will here do no more than set out the necessary requirements that the curve must fulfill & those that the equation thereby discovered must satisfy. It is the subject of Art. 75 (2) of the dissertation De Lege Virium, where the following problem is proposed. *Required to find the nature of the curve, whose abscissae represent distances & whose ordinates represent forces that are changed as the distances are changed in any manner, & pass from attractive forces to repulsive, & from repulsive to attractive, at any given number of limit-points: further the forces are repulsive at extremely small distances and increase in such a manner that they are capable of destroying any velocity, however great it may be.*

118. In addition to what is proposed in this Art. 75, I set forth in the article that follows it the following six conditions; these are the necessary and sufficient conditions for determining the curve that is required.

(i) The curve is regular, & simple, & not compounded of a number of arcs of different curves.
(ii) It shall cut the axis C'AC of Fig. 1, only in certain given points, whose distances, AE', AE, AG', AG, and so on, are equal in pairs on each side of A.
(iii) To each abscissa there shall correspond one ordinate & one only.
(iv) To equal abscissae, taken one on each side of A, there shall correspond equal ordinates.
(v) The straight line AB shall be an asymptote, and the asymptotic area BAED shall be infinite.
(vi) The arcs lying between any two intersections may vary to any extent, may recede to any distances whatever from the axis C'AC, and approximate to any arcs of any curves to any degree of closeness, cutting them, or touching them, or osculating them, at any points and in any manner (Boscovich, 1922).

Interpretation

Boscovich describes the arcs and areas and then offers an interpretation of the various sections of his curve. He states, in *Theoria* notes 167-168:

167. *With regard to the curve, there are three points that are especially to be considered; namely, the arcs of the curve, the area included between the axis and the curve swept out by the ordinate by its continuous motion, and those points in which the curve cuts the axis.*

168. *As regards the arcs, some may be called repulsive and others attractive, according indeed as they lie on the same side of the axis as the asymptotic branch ED or on the opposite side, and terminate ordinates that represent repulsive or attractive forces. The first art ED must certainly be asymptotic on the repulsive side of the axis, and continued indefinitely. The last arc TV, if gravity extends to indefinite distances according to a law of forces in the inverse ratio of the squares of the distances, must also be asymptotic on the attractive side of the axis, and by its nature also continued indefinitely. All the remaining arcs are represented in Fig. 1 as finite* (Boscovich, 1922).

Boscovich continues to describe the curve's analytical features in *Theoria* notes 179-180.

179. So much for the arcs & the areas; now we must consider in rather more careful manner those points of the axis to which the curve approaches. These points are either such that the curve cuts the axis in them, for instance, the points E, G, I, &c. in Fig. 1; or such that the curve only touches the axis at the points. Points of the first kind are those in which there is a transition from repulsions to attractions, or vice-versa; and these I call limit-points or boundaries, since indeed they are boundaries between the forces acting in opposite directions. Moreover these limit points are twofold in kind; in some, when the distance is increased, there is a transition from repulsion to attraction; in others, on the contrary, there is a transition from attraction to repulsion. The Points E, I, N, R are of the first kind, and G, L, P are of the second kind. Now, since at one intersection, the curve passes from the repulsive part to the attractive part, at the next following intersection it is bound to pass from the attractive to the repulsive part and vice-versa. It is clear then that the limit points will be alternately of the first and second kinds.

180. Further, there is a distinction between limit points of the first and those of the second kind. The former kind have this property in common; namely that, if two points are situated at a distance from one another equal to the distance of any one of these limit-points from the origin, they will have no mutual force; and thus, if they are relatively at rest with regard to one another, they will continue to be relatively at rest. Also, if they are moved apart from this position of relative rest, then, for a limit-point of the first kind, they will resist further separation and will strive to recover the original distance, and will attain to it if left to themselves; but, in a limit-point of the second kind, however small the separation, they will of themselves seek to get away from one another and will immediately depart from the original distance still more. For, if the distance is diminished, they will have, in a limit point of the first kind, a repulsive force, which will impede further approach and will impel the points to mutual recession, and this they will acquire if left to them; thus they will endeavor to maintain the original distance apart. But in a limit point of the second kind they will have an attraction, on account of which they will approach one another still more; and thus they will seek to depart still further from the original distance, which was a greater one. Similarly, if the distance is increased, in limit-points of the first kind, due to the attractive force which is immediately

> obtained at this greater distance; there will be a resistance to further recession and an endeavor to diminish the distance; and they will seek to recover the original distance if left to themselves by approaching one another. But, in limit-points of the second class a repulsion is produced, owing to which they try to get away from one another still further; and thus of themselves they will depart still more from the original distance, which was less. On this account indeed I have called those limit points of the first kind, which are tenacious of mutual position, limit-points of cohesion, and I have termed limit-points of the second kind limit-points of non-cohesion (Boscovich, 1922).

From Andronov, Vitt, & Khaikin (1966), these characteristics of Boscovich's curve may be expressed in terms of motion in a uni-dimensional phase space. According to Andronov et al. (1966), f(x) as in analytic function over the entire x-axis as shown in their Fig. 161.

> If f(x) has the real roots $x = x_1$, $x=x_2$, $x=x_3$.....$x=x_h$, then there can be paths of various types:
>
> (a) states of equilibrium
> (b) intervals between two roots
> (c) intervals between one of the roots and infinity (half straight lines)

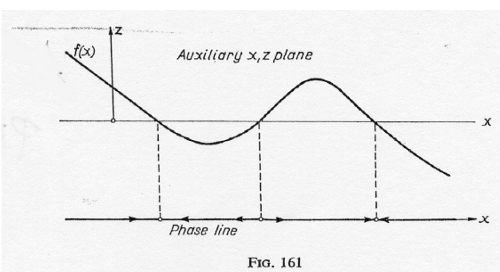

Fig. 2 (Fig. 161 from (Andronov et al., 1966))

> On each path the motion takes place in a determined direction, since the sign of f(x) does not vary over a path. If f(x)>0, the representative point moves towards the right; if f(x)<0 the representative point moves towards the left. The points where f(x)=0 correspond to states of equilibrium. Knowing the form of the curve z=f(x) and using these arguments we can divide the phase (straight) line into paths and indicate the direction of motion of the representative point along the paths. An example of such a construction is shown in Fig. 161. This gives a clear picture of the possible motions of a dynamic system described by one differential equation of the first order. Knowing the states of equilibrium and their stability will establish a qualitative picture of the possible motions (p. 214).

Andronov et al. (1966) discusses another representation of the stability of the states of equilibrium depending on the sign of the derivatives at the points of intersection of the curve.

> …it is easy to investigate stability directly from the properties of the function f(x) near to the state of equilibrium $x=x_0$. Since f(x)=0, three essentially different cases occur, and are illustrated in Figs. 163, 164 and 165.
>
> (1) F(x) changes its sign near $x=x_0$ from positive to negative as x increases (Fig. 164). Hence $f'(x_0)<0$ and x_0 is stable.
>
> (2) F(x) changes its sign near $x=x_0$ from negative to positive as x increases (Fig. 164). Hence $f'(x_0)>0$ and there is unstable point $x=x_0$.
>
> (3) F(x) does *not* change its sign in the vicinity of the state of equilibrium $x=x_0$ as x increases (Fig. 165). This means that a representative point, situated sufficiently close to the position of equilibrium on one side of it, will approach it, and one situated on the other side will move away from it. It is clear that the state of equilibrium proves unstable in the sense of Liapunov, for there is instability on one side and stability on the other. In this case $f'(x_0)=0$ (p. 218).

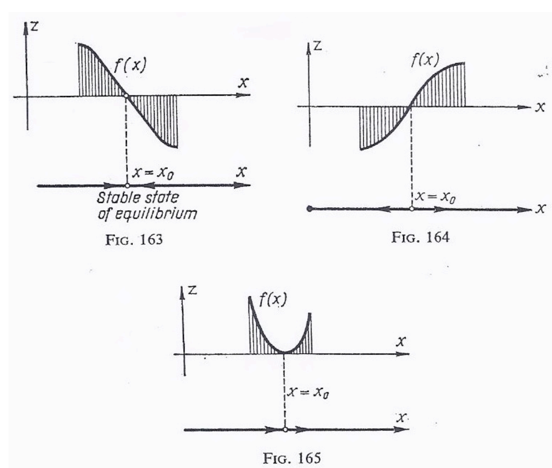

Fig. 3 (Fig. 163-165 from (Andronov et al., 1966))

Case 1 (Fig. 163) corresponds to what Boscovich calls "limit points of cohesion" and is illustrated at point E of his curve. Similarly his "limit of non-cohesion" or points of unstable equilibrium seen in Fig. 164 may be seen at point *G* on the curve.

Markovic succinctly described…(as cited in Whyte, 1961) the characteristics of Boscovich's curve by stating:

> The winding of the curve about the X-axis, in particular the behavior of arcs belonging to the repulsive and attractive forces respectively, have a bearing on the explanation of "fermentation", evaporation, sudden deflagrations and explosions, and also of light emission. "Fermentation" arises when the shape and the distribution of the repulsive and the attractive arcs of the curve are such that the particle is forced to oscillate rapidly within definite limits. In fact, Boscovich introduces, as well as the points in which the curve intersects the axis, X, also *limits of another kind* in which the transition from the repulsive force to the attractive, or vice versa, does not occur by cancellation of the force but by *transition through infinity*. Thus *new asymptotic branches* are introduced into the curve of forces in addition to that near the origin. For Boscovich this does not destroy the continuity of the curve, because in his theory of curves two such

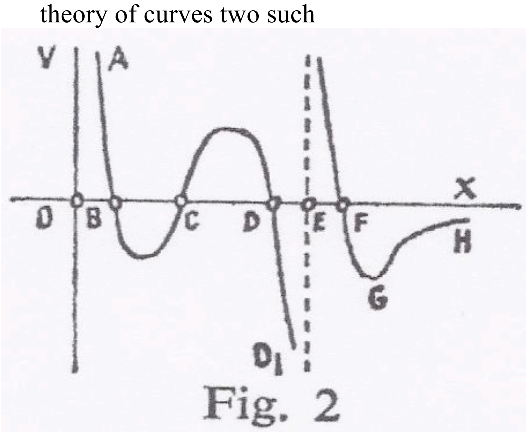

Fig. 4 (Fig. 2 from Marcovic…as stated in Whyte, 1961)

> asymptotic arcs, one of which recedes into positive infinity, while the other returns from the negative infinity, or vice versa, are connected at a "point of infinity". If the first of these vertical asymptotes falls, for instance, in a *limit of non-cohesion* E (Markovic's Fig. 2 in as stated in Whyte, 1961) in such a way that on the left of the asymptote the branch of the curve of forces tends towards negative infinity, and on the right towards positive infinity.
>
> The elements of matter contained in the interval between O and E will never be able to leave this interval however strong the mutual forces may be between them, and however great the effect of forces due to the point outside the interval. A detailed analysis shows that the particles will oscillate, even violently, and the fermentation which results from it – as intensive as it may be – will be able to persist for ever; the motions of single points will be accelerated or retarded, and the amplitude of oscillations will increase or decrease (p. 140-141).

This statement by Markovic clearly corresponds to Andronov's Fig. 165. It should be noted that Markovic's Fig. 2 displays all the features of Boscovich's Fig. 26 (1922) in the *Theoria.*

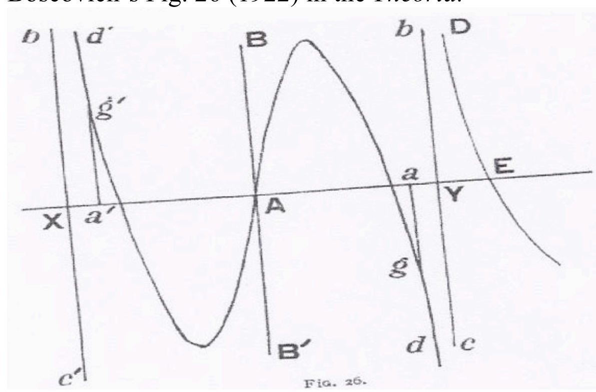

(Fig. 26 from Boscovich, 1922)

Qualitative Analysis: Development

In a paper by Prince (1989), it is stressed how important it is to establish physical laws from the phenomena, i.e.

> The observed phenomena must be examined according to some theory and described in terms of laws consistent with that theory. The laws derived from empirical data may be expressed by means of abstract concepts that permit them to be mathematically formulated and incorporated into the theory (p. 593).

This is further elucidated by Martinovic (1987).

> The curve of forces and physical phenomena are in a dichotomous, dialectical relationship. The curve can be used for the interpretation of many physical phenomena, and can help to solve very difficult problems dealt with in higher geometry and analysis. On the other hand, the curve of forces should be studied with regard to the phenomena: The nature of these curves, as well as the points [intersection with axes] which the curves cut, should be investigated with regard to phenomena. It is implied that phenomena should be studied as far as they are a manifestation of forces acting between particles of matter, which determines the properties of the flow of the curve of

forces. Boscovich's selection of phenomena has a decisive influence on the final form of the curve. The selection is not arbitrary. It reflects Boscovich's relationship towards Newton's general principles of motion: gravitation, cohesion and fermentation (p. 73).

Quantitative Analysis: The Process and Motivation

The motivation for investigating a possible quantitative expression for the Boscovich curve, with the hope that it would lead to substantiation of empirical data, was brought about by the publication of an article by Horadam & Shannon (1988). In this article, the authors produced an expression for determining Fibonacci numbers for non-integral values (Horadam & Shannon, 1988, p. 4). A parametric analysis, based on their equations given by:

$$x = \frac{\{A\alpha^{\theta} - B\alpha^{-\theta}\cos\theta\pi\}}{\sqrt{5}} \tag{2.3}$$

$$y = -\frac{B\alpha^{-\theta}\sin\theta\pi}{\sqrt{5}} \tag{2.4}$$

(Horadam & Shannon, 1988).

For the Fibonacci case A = B = 1, and (2.3) becomes

$$x = \frac{\{a^{\theta} - a^{-\theta}\cos\theta\pi\}}{\sqrt{5}} \, where \; \alpha = \frac{1+\sqrt{5}}{2} \tag{2.5}$$

(Hordam & Shannon, 1988).

Table 1 presents the parametric representational values for Fibonacci numbers (Horadam and Shannon, 1988). Table 1 sets out the values of *x* in (2.5), and *y* in (2.4) where *B* = 1, for the Fibonacci case α = 1, b = 0, when we proceed to increase θ by multiples of 0.2.

Table 1. The Fibonacci Curve

θ	x	y	θ	x	y
1	1	0			
1.2	0.999799314	0.14755316	6	8.000000000	0
1.4	0.947653586	0.216839615	6.2	8.817334649	-0.013304890
1.6	0.901827097	0.196943249	6.4	9.721923304	-0.019552416
1.8	0.911232402	0.110549283	6.6	10.71685400	-9.96822E-03
2	1	0	6.8	11.80690074	-9.96822E-03
2.2	1.163587341	-0.091192868	7	13.00000000	0
2.4	1.375792509	-0.134014252	7.2	14.3076953	8.22286E-03
2.6	1.602274541	-0.121717622	7.4	15.744608	0.012084058
2.8	1.814640707	-0.068323214	7.6	17.32733182	0.010975271
3	2.000000000	0	7.8	19.07328767	6.16070E-03
3.2	2.163386655	0.056360292	8	21.00000000	0
3.4	2.323446095	0.082825363	8.2	23.12502995	-5.08200E-03
3.6	2.504101639	0.075225627	8.4	25.4665313	-7.46836E-03
3.8	2.725873109	0.042226069	8.6	28.04418582	-6.78309E-03
4	3.000000000	0	8.8	30.8801884	-3.80752E-03
4.2	3.326973997	-0.034832576	9	34.00000000	0
4.4	3.699238605	-0.051188889	9.2	37.43272525	3.14085E-03
4.6	4.10637618	-0.046491995	9.4	41.21113931	4.611570E-03
4.8	4.540513816	-0.026097146	9.6	45.37151764	4.19218E-03
5	5.000000000	0	9.8	49.953447608	2.35318E-03
5.2	5.490360652	0.021527716	10	55.00000000	0
5.4	6.022684699	0.031636473			
5.6	6.610477819	0.028733633			
5.8	7.266386925	0.016128923			

Table 1
Fig. 1 shows the graph corresponding to the data in Table 1 called The Fibonacci Curve.

The similarity to the Boscovich curve is obvious with the intersections corresponding to the Fibonacci numbers 1, 2, 3, 5, 8, 13, 21, etc.

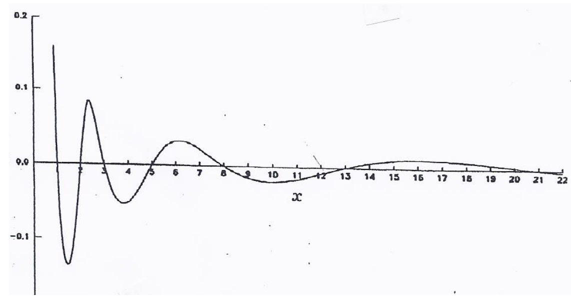

Fig. 5 (Fig. 1 from Hordam & Shannon, 1988). Fig. 1 shows the graph corresponding to the data in Table 1 called, The Fibonacci Curve.

$$\alpha = e^{\ln\alpha} \tag{1}$$

$$\alpha^{x} = e^{x\ln\alpha} = e^{kx} \tag{2}$$

(Hordam & Shannon, 1988).

Where $k = \ln\alpha = 0.481211825$

Then Horadam and Shannon's equations might be rewritten as:

$$x = \frac{e^{(k\theta)} - e^{(-k\theta)}\cos(\theta\pi)}{\sqrt{5}} \tag{3}$$

$$y = \frac{e^{(-k\theta)}\sin(\theta\pi)}{\sqrt{5}} \tag{4}$$

From Table 1, it can be seen that the non-integral values for the Fibonacci numbers can also be constructed from the preceding numbers:

$\theta_{2.2} + \theta_{3.2} = \theta_{4.2}$
$\theta_{3.2} + \theta_{4.2} = \theta_{5.2}$
etc.

These non-integral Fibonacci numbers I choose to call quasi-Fibonacci numbers. This relationship will prove to be very useful in the development of a quantitative value for the Boscovich curve. If we take a range of these quasi-Fibonacci numbers using the modified Horadam & Shannon (1988) equation they should show an oscillating characteristic similar to the Fig. 1 (The Fibonacci Curve). Based on this conjecture a curve is produced using:

$$F(x) = \sin\left\{\frac{\pi}{5}\left(e^{(kx)} - e^{(-kx)}\cos(\pi x)\right)\sqrt{5}\right\} \tag{5}$$

For x = 7 to 8 with the values of F(x) at 0.1 intervals, which is shown in Fig. 6 and values on Table 2.

Fig. 6

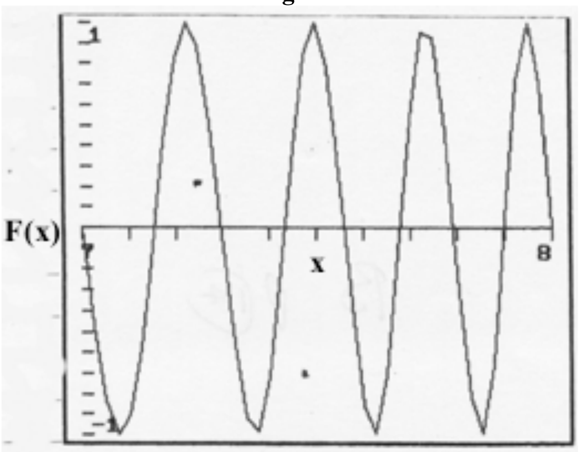

x	F(x)
7	0
7.1	−.906598
7.2	.822989
7.3	−.028252
7.4	−.718983
7.5	.99863
7.6	−.856445
7.7	.532663
7.8	−.228211
7.9	.040693
8	0

Table 2

Continuing the investigation, it is imperative that the intersections of the abscissa where f(x)=0 be determined. For this, it is necessary to go to the Binet approximation for the Fibonacci Series. This is given by:

$$u_n = \frac{1}{\sqrt{5}}\left(\frac{1+\sqrt{5}}{2}\right)^n - \frac{1}{\sqrt{5}}\left(\frac{1-\sqrt{5}}{2}\right)^n \ (n = 0,1,2,3,\ldots) \qquad (6)$$

While this equation reproduces the Fibonacci number fairly accurately, especially for large values of *n* ($n \geq 15$), it does not yield values for non-integer values, due to the fact that the second term means finding the n^{th} power of a negative number, when *n* is not an integer. However, it may be denoted that ignoring this term does yield approximate values for non-integers; exact values for $n \geq 15$. An example is shown in Table 3 and demonstrated in Fig. 7.

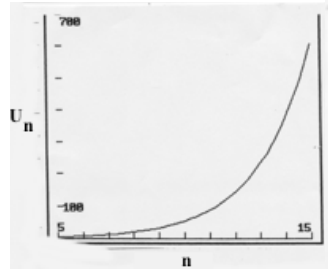

Fig. 7

n	U_n
5	4.95968
5.2	5.46073
5.4	6.01241
5.6	6.61981
5.8	7.28859
6	8.02492
6.2	8.83565
6.4	9.72828
6.6	10.7111
6.8	11.7932
7	12.9846
7.2	14.2964
7.4	15.7407
7.6	17.3309

Table 3

We are now in a position to determine the values of the x-intercepts using the Binet Formula for f(x) = 0. Using the first term of the Binet formula yields:

$$y = \frac{\ln(\sqrt{5}x)}{k} \qquad (7)$$

$$where\ k = \ln\left(\frac{\sqrt{5}+1}{2}\right) = 0.481211825$$

From Fig. 6 it can be noted that there are intersections at the 7^{th} & 8^{th} (real) Fibonacci number and seven intersections for the quasi-Fibonacci numbers, where $U_7 = 13$, $U_8 = 21$

Fig. 8

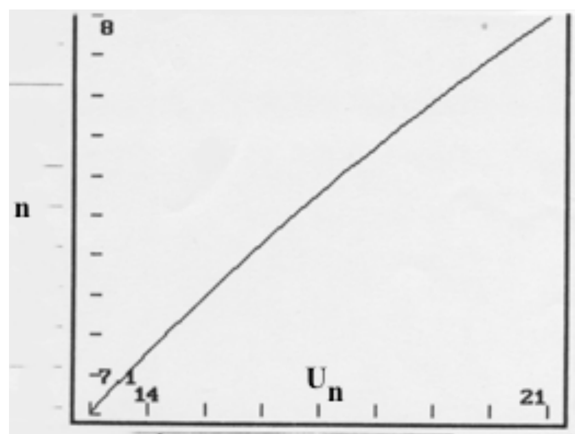

13	7.00246
14	7.15647
15	7.29984
16	7.43396
17	7.55994
18	7.67872
19	7.79108
20	7.89767
21	7.99906

Table 4

Thus, using Eq. 7 and starting at $U_7 = 13$, values of the other intersections are given in Fig. 8 and Table 4. A comparison of Table 4 and the roots of f(x) displayed in Fig. 8 is given in Table 5 and compared with the results using Newton's Method.

Fibonacci numbers	U_n	Intersection From Eq. 7	Intersection (Newton)	Δx Difference
13	$U_{7.0}$	7.00246	7.0	0.00246
14	U_{7a}	7.15647	7.15459	0.00188
15	U_{7b}	7.29484	7.29875	0.00109
16	U_{7c}	7.43396	7.43362	0.00034
17	U_{7d}	7.55994	7.36021	-0.00027
18	U_{7e}	7.67872	7.67940	-0.00068
19	U_{7f}	7.79108	7.79199	-0.00091
20	U_{7g}	7.89267	7.89063	-0.00098
21	U_8	7.99906	8.0	0.00094

Table 5

u_1 1	u_{11} 89	u_{21} 10946	u_{31} 1346269
u_2 1	u_{12} 144	u_{22} 17711	u_{32} 2178309
u_3 2	u_{13} 233	u_{23} 28657	u_{33} 3524578
u_4 3	u_{14} 377	u_{24} 46368	u_{34} 5702887
u_5 5	u_{15} 610	u_{25} 75025	u_{35} 9227465
u_6 8	u_{16} 987	u_{26} 121393	u_{36} 14930352
u_7 13	u_{17} 1597	u_{27} 196418	u_{37} 24157817
u_8 21	u_{18} 2584	u_{28} 317811	u_{38} 39088169
u_9 34	u_{19} 4181	u_{29} 514229	u_{39} 63245986
u_{10} 55	u_{20} 6765	u_{30} 832040	u_{40} 102334155

Table 6

For comparison purposes, a table for the first 40 numbers of the Fibonacci series is given in Table 6. From Table 6 it can be shown that the number and intercepts is given by the difference of two Fibonacci numbers plus one.

Example from Table 6:

$$u_{20} - u_{19} + 1 = 6765 - 4181 + 1 = 2585 \text{ intercepts} \quad (8)$$

$$u_{40} - u_{39} + 1 = 102334155 - 62345986 + 1 = 39088170 \text{ intercepts} \quad (9)$$

From this, one can see that for higher Fibonacci numbers, the distance between the x-intercepts becomes very small. The next step in the development of a quantitative analysis of the Boscovich curve will entail the magnitude of the various cycles. We now investigate the significance of an inverse cube type force. In Theorem note 121 in Supplement III, notes 74, Boscovich (1922) cites Newton and Kepler and mentions a force curve having the form given by $\frac{a}{x^2} + \frac{b}{x^3}$

In particular he emphasizes the significance of the fact that the inverse cube force $\frac{\mu}{r^m} - \frac{v}{r^{m+n}}$ is very important at very small distances. This is the region of the oscillating characteristic of his force curve and this is the region that will be of importance in the description of various microscopic phenomena.

Boscovich is not alone in this inverse curve assessment. Heilbron (1982, p. 52-86) mentions several attempts to modify Newton's Law of Gravitation. This includes names such as Lambert, Calendrini and Clairaut. Mention should also be made of an article by Lewis (1989, p. 652-653) who referred to the influence of Boscovich on Bertrand Russell who argued with Hannequin's criticism of both Boscovich and Kant. Russell defends Boscovich wherein he investigates the stability of a system based on Boscovich. Following Boscovich, Russell (1897, App II.1) determines that stability of four equidistance points acting according to an attractive-repulsive force may be given by:

$$\frac{\mu}{r^m} - \frac{v}{r^{m+n}} \quad (10)$$

For m = 2 and n = 1, this becomes:

$$\frac{\mu}{r^2} - \frac{v}{r^3}$$

All of the aforementioned concentrated their efforts in the macroscopic region, however, like Boscovich, there are some in the modern era who examined the significance at an inverse cube law in the microscopic (small distance) region.

Foremost among these were Thomson (1902, p. 160) where his interpretation of the structure of the atom assumed a radial repulsive force varying as the inverse cube of the distance from the center of the atom. Combined with a radial attractive force varying as an inverse square of the distance from the center. Quoting from Gill (1941):

> Thomson mentions Boscovich in his theory of electrons. In this connection, H. Strache's book, *Die Einheit der Materie, des Weltaters und der Naturkrafte,* 1909, is also worth consulting. For similar reasons to those of Boscovich's, Strache rectifies the law of gravitation for small distances. As an example of such a rectification he gives the following formula:
>
> $$y = k\frac{mm_1}{x^2}(1 - \frac{b}{x}) \quad (11)$$
>
> For great distances, $\frac{b}{x}$ is very small so that the formula passes into the Law of Gravitation. For x ≤ b is y positive; for x = b we have y = 0, whereas y is negative for x ≤ b. Then the attraction goes over into repulsion. For x = b, both masses are in equilibrium. With respect to the radii of action of the atoms and corpuscles, there must be several points of equilibrium. On p. 6 there is a reproduction of Boscovich's curve of forces with five neutral points (p. xiv).

Following Boscovich's idea of the fact that at small distances the inverse cube term predominates, leads to the assumption that this is the region of the oscillating position of the curve. With this in mind, an analytic function is given by:

$$F(x) = \frac{Be^{(-kx)}\sin\{\frac{1}{5}\pi\big(e^{(kx)} - e^{(-kx)}\cos(\pi x)\big)\sqrt{5}\}}{x^3} \quad (12)$$

Eq. 12 may be referred to as an analytical description of Boscovich's curve which represents its oscillating features. The following figures and tables depict the quantitative values for the calculated Boscovich curve. Note as $x \rightarrow 0$, $f(x) \rightarrow \infty$ in accordance with Boscovich's curve shown in Fig. 1 (Boscovich, 1922). At $x = 0.01$, $f(x) = 1.4143 \times 10^8$, as seen in Table 7.

Fig. 9

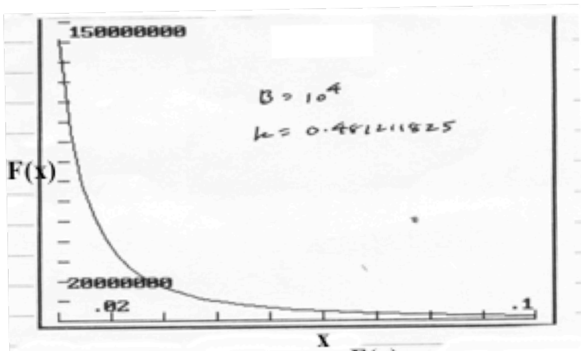

x	F(x)
.01	1.4143e+8
.02	3.68749e+7
.03	1.70467e+7
.04	9.94911e+6
.05	6.59153e+6
.06	4.72036e+6
.07	3.58113e+6
.08	2.82099e+6
.09	2.28909e+6
.1	1.90085e+6

Table 7

F(x) for x = 0.2 to x = 1.0 is shown in Fig. 10 with its values given in Table 8.
The oscillatory features of the curve starts at x = 1.0 and is shown in Fig. 11 to 15 and Tables 9 to 12. It should be noted that the quantitative results are arbitrary where $B = 10^4$ was used.

Fig. 10

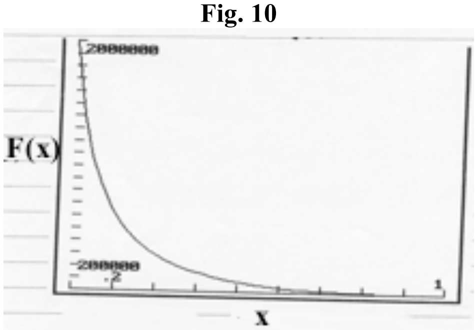

x	F(x)
.2	615185.
.3	292034.
.4	152285.
.5	78135.1
.6	37416.2
.7	16001.1
.8	5836.25
.9	1406.65
1	.000001

Table 8

Fig. 11

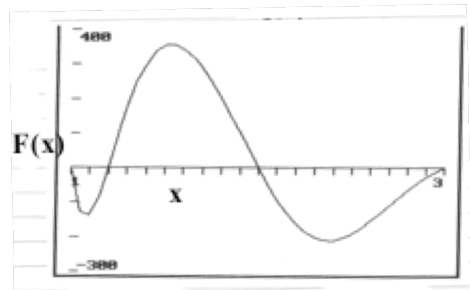

x	F(x)
1	.000001
1.2	2.04003
1.4	304.166
1.6	343.158
1.8	190.582
2	0
2.2	-160.166
2.4	-218.794
2.6	-154.409
2.8	-65.1173
3	0

Table 9

Fig. 12

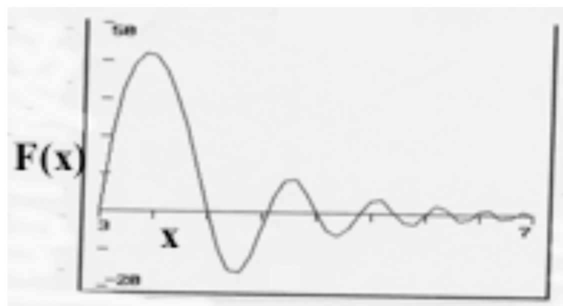

x	F(x)
3	0
3.2	32.1303
3.4	42.1177
3.6	37.9054
3.8	22.2006
4	0
4.2	-15.3077
4.4	-11.45
4.6	3.60352
4.8	8.90448
5	0
5.2	-5.02177
5.4	.336357
5.6	3.61747
5.8	-2.33516
6	0
6.2	1.15293
6.4	-1.34442
6.6	1.12009
6.8	-.607560
7	0

Table 10

Fig. 13

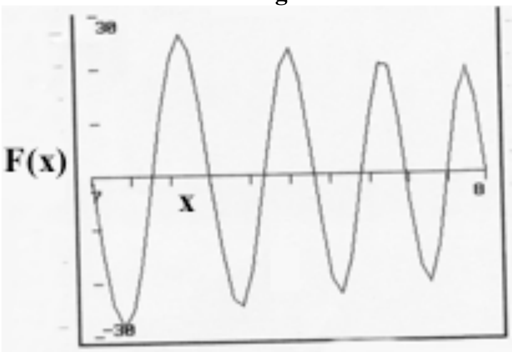

x	F(x)
7	0
7.1	-25.3303
7.2	22.0494
7.3	-.726238
7.4	-17.7428
7.5	23.6712
7.6	-19.5101
7.7	11.6676
7.8	-4.00098
7.9	.025344
8	.000001

Table 11

As *x* increases, the curve exhibits the same oscillating characteristics as the Boscovich curve, the x intercept occurring at both the real and quasi-Fibonacci numbers. In Fig. 14, we see the irregular features at the curve where the roots for f(x) = 0 using Eq. 12 are displayed in Table 11, but Table 12 shows that the intercepts still occur for the Fibonacci numbers $U_{10} = 55$ & $U_{20} = 6765$. Thus, 6765 – 55 + 1 = 6711 intercepts which of course cannot be demonstrated in the figure.

Fig. 14

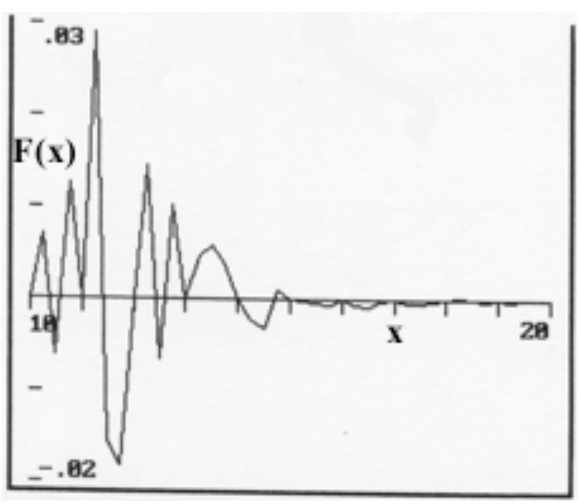

x	F(x)
10	0
11	0
12	0
13	0
14	0
15	0
16	0
17	0
18	0
19	0
20	0

Table 12

Fig. 15

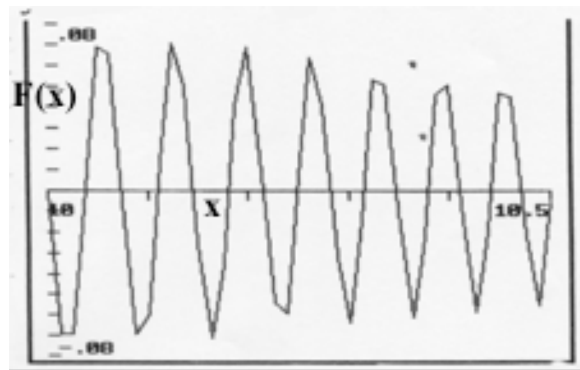

x	F(x)	
55	9.99986	$< U_{10}$
56	10.0373	
57	10.0741	
58	10.1102	
59	10.1458	
60	10.1807	
61	10.215	
62	10.2488	
63	10.2821	
64	10.3148	
65	10.347	
66	10.3787	
67	10.41	
68	10.4408	
69	10.4711	
70	10.501	$< U_{10.5}$

Table 13

In Table 12, the only real Fibonacci numbers occur at integral values, while between the integral values, the quasi-Fibonacci occur, e.g. between the tenth Fibonacci number, $U_{10} = 55$ and the eleventh Fibonacci number, $U_{11} = 89$. An example is given in Fig. 15 & Table 13, where the calculated curve is shown for U_{10} to $U_{10.5}$ with values given in Table 13.

Fig. 15 shows a graphical representation of the named values indicated in Table 13 using Eq. 12. The sixteen *x* intercepts from y_{10} to $y_{10.5}$ represents less than 0.25% of the total number of 6710 intercepts.

Boscovich in Supplement III entitled *Analytical Solution of the Problem to Determine the Nature of* *the Law of Forces*, (note 25) sets out to find an algebraic formula that will determine the number of intersections of the curve at given points where for each intercept there will be one and only one ordinate. His formula is given by

$$P = z^m + az^{m-1} + bz^{m-2} + cz^{m-3} + \cdots \qquad (13)$$

Setting P = 0, all the roots of this equation will be real and positive. It should be noted that this pre-empts Gauss, who in 1799, produced a rigorous proof now called *The Fundamental Theorem of Algebra*, which states that every complex polynomial of degree n ≥ 1 has a complex zero. If the coefficients in Boscovich's expression are real or complex then there is at least one solution in the domain of complex numbers. This leads to the form

$$(z - z_1)(z - z_2)(z - z_3) \ldots (z - z_\infty) = 0 \qquad (14)$$

It is interesting to note that the letter *z* is now the accepted notation for complex numbers in engineering, etc. Rider (1988) has addressed Boscovich's method of using imaginary numbers. Others have used Boscovich's method of using a power series to represent empirical data. For example, Whyte (1961) states that a special case employed by Poynting uses an expression defined by:

$$F = \frac{m(r-a)(r-2a)(r-3a)}{r^5} \qquad (15)$$

These series representations, which may be important for finding the intercepts of a function does nothing for determining the shape of the function.

One attempt to determine the points of intersection with the Boscovich curve was undertaken by Thomson (as stated in Kelvin, 1904, p. 675). In describing the crystallography, elasticity of solids and the thermo-elastic properties of solids, liquids and gases, he produced these points on the Boscovich curve (inverted as was the British custom), shown in Fig. 17.

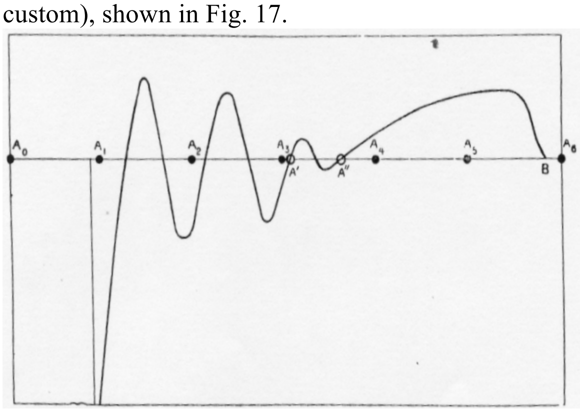

Fig. 17 (Fig. 6 from (Kelvin, 1908))

Kelvin's (1908) description of the curve and point of intersection states:

> The accompanying diagram, Fig. 6, copied from Fig. 1 of Boscovich's great book, with slight modifications (including positive instead of negative ordinates to indicate attraction) to suit our present purpose, shows for this particular curve three of the solutions of the Eq. 8 (There are obviously several other solutions.) In two of the solutions, respectively, A_0, A', and A_0, A", are consecutive atoms at distances at which the force between them is zero. These are the configurations of equilibrium, because A_0B, the extreme distance at this there is mutual action, is less than twice A_0A', and less than A_0A''. In the other of the solutions shown, A_0, A_1, A_2, A_3, A_4, A_5, A_6 are seven equidistant consecutive atom of an infinite row in equilibrium in which A_5 is within range of the force of A_0, and A_6 is beyond it. The algebraic sum of the ordinates with their proper multipliers is zero and so the diagram represents a solution of Eq. 9 (p. 675).

The Boscovich curve shown earlier in his Fig. 1 is only a qualitative representation showing its oscillating features leading to its gravitational features. The range is from very small distances to extremely large distances. Any attempt to show its quantitative features is hampered by the extreme range of the curve. This is the reason that Figs. 9-15 were presented in the previous sections.

Determination of the x-intercepts

If one looks at Fig. 8 and compares it with Fig. 6 generated by Eq. 12, which leads to the quantitative values for the Boscovich curve. It can be shown that the intercepts are the same based on Newton's method, as shown in Table 5. This differs from the aforementioned power series representation, since Eq. 12 is a real value foundation of the variable, parameter *x*, which leads to a shape consistent with Boscovich's curve.

Further Development

We are now in position to examine in detail the results and consequences using this mathematically generated Boscovich curve. Attention can be drawn to Thomson's (1907) use of Boscovich's curve in his interpretation of the hydrogen line spectra. Thomson (1907), in his book, entitled *Corpuscular Theory of Matter,* speculated that in order to get rid of the assumed continuous spectrum due to a revolving electron, one would have to formulate a theory in which an electron could only revolve in "allowed" orbits. He hypothesized that by using Boscovich's curve he could produce a theory of "allowed" and "forbidden" orbits.

The following interpretation is taken from Gill (1941), which is essentially the same as *Theoria* (notes 179 and 180) but repeated here differently for further clarification.

> The direction of motion of one particle towards another may be deduced from Fig. 1 where A is one of the points and the other somewhere along the line AP. The Points E, G, I, L, N, P, etc., are the intersections of the curve with the line AP, as already shown in Fig. 1. As already explained, A, G, L, P are limits of non-cohesion, while E, I, N, etc., are limit points of cohesion. A point between A and E will be repelled towards E. A point between E and G will be attracted towards E. The point will, therefore, tend to remain at E, and if slightly displaced, to return to it. The above is true of the points I, N, etc.
>
> A point between E and G will tend to move away from G towards E. A point between G and I will also move from G towards I. Thus the points G, L, P, etc., are such that no point tends to remain there. The slightest disturbance makes them move away from these points with a velocity that at first increases rapidly, and never to return.
>
> If a point is repelled with the absolutely correct force from A it will just reach E and remain there, but in general the force will cause it to pass into the space EG, where it will be attracted back to E, where, after some oscillations, it will come to rest. If the force of repulsion is strong enough to cause the point to pass over several spaces, it will finally settle down at one or other of the limit points of cohesion, I, N, R, etc., but never at the limit points of non-cohesion, G, L, P, etc. Finally, if the force is strong enough to repel the points beyond all the arcs (of Fig. 1) into the distant region RC, it will reach some point where it is subject to the Newtonian Law of Attraction.
>
> In this way a point near A will come to rest at one of the points E, I, N, etc., but never at G, L, P, etc. The same is true of points E', I', N', etc., on the other side of A. Evidently the same considerations apply to a point along a line in any direction from A (p. 19).

Gill (1941) continues to quote Thomson's (1907) interpretation of a revolving electron:

> Suppose we regard the charged ion as a Boscovichian atom exerting a central force on a corpuscle which changes from repulsion to attraction and from attraction to repulsion several times between the surface of the ion and a point from the surface comparable with molecular distance, such a force, for example, as is represented graphically in Gill's (1941) Fig. 2 where the abscissae represent distances from the atom, and the ordinates of the forces exerted by the atom on a corpuscle at a distance represented by the abscissae, the forces being repulsions when the representative point is below the line, attractions when it is above it. (The figure here reproduced is simply the Boscovich curve inverted, in accordance with the English practice of representing attractions by positive ordinates).

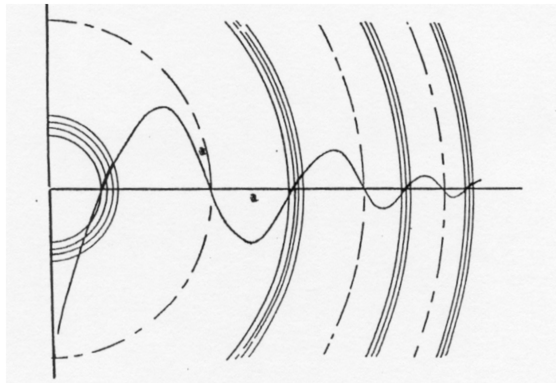

FIG. 2.

The curve is that of J. J. Thompson, from The Corpuscular Theory of Matter, p. 160. The orbits have been added. The continuous zones represent the "favoured orbits." The broken circles represent the "forbidden orbits."

Fig. 18 (Fig. 2 from (Gill, 1941))

Gill concludes that Boscovich, without the concept of "allowed" and "forbidden" orbits, showed that alternate limit points of cohesion and non-cohesion are on the perimeter of an ellipse. From Fig. 33 in the *Theoria*, Gill (1941) represents a system of con-focal ellipses. He states:

> As before, we need not discuss the proof or construction. The semiaxes DO, DO', D'' etc., correspond in length to limit points of cohesions and non-cohesion alternately, i.e., to L, N, P, etc., in Fig. 1. As before, a point on certain perimeters can make a continuous circuit of its ellipse:

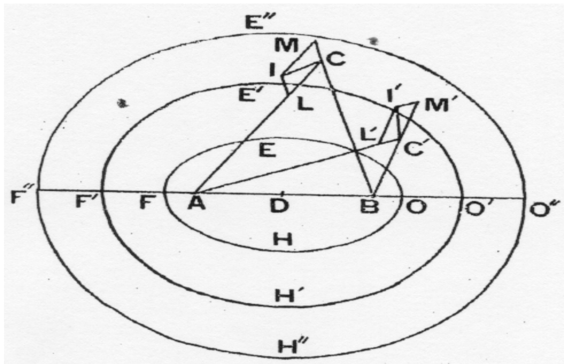

Fig. 19 (Fig. 33 from *Theoria*)

Gill continues to quote Boscovich (1922) from *Theoria*:

> Let us consider a number of ellipses having the same foci, of which the semiaxes are in order equal to the distances corresponding to the limit-points in Fig. 1, namely, one of cohesion for one, to that of non-cohesion next to it for the second, and so on alternately… and that each ellipse has four limit-points, one at each of the four vertices of the axes. The whole set of such perimeters will be somewhat of the nature of limit points as regards approach to or recession from the center. A point situated on any one of these perimeters will have a propensity for motion along that perimeter. If it be situated between two perimeters, it will always direct its force in such a way that it will tend towards a perimeter corresponding to a limit-point of cohesion in Fig. 1, and will recede from a perimeter corresponding to a limit point of non-cohesion. Hence, if a point is disturbed out of a position on a perimeter of the first kind, it will endeavor to return to it; but if disturbed from a position on a perimeter of the second kind, it will of its own accord try to get away from it still further, and will recede from it (note 245).

This can be interpreted as: since the perimeter of those limit points of non-cohesion manifest instability, then no points can move on these ellipses resulting in movement of points in alternate orbits.

This is a clear verification of Thomson's "allowed" and "forbidden" orbits. It should be noted that Martinovic (1988, p. 206-210) explained this concept in his article, *Boscovich's Model of the Atom.* Martinovic (1988) employed Boscovich's (1748) ideas from his work, *Dissertations de lumine pars* secunda, that was written 10 years before the *Theoria*. In the *de lumine*, Boscovich (1748) investigated the null points of his curve and from three analogies, which culminated in a system of confocal ellipses each having alternate cohesive and non-cohesive characteristics. The fourth analog depicted the idea of confocal spheroidal shells where their surfaces represented limits of equilibrium and non-equilibrium states. This illustrates particles moving between their spherical shells when they could be attracted to that shell corresponding to a limit of cohesion and being repelled from that shell corresponding to a limit of non-cohesion. This allows a 3-dimensional analysis, which might be of great importance for future scientific investigations.
Figs. 20 and 21 show Martinovic's (1988) depiction of Boscovich's theory of fourth analogy:

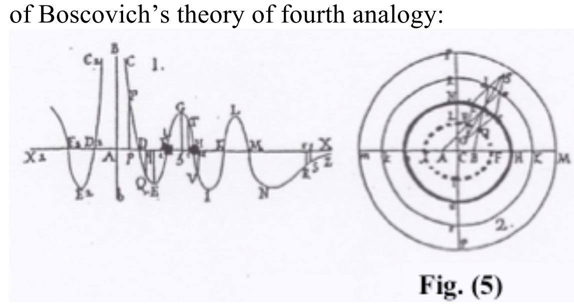

Fig. 20 (Fig. 5 from (Martinovic, 1988))

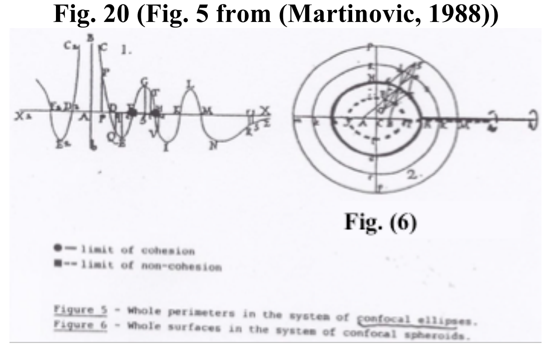

Fig. 21 (Fig. 6 from (Martinovic, 1988))

It can be seen in Martinovic (1988) that Fig. 5 is essentially identical to Fig. 33 shown by Gill (1941). Thus an alternating series of limits of cohesion and non-cohesion from Boscovich's third analogy leads to the modern concept of limit cycles. At this point, these aforementioned concepts can be extended to what is commonly referred to as stable and unstable limit points. These terms might be interpreted as replacing Boscovich's "cohesion and non-cohesion" limit points. His stable and unstable limit points lead to the concept of "limit cycles", which is a modern means of visualizing and explaining oscillating systems.

It was Poincare (1881) who, in his work on differential equations, showed that under certain conditions, special solutions could be represented by closed curves, which are called limit cycles. These curves are in what is called a "phase plane". This plane represents the totality of all possible states in a system. To each new state a new point results, thus for each point whose variations may be associated with the motion of a certain point, is called the "representative" point in the phase plane.

It should be emphasized that this motion corresponding to the various curves in the phase plane (phase trajectories) have nothing in common with actual movement of points in a system. Not withstanding this difference, an analogy can be made to the limit points of Boscovich leading to his system of confocal ellipses.

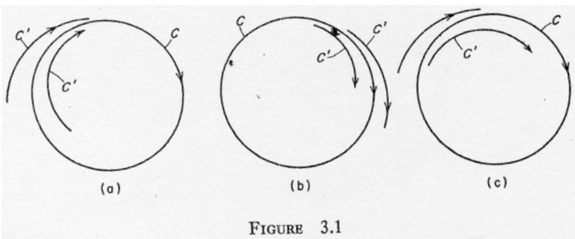

Fig. 22 (Fig. 3.1 from (Minorsky, 1962))

Following Minorsky (1962), a limit cycle being an isolated closed trajectory, then

> every trajectory beginning sufficiently near a limit cycle approaches it either for $t \to \infty$ or for $t \to -\infty$, that is, it either winds itself upon the limit cycle, or unwinds from it. If all nearby trajectories approach a limit cycle C as $t \to \infty$, we say that C is *stable* (Fig. 3.1a); if they approach a limit cycle C as $t \to -\infty$ we say that C is *unstable* (Fig. 3.1b). If the trajectories on one side of C approach it while those on the other side depart from it, we sometimes say that C is *semi-stable* (Fig. 3.1c) although from a practical point of view C must be considered unstable (p. 71).

Carrying out this analogy, one might now think in terms of Boscovich's limit points of cohesion and non-cohesion to be identified with stable and unstable limit points in limit cycles. With this in mind, lets consider a set of confocal limit cycles as depicted in Fig. 23 from Minorsky's (1947, p. 70) Fig. 24.4.

Here we consider a single point surrounded by several limit cycles.

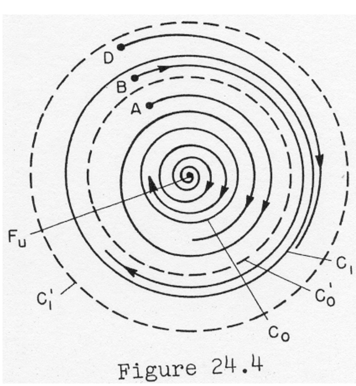

Fig. 23 (Fig. 24.4 from (Minorsky, 1947))

A point singularity F_u, which we shall assume to be an unstable focal point, is surrounded by several limit cycles, represented by closed curves shown as circles C_0, C'_0, C_1, etc., in Fig 24.4 (Minorsky, 1947, p. 70); the circles in full lines represent the stable limit cycles and those in broken lines, the unstable ones. The fact that we assume that the limit cycles are circles is not essential since we are primarily interested in the topology of trajectories in the various domains which we are now going to specify. In order to include the half-stable limit cycles, the following terminology is convenient. A limit cycle is *inwardly* or *outwardly* stable according to the side on which stability exists; similarly, a limit cycle may be inwardly or outwardly unstable. A stable limit cycle in this terminology is one that is both inwardly and outwardly stable and an unstable limit cycle is both inwardly and outwardly unstable.

In a succession of concentric limit cycles considered from the center outward, one that is inwardly unstable follows an outwardly stable limit cycle and one that is inwardly stable follows a cycle that is outwardly unstable. Minorsky's (1947) Fig 24.4 exhibits an unstable singularity F_u surrounded by a stable limit cycle C_0 and a few other cycles (C'_0, C'_1 unstable, C_1 stable, etc.). It is apparent that, since the state of rest F_u is unstable, a spiral trajectory will originate at F_u and will approach C_0, which represents the state of the ultimate stable stationary oscillation on the limit cycle. It is thus seen that the unstable limit cycles C'_0, C'_1 constitute a kind of divide or "barrier" for the initial conditions from which various stable limit cycles such as C_1, C_2… can be reached by trajectories.

Minorsky (1947) continues to investigate and explain the configuration of the limit cycles when there is a stable focal point. This is depicted in his Fig 24.5.

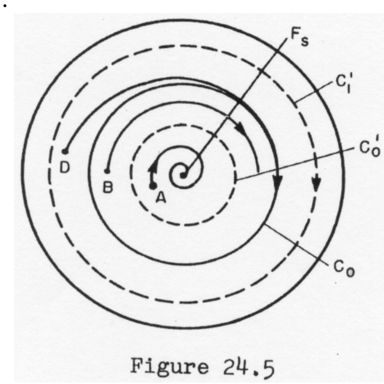

Fig. 24 (Fig. 24.5 from (Minorsky, 1947))

If there exists a stable limit cycle C_0, it follows that there must necessarily be an unstable limit cycle C'_0 between F_s and C_0. Therefore the system cannot become self-excited and reach the stable limit cycle either from rest or from any initial conditions represented by a point A inside C'$_0$. In fact, in the latter case, Fig. 24.5, the trajectory starting from A will approach the state of rest at F$_{s.}$ The stable limit cycle C$_0$ can be approached, however, if a trajectory originates either at B or at D, which represent points of the annular region between the divides C'$_0$ and C'$_1$, that is, the system must be given initial conditions represented by any point in this annular region.

Based on this analysis, it can be interpreted that if the singular point is found to be unstable, the innermost cycle is stable with alternate cycles being unstable. Similarly, if the singularity is stable, the innermost cycle is unstable followed by alternate stable cycles.

The preceding descriptions by Minorsky (1947) concerning limit cycles having stable or unstable foci may be compared with Boscovich's analysis where the perimeter of several ellipses are equivalent to limit points. He states,

> Now there is yet another analogy with these limit points. Let us consider a number of ellipses having the same foci, of which the semiaxes are in order equal to the distances corresponding to the limit-points in Fig. 1, namely to one of cohesion for one, to that of non-cohesion next to it for the second, and so on alternately; also suppose that the eccentricity is still smaller than any width of the arcs of the limit-points of Fig. 1 so that each of the elliptic parameters has only four limit-points, one at each of the four vertices of the axis. The whole set of such perimeters will be somewhat of the nature of limit points as regards approach to, or recession from the centre. A point situated in any one of the perimeters will have a propensity for motion along that perimeter. If it is situated between two perimeters, it will always direct its force in such a way that it will tend towards a perimeter corresponding to a limit-point of cohesion in Fig. 1, and will recede from a perimeter corresponding to a limit-point of non-cohesion. Hence, if a point is disturbed out of a position on a perimeter of the first kind, it will endeavor to return to it; but if disturbed from a position on a perimeter of the second kind, it will of its own accord try to get away from it still further, and will recede from it (*Theoria* note 234).

Boscovich follows this with a very concise demonstration in *Theoria* (note 235) where he employs the series of confocal ellipses in Fig. 33.

If one looks at Poincare's theory on differential equations the effect of changing parameters on solutions, it can be shown that a concentric pattern of limit cycles may undergo various qualitative changes. Given a function:

$$\emptyset(p) = -K(p-p_1)(p-p_2)\dots(p-p_n) \qquad (16)$$

Which corresponds to the roots $p_1 p_2 \dots$; if these roots are distinct $(p_1 \leq p_2 \leq p_3 \leq \cdots)$ one has a graph of $\emptyset(p)$ shown in his Fig. 7.10 (Minorsky, 1962). Then, if the roots are real positive then it may be shown that when:

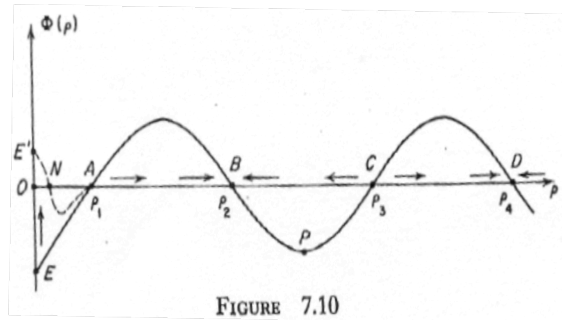

Fig. 25 (Fig. 7.10 from (Minorsky, 1962))

> The alternate stabilities of limit cycles result directly from the signs of the slopes, $\emptyset_p(p_i)$ at points A, B, C, … (Fig 7.10) and thus roots p_1, p_3 are unstable and p_2, p_4 are stable. For the configuration shown, the state of rest $p \approx 0$ must be stable in order to have a regular configuration with alternate stable and unstable cycles, with the singular point at the center considered as a cycle reduced to one point (Minorsky, 1962).

It is obvious that the treatment of limit points and limit cycles provides an ideal analogy with both Gill's (1941) treatment of Thomson's (1907) interpretation of Boscovich (1922) and also Martinovic (1987).

The pictorial representations as shown by Gill (1941) on Thomson (1907) and Martinovic (1987) differ in that Thomson assumes circular orbits, while Martinovic's interpretation, which is geometrical, exhibits concentric ellipses. Nonetheless both can be shown to yield a power series representation.

It will later be shown that the spiraling can be described via equiangular spirals. Fig. 26 shows the states of equilibrium, both stable and unstable on the Boscovich Curve.

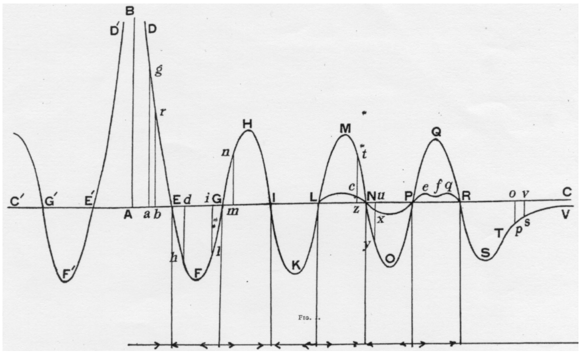

Fig. 26 States of Equilibrium (Fig. 1 from *Theoria*)

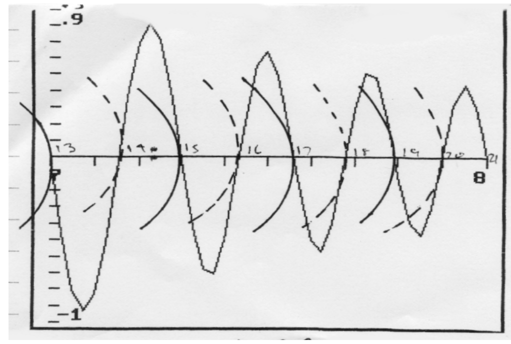

Fig. 27

Development

Returning to Thomson's (1907) description of what he refers to as the "Boscovichian atom," we should note that the "favored orbits" are the solid curves, while the "forbidden orbits" are represented by the broken curves. Thomson assumes that these curves are circles. If one considers that these curves might be analogous to the boundaries of the limit cycles of Poincare (1881) mentioned earlier, then there is no reason not to assume that these curves might be represented by other means. We can think of Martinovic's (1987) geometrical interpretation that they might be ellipses.

At this point, another interpretation can be brought to our attention since the analytical function derived as a quantitative representation of the Boscovichian curve has an inverse cube dependence, then the curve generated by a point moving under such a central force is a logarithmic spiral (Smith & Longley, 1910, p. 106-108) oftentimes referred to as an equiangular spiral after Descartes.

We are now in a position to discuss the series of curves in terms of the Fibonacci and quasi-Fibonacci numbers. Looking at the generated Boscovichian curve given by Eq. 12 for Fibonacci numbers U_7 to U_8 illustrated in Fig. 14 and assuming stable and unstable limit cycles, the Fibonacci and quasi-Fibonacci numbers make possible a qualitative descriptive portrait of the stable and unstable boundaries of the limit cycles. The stable limit cycles are shown as solid curves and correspond to $U_7 = 13$, $U_{7b} = 15$, $U_{7d} = 17$, $U_{7f} = 19$, and $U_8 = 21$. The unstable boundaries are $U_{7a} = 14$, $U_{7c} = 16$, $U_{7e} = 18$, and $U_{7g} = 20$.

The identities and intercept points were shown in Table 5. The role of Fibonacci numbers used in science spans several disciplines. Jean (1944) discusses the phyllotactic patterns outside botany. Since these numbers were used in the development of the analytical form of the Boscovician curve, it is now of interest to see how these Fibonacci sequences can be applied to other areas with emphasis on the microscopic region of matter. We can start with the analysis of the Balmer series of the hydrogen line spectra to develop an algorithm that also will explain the accompanying series.

The hydrogen spectra consist of consecutive lines called a series. Analyzing this series, spectroscopists determined the frequencies of these lines. Such a discrete spectrum of frequencies was assumed to be due to periodic motions similar to planetary motions. Many attempts were made to find a model based on the classical laws of mechanics and electrodynamics.

These proved to be incapable at predicting the structure of the spectra, thus all efforts were applied to empirical relationships. Later developments led to replacing classical mechanics with quantum mechanics. However, this leads to very complicated computations with the result that even though quantum mechanics explains the basic features of spectral structure, it still leaves a lot to be desired. It is now proposed to make another approach using algorithms obtained from phyllotaxis.

A brief description of phyllotaxis is necessary to explain its algorithmic role, which hopefully will be the beginning of a unique role in explaining these spectra. Phyllotaxis is a branch of plant morphogenesis, which studies the symmetrical and asymmetrical patterns of leaves around a stem, the scales on a pineapple or pinecone, etc. These phyllotactic patterns are called primordial which vary in number, size, position, etc. One of the leading authorities in phyllotaxis is Jean (1994), whose book, *Phyllataxis – A Systematic Study in Plant Morphogenesis,* is to many the most extensive source on phyllotaxis.

Thornley (1975, p. 510) shows that the patterns exhibited by the primordia may be expressed in terms of a logarithmic spiral which in turn produces the logarithmic spiral when a constant angle ϕ with the radius vector *r*. His derivation is presented below, along with his Fig. 1

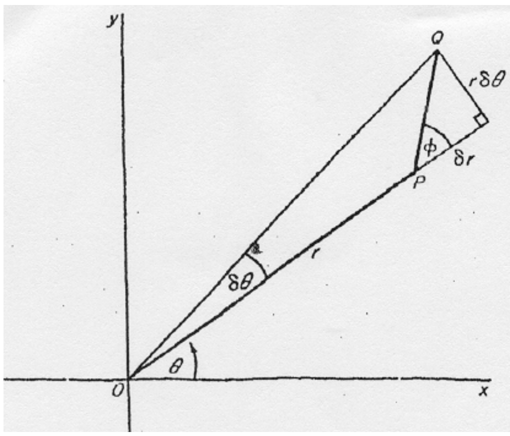

Fig. 1. Relationship between polar coordinates (r,Θ) and Cartesian co-ordinates (x,y). *PQ* is an element of a curve, and ϕ is the angle between *PQ* and the radius vector *OP*. See Eqns (1) and (2).

$$x = r\cos\emptyset, \quad and \quad y = r\sin\emptyset \quad (1)$$

Let *P* (Fig. 1) be a point on a curve with co-ordinates (r,Θ), and *Q* be another point on the same curve a short distance away from *P* with co-ordinates (*r*+*δr*,*Θ*+*δΘ*), where *δr* and *dΘ* are small increments in *r* and *Θ*. If ϕ is the angle between the portion of the curve *PQ* and the radius vector *OP*, then

$$\tan\emptyset = r\frac{d\theta}{dr} \quad (2)$$

Assuming that *PQ* is so small that *δΘ*/*δr* may be replaced by *dΘ*/*dr*. The logarithmic spiral is described by the equation

$$r = ae^{\theta\cot\emptyset} \quad (3)$$

Fig. 28 (Fig. 1 from (Thornley, 1975))

From his Eq. 2, Thornley (1975) gives Eq. 4:

$$\frac{dr}{d\theta} = r\cot\emptyset$$

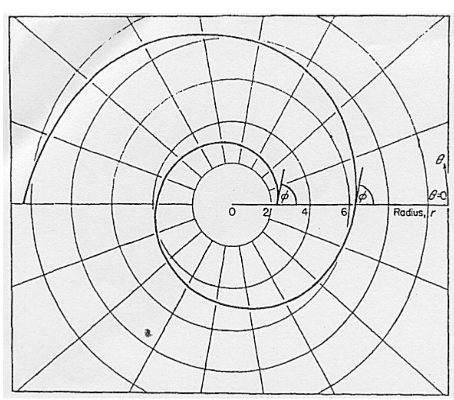

Fig. 2. Logarithmic spiral: Eqn (3) with α=2π/2 and cotϕ=1/2π. Comparing Eqns (4) and (2) shows that the logarithmic spiral always makes a constant angle ϕ with the radius vector. A logarithmic spiral is drawn out in Fig. 2.

Fig. 29 (Fig. 2 from (Thornley, 1975))

Using different symbols for Thornley's (1975) equations, Thomas & Cannell (1980, p. 1) discusses what they call "The Generative Spiral in Phyllotaxis Theory." Basically, this is the constant angle between any tangent to the logarithmic generative spiral and the radius, which is called the generative angle ϕ. A representation of a logarithmic spiral displaying two successive primordia is shown in Fig. 30.

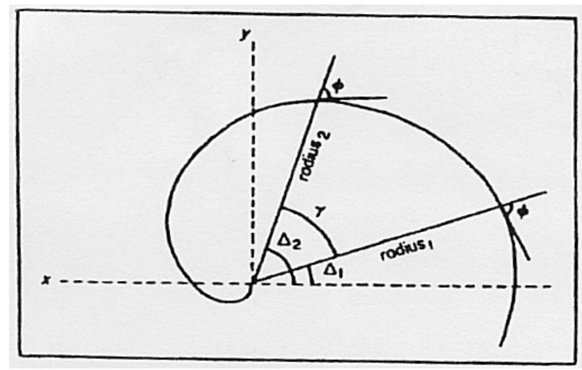

Fig. 30 (Fig 1 from (Thomas & Cannell, 1980))

From their Fig. 1, Thomas & Cannell produced a logarithmic generative spiral drawn through nine primordia using their Eqs. 1 and 2. (Note Δ is θ in Thornley (1975)).

Thomas & Cannell (1980) state:

> Assuming the generative spiral to be a logarithmic or equi-angular spiral, any radius may be defined with reference to the angle, Δ, it makes with the normal Cartesian coordinates (*x,y*), for instance, in Fig. 1:
>
> $radius = \exp[(\cot\emptyset)\Delta],$ (1)
>
> where ϕ is the constant angle (hence equiangular spiral) between the tangent to any point on the spiral and a radius (Fig. 1; also Thornley (1975)). This angle, ϕ, we shall call the *generative angle*. The ratio of any two radii is given by:
>
> $\frac{radius_2}{radius_1} = \exp[(\cot\emptyset)(\Delta_2 - \Delta_1)] = \frac{r_2}{r_1}$ (2)
>
> (p. 238).

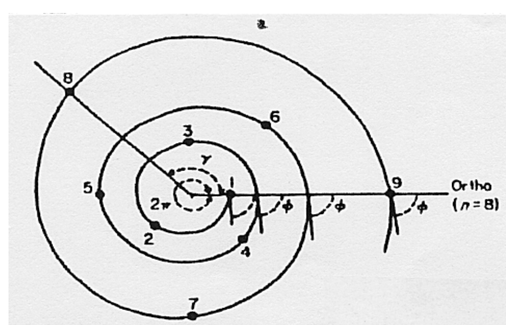

Fig. 31 (Fig. 2 from (Thomas & Cannell, 1980))
Logarithmic Generative Spiral Drawn Through Primordia

Following Thornley (1975) and Thomas & Cannell (1980), a parametric representation produced a logarithmic spiral, which is consistent with an inverse cube. Fig. 32 shows the spiral using Boscovich term expressions.

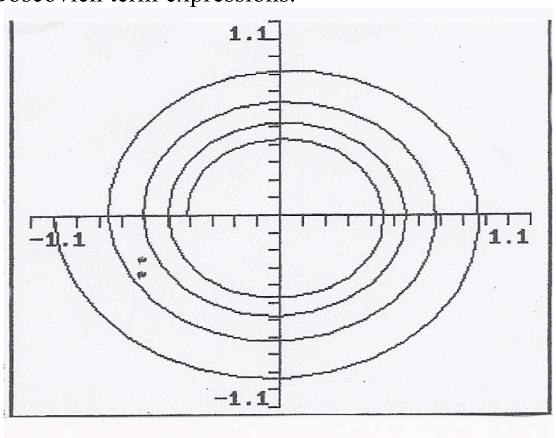

Fig. 32

$$\frac{Be^{(-kx)}\cos\left(\frac{1}{5}\pi\left(e^{(kx)}-e^{(-kx)}\cos(\pi x)\right)\sqrt{5}\right)}{x^3} \quad (17)$$

$$\frac{Be^{(-kx)}\sin\left(\frac{1}{5}\pi\left(e^{(kx)}-e^{(-kx)}\cos(\pi x)\right)\sqrt{5}\right)}{x^3} \quad (18)$$

$B = 10^4$

For purposes of comparison, Fig. 33 represents a logarithmic spiral using the Binet approximation form based on the fact that the x-intercepts occur at the integer Fibonacci numbers as well as the quasi-Fibonacci numbers.

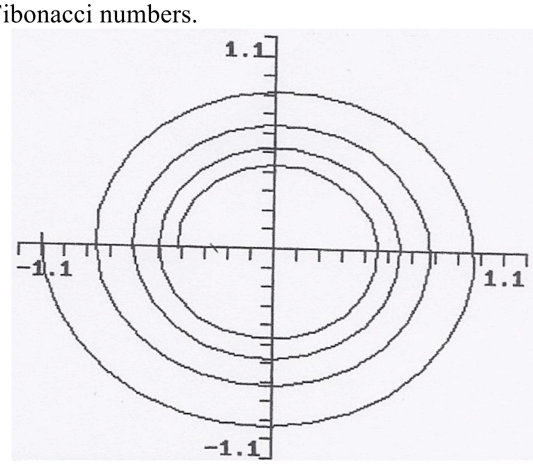

Fig. 33

$$x = \frac{Be^{(-kx)}cos\left(\frac{\pi 1.618034^{x}\sqrt{5}}{5}\right)}{x^3} \quad (19)$$

$$y = \frac{Be^{(-kx)}sin\left(\frac{\pi 1.618034^{x}\sqrt{5}}{5}\right)}{x^3} \quad (20)$$

$B = 10^4$

It is readily seen that there is hardly any difference between Figs. 32 and 33. It should be noted that the same set of spirals could have been obtained using the integer-non-integer Fibonacci number representation from Horadam & Shannon (1988) and converted by the writer. Note that there are nine intersections in both figures when there are two integers Fibonacci numbers (13 and 21) and seven quasi-Fibonacci numbers as mentioned earlier in Fig. 27 and Table 5.

Applications

Atomic Spectra and Empirical Data

From the foregoing, it is now time to apply the foregoing analysis in the form of an algorithm for predicting atomic line spectra. In keeping with tradition, the hydrogen atom is to be used in the prognosis with emphasis on the empirical Balmer series. Following this, the other prevalent hydrogen line spectra of Lyman, Paschen, and Brackett are presented.

It has been observed that heated solid bodies emit a continuous spectrum when they glow; however, for gases and vapors, one observes what is commonly called discrete line spectra. It is assumed that these lines are for atoms only, although continuous spectra can occur for both atoms and molecules as well. The history of spectra both for line and continuous is very extensive and is beyond the purpose of this work.

The discrete spectra exhibit a regular sequence of lines, which are referred to as a series.
It was Balmer (1885) who first produced an empirical relationship for the hydrogen spectra, which became the model for all subsequent investigations. Balmer's interpretation was in what is called the wavelength and is given by the Greek letter; λ. Balmer's formula was given as a series of fractions defined by:

$$\lambda = b\frac{m^2}{m^2-n^2} \quad (21)$$

Where b is the fundamental number and λ is the wavelength of any hydrogen line in Angstrom units (10^{-8} cm) and b = 3645.6. If n = 2 and m = 3, 4, 5, etc., the formula gives the series of lines in the visible hydrogen spectrum.
Balmer (1885), in his landmark paper, stated that the wavelength might be represented as

$$\frac{9}{5}b, \frac{4}{3}b = \frac{16}{12}b, \frac{25}{21}b, \frac{9}{8}b = \frac{36}{32}b \quad (22)$$

It is interesting to note that the integer Fibonacci number 5, 3, 21, and 8 appear. This intriguing association leads one to infer that there might be some correlation between the Balmer series and Fibonacci numbers. With this in mind it was decided to see what the ratio of the Balmer series and the Fibonacci sequence looked like. Based on this, it was decided to first see what a plot of the Balmer series as a function of its wavelength looked like. This is not unusual in science since a pictorial representation can form as a guide in an analysis.

Fig. 34 shows the shape of the series as a function of its wavelength λ. The associated table is also shown for n = 3 to 16. To my knowledge, this may be the first time that a pictorial representation has been shown for the Balmer series.

n	λ (10^{-8} cm)
3	6562.08
4	4860.8
5	4340
6	4101.3
7	3969.65
8	3888.64
9	3834.98
10	3797.5
11	3770.24
12	3749.76
13	3733.98
14	3721.55
15	3711.58
16	3703.47

Table 14

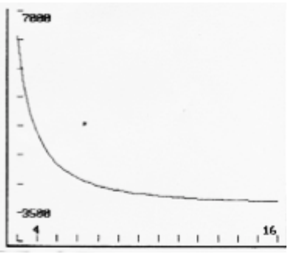

Fig. 34

This brings us to the point where it might prove feasible to compare the Balmer series to the Fibonacci sequence. We first investigate the ratio of the Balmer series to the Fibonacci numbers to see what the form of the graph presents. Fig. 35 shows the ratio of the Balmer series to the Horadam & Shannon (1988) and Prince (1989) Fibonacci sequence. The table is also shown:

n	Ratio
3	3281.04
4	1620.27
5	868
6	512.663
7	305.358
8	185.173
9	112.794
10	69.0455
11	42.3622
12	26.04
13	16.0257
14	9.87148
15	6.08456
16	3.75225

Table 15

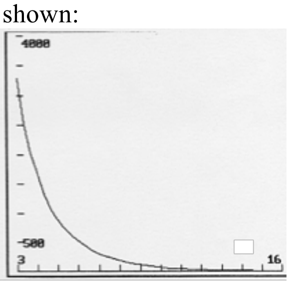

Fig. 35

The ratio of the Balmer series and the Binet approximations is shown in Fig. 36 along with an accompanying table:

n	Ratio
3	7164.58
4	4610.27
5	3735.04
6	3282.47
7	2999.05
8	2801.83
9	2654.76
10	2539.67
11	2446.4
12	2368.76
13	2302.76
14	2245.7
15	2195.7
16	2151.37

Table 16

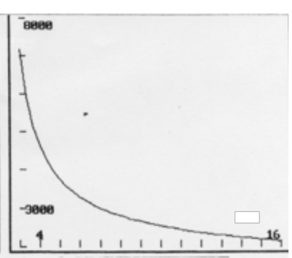

Fig. 36

Except for magnitudes, one sees that both curves Figs. 35 and 36 have very similar shapes. This implies that there might be a linear or non-linear function that would bring these curves and quantities into agreement. Before doing this, it would behoove us to return to the statements made by Boscovich (1922) in studying the limit points of cohesion and non-cohesion using his Fig. 33 of con-focal ellipses.

From his Fig. 1 (the Boscovich curve), he establishes a relationship with the associated limit points of cohesion and non-cohesion as one goes around the perimeter of the ellipse. Boscovich asserts that, "…it must be practically an ellipse, yet will neither be an ellipse accurately…" (1922, note 236).

This essentially leaves room for determining the actual forms of the confocal perimeters and their influence as a point lies between these perimeters. From the inverse cube form of the force, then as mentioned earlier, the resulting curve will be an equiangular (logarithmic) spiral. We will now investigate how this configuration can be applied to the description of atomic spectra using the hydrogen atom and the Balmer series.

In present day analysis of spectra, it is more convenient to use the Balmer series equation in terms of the number of wavelengths per centimeter instead of frequency. This designation is called "wavelength number" and is defined as

$$v = \frac{1}{\lambda_0} cm^{-1} \tag{23}$$

Accordingly, this interpretation allows the Balmer equation to be rewritten as

$$\frac{1}{\lambda} = v = R\left(\frac{1}{n^2} - \frac{1}{m^2}\right) \tag{24}$$

n = 2; m = 3, 4, 5, …; and R = 109721.3 (this work)

Where by setting n = 2 in Balmer and R is called the Rydberg constant.

$$b = \frac{4x10^8}{R}$$

The denominator in Balmer's formula yields the difference between two integers, and going to the v representation results in the difference of two terms, which can be interpreted as the difference of two orders.

Following Thomson's (1907) designation of Boscovich's curve, where he discusses "favored orbits" and "forbidden orbits," or in Boscovichan terms, "cohesion" and "non-cohesion," which can be carried over to "stable" and "unstable" limit cycles, we see that the difference between these quantities are essentially the difference of two terms which for our purpose will be denoted as the difference of two distances. This allows us to investigate the relationship between these differences and the Balmer formula. Returning to Fig. 27 reproduced below; we see that the favorable (allowed) orbits appear for at alternate Fibonacci or Quasi-Fibonacci numbers as well as unfavorable (forbidden) orbits.

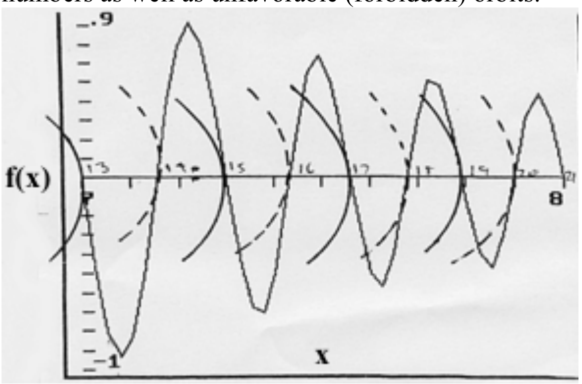

Fig. 27

In either case, the difference is between $x_n - x_{n-2}$ e.g.: $x_{15} - x_{13}, x_{17} - x_{15}$, etc.

The difference of these intersections may be described by:

$$f_{(x)} = \frac{\ln(\sqrt{5}x)}{k} - \frac{\ln(\sqrt{5}(x-2))}{k} \tag{25}$$

Where k = 0.481211825

The graph of this expression is shown below:

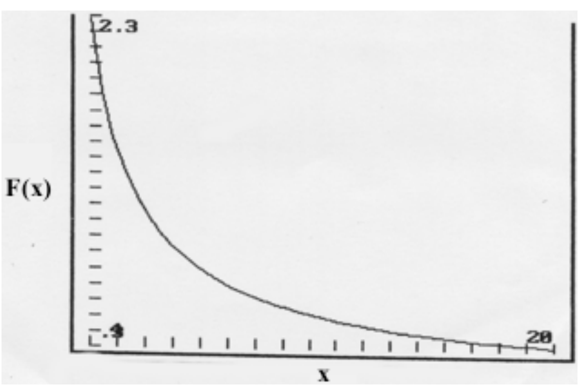

Fig. 37

If one ignores the magnitudes, this curve is similar to the Balmer curve, which implies some type of correlation may result. With this in mind, it was decided to find the ratio of Balmer and the aforementioned expression. This resulted in the following graph:

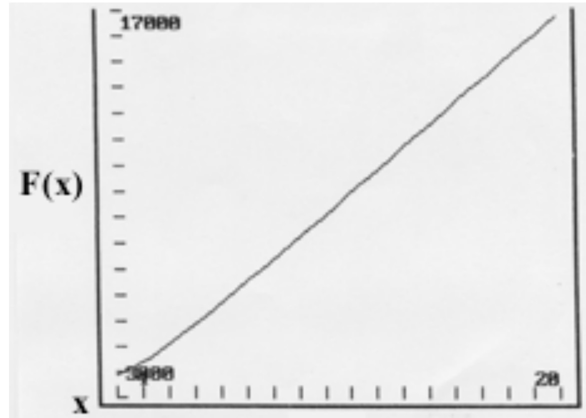

Fig. 38

While this curve looks linear, upon numerical evaluation, it is not; therefore, it was necessary to perform a nonlinear regression analysis to produce a particular functional form. The nonlinear regression analysis was performed using the assumption that the premonitory equation depends nonlinearly on one or more unknown parameters, ever mindful that it should follow a particular functional form. In this case, the concept of the relation between a logarithmic spiral and its significance in phyllotaxis proved to be very advantageous. The resulting equation is given below.

$$\frac{\left(\ln(\sqrt{5}x) - \ln\left(\sqrt{5}(x-2)\right)\right) a e^{(dx\cot(e))} x}{k\cos(\frac{b}{x+c})} \tag{26}$$

The designated parameters are:
a = 808.0643
b = -0.33385
c = 2.405
d = 0.001347
e = 45°
k = 0.481211825

A physical meaning to these parameters will be studied with the hope that they will be useful in other investigations. As mentioned earlier, the Balmer series was purely empirical and only applicable to the hydrogen atom. The hydrogen spectra series was subsequently calculated using Eq. 26, with the graphical and tabular results shown in Fig. 39 and Table 17 respectively.

n	λ (10^{-8} cm)
3	6563.18
4	4785.41
5	4353.93
6	4136.19
7	4003.13
8	3913.51
9	3849.39
10	3801.58
11	3764.87
12	3736.05
13	3713.06
14	3694.49
15	3679.36
16	3666.95

Table 17

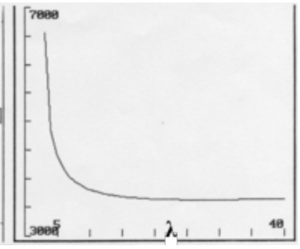

Fig. 39

A comparison of the calculation and the Balmer series also showed excellent agreement as shown below in Fig. 40. The results were almost identical.

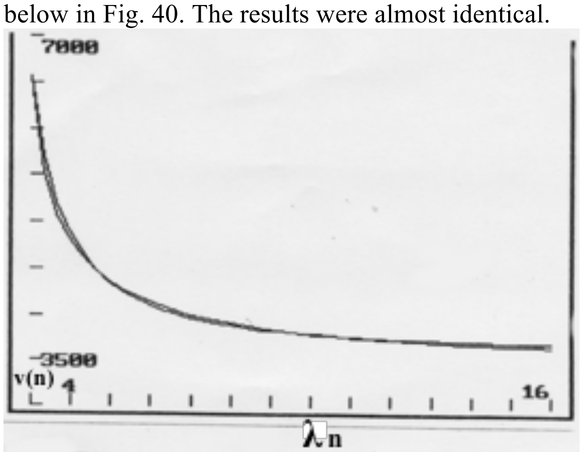

Fig. 40

Using the relationship between the wavelength number and wavelength

$$v_n = \frac{10^8}{\lambda_n} \tag{27}$$

Provided Table 17 and Fig. 41 for the Balmer wavelength numbers as a function of *n*.

n	v (10^8 / λ)
3	15236.5
4	20896.9
5	22967.8
6	24176.9
7	24980.5
8	25552.5
9	25978.2
10	26304.9
11	26561.4
12	26766.3
13	26932.
14	27067.4
15	27178.7
16	27270.6

Table 18

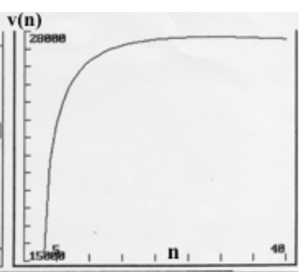

Fig. 41

Table 19 shows the actual data for the calculated wavelength based on Eq. 26 and the wavelength according to the Balmer formula. It can be seen that for *n* values up to 16, the percentage differences are less than one percent. For higher *n* values, the percentage difference is somewhat greater than one percent (approximately 1.3%). At any rate, it is felt that this approach is within experimental accuracy.

Wavelength for the Hydrogen Atom

n	Eq. 26	Balmer
3	6563.15	6562.08
4	4785.39	4860.8
5	4353.91	4340
6	4136.17	4101.3
7	4003.11	3969.65
8	3913.49	3888.64
9	3849.37	3834.98
10	3801.56	3797.5
11	3764.85	3770.24
12	3736.03	3749.76
13	3713.04	3733.98
14	3694.46	3721.55
15	3679.33	3711.58
16	3666.93	3703.47

Table 19

A comparison of the experimental and calculated values are given by Baly (1927), as shown in his Table I (b=3646.13)

Hydrogen Spectrum

Designation	Observed	Calculated	Difference
a	6563.07	6563.03	+ 0.04
β	4861.57	4861.52	+ 0.05
ν	4340.53	4340.63	- 0.10
σ	4102.00	4101.90	+ 0.10
ε	3970.33	3970.22	+ 0.11
ζ	3889.15	3889.20	- 0.05
η	3835.51	3835.53	+ 0.02
θ	3798.00	3798.04	- 0.04
ι	3770.73	3770.77	- 0.04
κ	3750.27	3750.30	- 0.03
λ	3734.53	3734.51	+ 0.02
μ	3721.98	3722.08	- 0.10
ν	3712.13	3712.11	+ 0.02
ξ	3704.01	3704.00	+ 0.01
ο	3697.28	3797.29	- 0.01
π	3691.70	3691.70	± 0.00
ρ	3686.96	3686.97	- 0.01
σ	3682.94	3682.95	- 0.01
τ	3679.52	3679.49	+ 0.03
υ	3676.51	3676.50	+ 0.01
φ	3673.87	3673.90	- 0.03
χ	3671.53	3671.48	+ 0.05
ψ	3669.55	3669.60	- 0.05
ω	3667.83	3667.82	+ 0.01
Series No. 27	3666.25	3666.24	+ 0.01
Series No. 28	3664.74	3664.82	- 0.08
Series No. 29	3663.55	3663.54	+ 0.01
Series No. 30	3662.36	3662.40	- 0.04
Series No. 31	3661.31	3661.35	- 0.04
Series No. ∞	Theoretical limit	3646.13	----

Table 20 (Table I from (Baly, 1927))

Another tabulation for the Balmer series was presented by Fowler (1922, p. 89) and is shown below with his tabulation using this formula, which is displayed in Table 21.

$$v = 109678.28[\frac{1}{(2-0.00000383)^2} - \frac{1}{(m+0.00000210^2)}] \quad (28)$$

H. BALMER SERIES Limit = A = 27419.674			
m	λ, *I.A.*	ν	$A - v$
1	---	---	109677.82
2	---	---	27419.512
3	6562.793	15233.216	12186.458
4	4861.327	20564.793	6854.881
5	4340.466	23032.543	4387.131
6	4101.738	24373.055	3046.619
7	3970.075	25181.343	2238.331
8	3889.052	25705.957	1713.717
9	3835.387	26065.61	1354.06
10	3797.900	322.90	1096.77
11	70.633	513.24	906.43
12	50.154	658.01	761.64
13	34.371	770.68	648.99
14	21.941	860.09	559.58
15	11.973	932.21	487.46
16	03.855	991.24	428.43
17	3697.154	27040.16	379.51
18	91.557	81.16	338.51
19	86.834	27115.85	303.82
20	82.810	45.47	274.20
21	79.355	70.96	248.71
22	76.365	93.07	226.60
23	73.761	27212.35	207.32
24	71.478	29.26	190.41
25	69.466	44.19	175.48
26	67.684	57.42	162.25
27	66.097	69.23	150.44
28	64.679	79.78	139.89
29	63.405	89.26	130.41
30	62.258	97.81	121.86
31	61.221	27305.54	114.13
32	60.280	12.55	107.12
33	59.423	18.94	100.73
34	58.641	24.79	94.88
35	57.926	30.14	89.53
36	57.269	35.05	84.62
37	56.666	39.55	80.12
∞	45.981	27419.674	0

Table 21 (Fowler, 1922)

We can now turn our attention to other spectra associated with atomic hydrogen. The main ones are given for n = 1, 3, 4, and 5 referred to as the Lyman, Paschen, Brackett, and Pfund series. To investigate these sets of series, it was decided to use the wavelength and wavenumber calculations employing the Rydberg-Ritz combination principle.
As mentioned earlier, the wave number v is the difference of two terms where n is a constant and m is a variable term given by $v = R\left(\frac{1}{n^2} - \frac{1}{m^2}\right)$.

Rydberg (1896) and Ritz (1908) formulated what is now called "Principle of Combination", showed that by adding or subtracting and using a certain combination allows the calculation of new lines based on the knowledge of previous discovered or calculated wave numbers. It should be mentioned that the combination principle was obtained by purely empirical techniques and to date has never been analyzed by classical means.

The following exemplary description is based on an interpretation from Shpol'skii (1969), and it is applied to determining the second line in the Paschin series. From Eq. 24, let $T_n = \frac{R}{n^2}$, $T_m = \frac{R}{m^2}$ where m > n. Then, letting $v = T_n - T_m$. Knowing the wave numbers of the first and third lines in the Balmer series (n = 3 and n = 5, respectively) yields $v_1 = T_3 - T_2$ *and* $v_3 = T_5 - T_2$. Then, the difference of $v_3 - v_1$ is the wavenumber of the second line in the Paschen series. e.g., $v_3 - v_1 = T_5 - T_3$

From the calculated values in Table 17 on the Balmer series $v_1 = 15236.5$, $v_3 = 22967.8$. Thus, $v_3 - v_1 = 7731.3$ using $\lambda = \frac{10^8}{v}$ yields $\lambda = 12934.3$.

Comparing this with the observed value of λ = 12817.6 (Shpol'skii (1969) Table 12) is less than 1%. Using this combination principle, the wavenumber of all of the series were calculated and the associated wavelengths were determined. It should be pointed out that the comparisons of this work with the calculated Balmer series using b = 3645.6 produced a small percentage error of approximately 1.0 to 1.5%.

On going to the higher values of m (m > 30) there is a slight increase of λ using Eq. 26. This could be due to the fact that the experimental value of the Rydberg constant has been shown to decrease as the order number m increases. Both Fowler (1922, p. 29) and Baly (1927, p. 39) have addressed this situation and reported that there would be a slight departure from Balmer's (1885) formula. In fact, Baly states the Balmer series is not quite exact (1927, p. 40).

When one looks at the range of m values associated with the observed Balmer series (see Table 20), the highest value of m is m = 31. For the range of m values between m = 31 and the series limit at infinity, no observed values of the wavelengths exist, however at the theoretical limit Baly (1927) calculates λ = 3646.13.

Now, this really is an extrapolation and does not guarantee that the wavelengths series continue to decrease; in fact the lines in the series tend to slightly increase using Eq. 26. Whether this is true or not will depend upon more experimental data for the higher values of m.

The following figures show the wavenumbers and wavelengths for the Lyman, Paschen, Brackett, and Pfund series. Only the numerical values associated with the Lyman series are shown. The numerical values for the others have been calculated also and show appreciable comparisons with the available experimental data.

Wavelength for the Lyman Series

Fig. 42

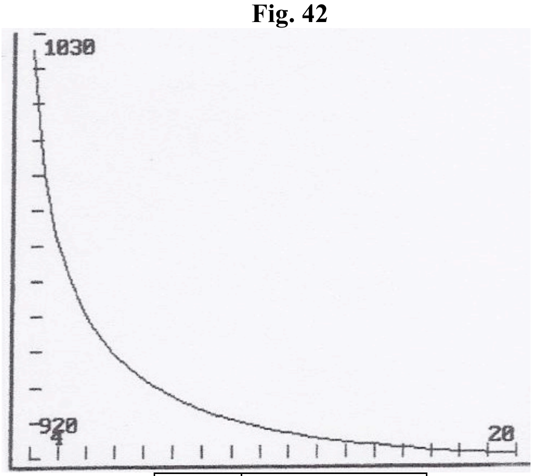

n	$\lambda(10^{-8}cm)$
3	1025.35
4	969.106
5	950.04
6	939.251
7	932.214
8	927.269
9	923.624
10	920.845
11	918.675
12	916.949
13	915.550
14	914.425
15	913.495
16	912.728

Table 22

Wavenumber for the Lyman Series

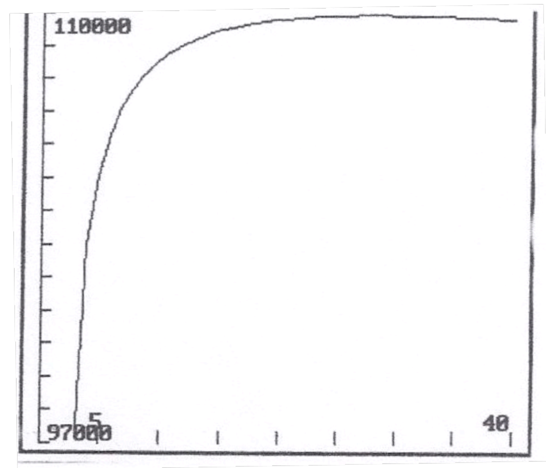

Fig. 43

n	$v = \left(\frac{10^8}{x}\right)$
3	97527.5
4	103188
5	105259
6	106468
7	107271
8	107844
9	108269
10	108596
11	108852
12	109857
13	109223
14	109358
15	109478
16	109562

Table 23

The Paschen Series

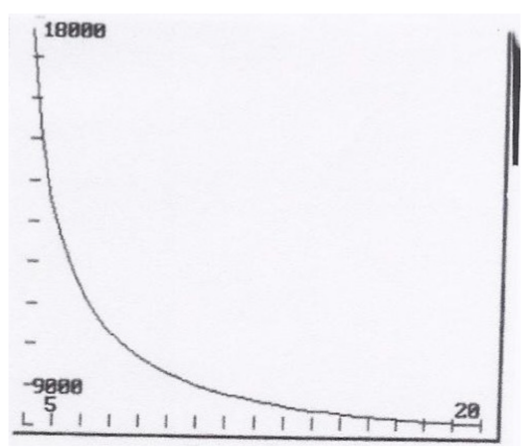

Fig. 44
Wavelength for Paschen Series

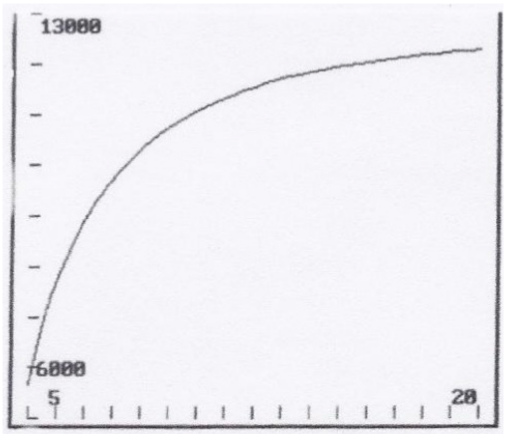

Fig. 45
Wavenumber for Paschen Series

The Brackett Series

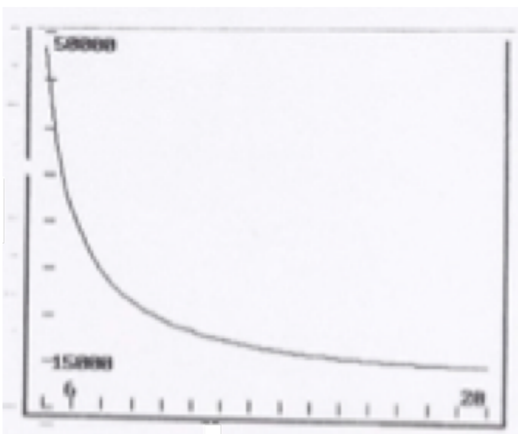

Fig. 46
Wavelength for Brackett Series

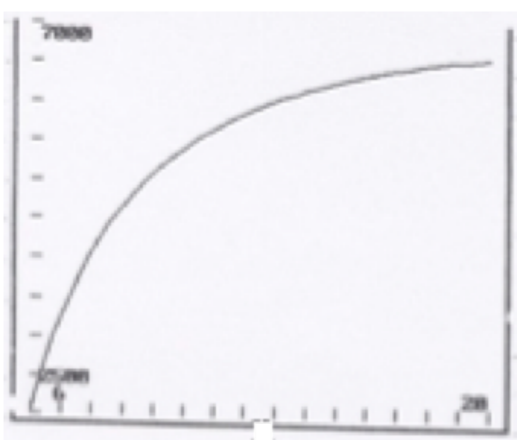

Fig. 47
Wavenumber for Brackett Series

The Pfund Series

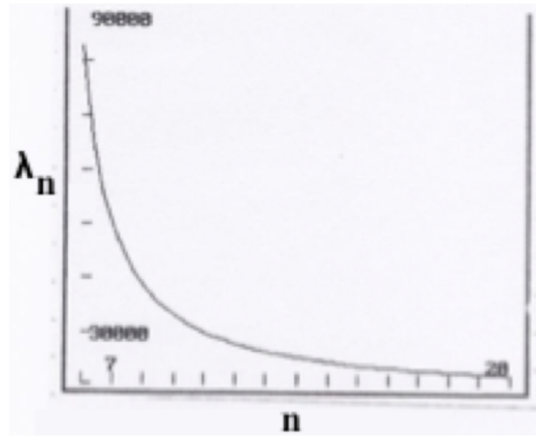

Fig. 48
Wavelength for Pfund Series

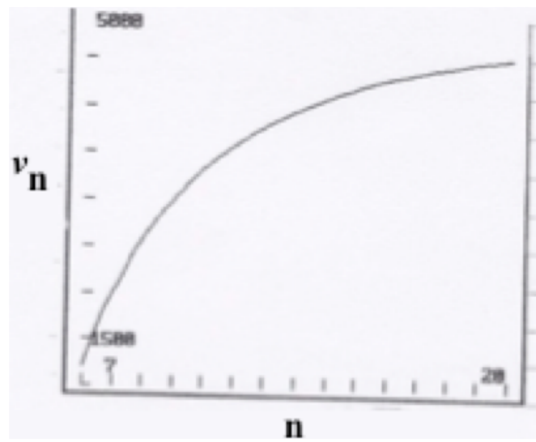

Fig. 49
Wavenumber for Pfund Series

A comment should be made about the differences in numerical values for the Rydberg constant. Rydberg used a value R = 109675.00, but as pointed out by Baly (1927, p. 39), the value tends to decrease as the order number *m* increases. These differences may be attributed to the measured "optical center of gravity." These will not conform strictly to the Balmer formula.

The ensuing years have seen more than 500 scientific papers on the Hydrogen spectrum many of which used various numerical values for the Rydberg constant. An international standard of *R* = 109,737.31568 has been established based on The Task Group and Fundamental Constants of the Committee on Data for Science and Technology, (CODATA). (Mohr & Taylor, 2000; Mohr & Taylor, 2005; Mohr, Taylor & Newell, 2008). The latest compilation on the Hydrogen series may be found in the Atomic Data and Nuclear Data Tables. (Kramides, 2010).

Previous studies of discrete and continuous spectra have led to inconsistencies with classical interpretations. The arithmetical relationship of the wavelengths or wavenumbers of the various spectral lines using consecutive integral numbers have been reanalyzed in this work, so to speak in terms of Fibonacci numbers. Up to this point, the analysis has concentrated only on the hydrogen atom spectrum. The method was derived using an empirical analysis which also can be applied to hydrogen-like atoms, such as ionized helium.

The hydrogen spectral series was successfully demonstrated in the Rutherford-Bohr model. This led to a rather comprehensive interpretation of the hydrogen spectrum which subsequently led to the development of quantum electrodynamics. When one goes to multi-electron atoms and molecular spectrum, the situation becomes much more complex and requires very extensive mathmatical calculations using very sophisticated quantum-mechanical interpretation.

As has been shown, using the mathematical interpretation of the famous Boscovich curve, a new paradigm was established which led to a new method for depicting the hydrogen spectrum. This paradigm led to an algorithm based on Fibonacci numbers and does not need the use of the Rydberg constant. It does, however, use what the author describes as a "senescence function" as shown in the denominator of Eq. 26 given by: $kcos(\frac{b}{x+c})$.

The development and reasons for this function will be addressed in the following analysis used in the so called "Black Body Radiation" interpretation for continuous spectra. The parameters *b* and *c* remain to be identified with a particular physical interpretation which, like the b = 3647.1, which was used by Rydberg to establish his constant. $R = \frac{4x10^8}{b} = 109721.3$ is used in this work.

The Rydberg constant was subsequently given a scientific explanation by Bohr (1913), who, using the frequency instead of wavenumbers, produced a value for the Rydberg constant which was in close agreement with the observed value.

A rather extensive description of Bohr's ideas may be found in Heilbron & Kuhn (1969). Refinement in experimental methods have improved the value for the Rydberg constant. It is hoped that a physical interpretation of the "senescence function" will follow the same course. A hint may be found in the use of an analysis by Church (1904), where the use of "energy fields" are assumed. Church describes a method for analyzing phyllotaxis phenomena where the concept of periodicity is assumed. He states,

> There must, in fact, be some still more hidden meaning in the construction from which the periodicity as expressed in a time-diagram, and in actual ontogeny, follows as naturally as does the geometrical construction by logarithmic spirals from the addition of similar members (p. 227).

Church (1904) continues,

> Thus, in the postulated construction of circular growth-centres plotted along orthogonally intersecting log. spirals, the numbers of which are taken from observation of the plant, it follows that these initial centres must also have been laid down at the intersection of orthogonally intersecting log. spirals of the same ratio. The main question at issue, therefore, is to determine why these points should be found at the intersection of certain orthogonal trajectory paths, and what may such paths and intersections possible mean from a physical standpoint – that is to say, to what extent may the diagrams be also taken as the expression of a field of distribution of growth-energy, comparable, for example, to manifestations of distribution of the physical energy of the electro-magnetic field?
>
> To what extent one may be justified in thus passing from a *kinematic* to a *kinetic* standpoint is, of course, very questionable; and similarly little can be said beyond mere speculation until more is known as to what is actually meant by the expression *growth-energy,* or the energy of life, and how far it is comparable, for example, with "electrical" energy. One point may, however, be conceded: that in the case of living matter, *the actual mechanical energy accompanying life obeys physical laws just as surely as its material substance obeys chemical laws.*
>
> The data afforded by the plant are these:---
>
> I. A growing, expanding system, containing, therefore, moving particles; in which
>
> II. Growth-energy is being introduced from a central "growing- point"; and
>
> III. A construction which, as expressed in the transverse component of the formation of lateral members, has been put forward as implying primarily the geometrical properties of orthogonal trajectories (p. 228-229).

In regard to the intersection of orthogonally intersecting logarithmic spirals, Church maintains that these curves should, therefore, have some meaning attached to them. If, as the log. spiral theory suggests, these curves imply lines of equal distribution of growth-energy, it may be possible to give an explanation in physical terms (1904).

Church (1904) follows with,

> Two points may here be conceded: there must be, as already stated, some mechanical law implying a fundamental property of force and matter underlying these phenomena of rhythm; and it will again be hardly possible to discuss such speculations without trespassing on the terminology of some branch of physical science, the fundamental laws of which are equally obscure (p. 232)

Church (1904) felt that if a geometrical theory can be established for phyllotaxis, certain inferences may be drawn from it such that physicists might be able to use it as an analog to explain mathematical laws of scientific phenomena. He mentions,

> If the introduction of a mathematical conception of growth and growth-centres can lead to any better method of dealing with the facts, there will be no harm in trying to apply it so long as "growth-movement" and "growth-energy" are recognized as being in someway comparable, though not necessarily identical, with more strictly physical phenomena. While, again, the application of the strictly mathematical conception of a uniform distribution of growth-energy around an initial growth-centre must remain necessarily in the condition of a working hypothesis, …. *There can be no doubt that such an hypothesis must continue to form the basis of all considerations of the geometrical representation of the growth-phenomena presented by the plant-body;…* (Church, 1904, p. 232-233).

Church's concept of a field distribution of growth energy in phyllotaxis, may be construed as being analogous to kinetic energy rather than potential energy. Thus, since this involves motion, it is hoped that using Boscovich's concept of "point centers" it might be analogously carried over to the explanation of the "senescence function" and subsequently to a mathematical justification.

The treatment used in this work for calculating the Hydrogen spectra is strictly semi-empirical. As mentioned earlier, the clarification of the various perimeters and their interpretation remains to be achieved. It is hoped that a scientific inquiry based on Church's description of field theory in phyllotaxis will carry over to an analogous treatment of spectra, not only for single electron atoms like Hydrogen or ionized Helium, but also molecular spectra. With this in mind, the following section will also deal with the microscopic region namely the "thermal radiation" often called "blackbody radiation".

The employment of Boscovich's ideas will be coupled with the methods used in the foregoing line spectrum study. In the course of developing an algorithm for explaining what is commonly called blackbody radiation, several concepts were investigated. The primary one was that Boscovich (1922) made a distinction between different kinds of particles resulting from the number of points in them, the corresponding volume, density and shape. The shape is dependent upon the forces between the points. He outlines this in the *Theoria*:

> 419. The first thing that presents itself is the huge difference, of many kinds, which there can be amongst different groups of points such as form the different kinds of particles of which bodies are formed. The first difference that calls our attention can be derived from the number of points that form the particle; this number can be quite different within the same volume. Then, the volume itself may be different, as also may the density; for, of course, two particles need not have equal masses, equal volumes or equal densities. Then, even if the mass and the volume were given, that is to say even the mean density of the particle is given, there may be a huge difference in shape, that is to say, in the surface enclosing all the points and conforming to them. For, the points in one particle may be disposed in a sphere, in another in a pyramid, or a square or a triangular prism. Take any such figure, and suppose the points are disposed in any particular manner whatever; then there will be as many distances as there are pairs of points, and their number will be finite in every case. The curve of forces can have any number of limit points of cohesion, and these can occur anywhere along it. Therefore it must be the case that limit points can be found to correspond with those distances, and on account of these, the particle will have that particular form and can be extremely tenacious in keeping that form. Indeed, through a single distance, with a restraint of infinite resistance arising from a pair of parallel asymptotes close to one another, having the area on one side attractive and on the other side repulsive, there can be obtained in any mass of any form whatever a solidity that is also infinite, or a force that would prevent any change of disposition of the particles equal to or greater than any given change.
>
> Hence, the density can be varied to any extent, but apart from the fact that to each distance there corresponds a limit point in the primary curve, or that there are pairs of asymptotes, or any other asymptotes of the sort except the

> first, there are really an innumerable number of kinds of figures, in which with a given number of points there can be equilibrium, and a limit point of cohesion due to the canceling of equal and opposite forces, as can be seen from the solution of the problem indicated in Art. 412. The following distinction is especially worth remark.
> 420. Even if the figure is given, there can still be obtained a great difference between different particles on account of the different disposition of the points that form it. Thus, in the same sphere, the points may be quite unequally distributed, in such a way that, even at equal distances, there may be very many in one part and very few in another; or in different places on the same concentric surface there may be very many groups of points condensed together, whilst in others there are very few of them; these very places may be at quite different distances in different places even within the same particle, and in different particles at the same distance from the center they may be distributed in ways that are altogether different. Further, even if particles have the same figure, say spherical, and in each of them, round about, and at the same distance from, the center the points are distributed uniformly; yet even then there may be a huge difference in the density corresponding to different distances from the center. For, in the one, they may all be grouped near the center, in another toward the middle surface, and in a third close to the outer surface. In these, the differences, both as regards to the positions of equal density and also as regards the ratio of the different densities, can be varied indefinitely (notes 419 and 420).

It should be noted that Boscovich in notes 419 and 420 mentions two characteristics associated with his point distribution, namely the “surface area” and “volume”. He alludes to the homogeneity of the disposition of points and their relation to the alternation and transformation of bodies in *Theoria*

> 519. But, to return to my theory of homogeneous elements, the several forms of bodies will consist of a combination of homogeneous points, which comes from their distances and positions, and, in addition, to combination alone, the velocity and direction of the motion of each of the points; also for individual masses of bodies there is to be added the number of points that form them. Given the number and disposition of the points in a given mass, the basis of all its properties, which are inherent in the mass, is given; and also that of all the relations that the same mass must have with other masses; that is to say, those determined by their numbers, combinations and motions; moreover, the basis of all changes that can happen to it is also given. Now, since there are special combinations, representing certain special constant properties, which we have determined and explained, namely those corresponding to cohesion, and various degrees of solidity, those for fluidity, for elasticity, for softness, for the acquisition of certain shapes, for the existence of certain oscillations, which combinations, both of themselves and through forces connected with them, produce different tastes and different smells, and exhibit the different constant properties of colors; and also there are other combinations, which induce motions and changes that are not permanent, like all sorts of fermentations; there can be derived from the primary combinations of constant properties the specific forms of bodies and their differences, and from the latter also can be obtained alterations and transformations in these forms.
> 520. Now, amongst these constant properties there may be some that are chosen more constant than others; such as do not depend upon admixture with other particles, and also such as, if they should be lost, would be easily and quickly acquired. These properties could be considered to be essential to the species; and if such properties suffered a permanent change, we should have a transformation; whereas, if they persisted, there would only be an alteration. Thus also, a body would be said to be altered, but not specifically changed, if the quantity of fiery matter, which it contains in its pores, is increased; or if there is an increase in its motion, or even in some oscillation of its parts; similarly, it would be said to be merely altered by a fresh accession of heat (notes 519 and 520).

The reason for mentioning the foregoing quotes from Boscovich’s (1922) *Theoria* is due to the fact that these quotations serve to begin the analysis of blackbody radiation from a classical viewpoint. When one researches the literature on this topic, we find many publications. The most extensive of these is by Kangro (1976). Kangro (1976) traces the history of attempts to establish a theoretical basis for this phenomena starting from the mid 19th century to the beginning of the 20th century with Max Planck’s investigation on radiation, which subsequently led to the concept of quantum mechanics.

A brief review might begin with the common definition of "blackbody radiation". When a body is heated it radiates a specific spectrum. At the turn of the century, it was assumed that heat caused the molecules and atoms of a solid to vibrate, inducing charge oscillations, which from Maxwell's Theory of Electromagnetic Radiation, produced light. The puzzle that confronted the early experimenters at the turn of the century was that the radiations could not be predicted using classical physics. This was a motivating factor in Planck's successful theoretical analysis, which subsequently led to what is now termed "Quantum Theory".

One is then tempted to ask, "Just how does Boscovic and his ideas outlined in the *Theoria* apply to explaining blackbody radiation?" Perhaps a way to begin is to quote Kangro (1976),

> How, then, is the radiation which succeeds absorption to be explained? Experience shows, as Lommel points out, that there are two types of spectra, and therefore that there are two causes. On heating a solid body "the *vis viva* of its intermolecular vibrations (i.e., vibrations of whole molecules) is increased", and opposes the "cohesive forces" of the solid state. The result is a continuous spectrum. Sharp lines of "molecular vibrations", caused by "intramolecular forces (chemical "affinity") can only be detected (as Lommel concludes) when the "cohesion" has disappeared, i.e. when the body has become gaseous. Both kinds of vibrations are propagated as waves through the aether, which fills all space and also flows freely around the molecules of bodies" (Lommel 1871, p. 41, as cited in Kangro, 1976). It is assumed by him "that the elastic force, which sustains the vibrations of an aether atom, is proportional to the distance of the atom from its equilibrium position" (elongation) (Lommel 1871, p. 41-42, as cited in Kangro, 1976). (p. 28).

Lommel…(as cited in Kangro, 1976, p. 29) felt that "vis viva" increases continuously with time and derived an equation comprised of vibrations at the "aether" and proper vibrations of the atom. Michelson looked at the problem a few years later (Kangro, 1976) and was stimulated to treat the matter hypothetically in which he stated:

> Absolute continuity of the spectra emitted by solid bodies can only be explained by the complete irregularity of the vibrations of their atoms. Hence the distribution of radiation energy with respect to individual vibrations must be undertaken by means of probability calculations (p. 30).

Michelson subsequently derived an equation that produced an energy distribution curve (Kangro 1976, p. 33-34). As pointed out in Kangro (1976), it was Planck who, thirteen years later, also arrived at a statistical deduction of the radiation law. This will be discussed in the ensuing pages.

At this point, it should serve well to discuss the status of the existing radiation theories near the end of the 19th century. Kangro (1976) does an excellent job in reviewing the various attempts to explain the spectral distributions, mostly geared to classical treatments.

Another excellent source may be found in Whittaker (1989, Chapter XII). The following will be to outline how far the complications surrounding the attempts to solve the blackbody radiation and how all classical attempts failed.

When bodies are heated, they emit radiant energy. The quality, as will be shown later, along with the quantity of this emission, depends exclusively on the temperature. It should also be mentioned that the radiation only occurs in solids and in some cases, liquids.

Following a description of how the energy distribution e_λ varies with λT (λ = wavelength and T = temperature) as given by Richtmyer & Kennard (1947, p. 158-159) the relationship

$$\frac{e_\lambda}{T^5} = f(\lambda T) \tag{29}$$

is shown in Fig. 50 below.

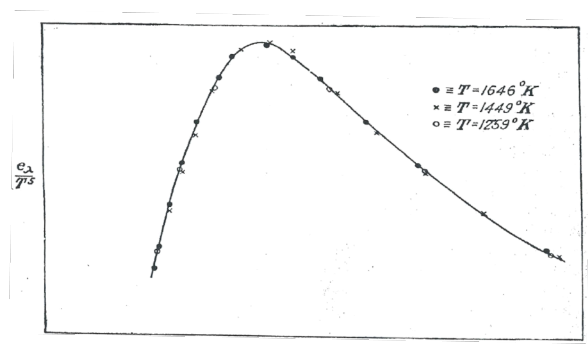

Fig. 50 Experimental Verification of the Blackbody Displacement Law From Eq. (29)

$$e_\lambda = T^5 f(\lambda T) = (\lambda T)^5 \frac{f(\lambda T)}{\lambda^5} \tag{30}$$

we can write

$$e_\lambda = \frac{1}{\lambda^5} F(\lambda T) \tag{31}$$

where

$$F(\lambda T) = (\lambda T)^5 f(\lambda T) \tag{32}$$

We may define the *monochromatic emissive* power, e_λ at any given wavelength λ by saying that the radiant energy emitted in the spectral range λ to λ + dλ, per unit area per unit time, is given by $e_\lambda d\lambda$. The total emissive power, *E*, is given by:

$$E = \int_0^\infty e_\lambda d\lambda \tag{33}$$

According to Whittaker (1989),

> At the end of the nineteenth century, the theory of radiation was in a most unsatisfactory state. For the energy per cm^3 of pure-temperature of blackbody radiation, in the range of wavelengths from λ to λ + dλ, two different formulae had been proposed. Firstly, that of Wien, (1896, p. 667) $E = C\lambda^{-5}e^{-bl\lambda T}d\lambda$. Where λ is wavelength, *T* is absolute temperature, and *b* and C are constants. This formula is asymptotically correct in the region of short waves (more precisely, when λT is small); but is irreconcilable with the observational results for long waves. Secondly, that of Rayleigh (1900, p. 539-540) $E = 8\pi kT\lambda^{-4}d\lambda$. Where *k* is Boltzmann's constant; which, as shown by the experiments is asymptotically correct for the long waves but is inapplicable at the other end of the spectrum. What was wanted was a formula, which for the extreme limits λ→0 and λ→∞ would tend asymptotically to Wien's (1896) and Rayleigh's (1900) formulae respectively, and which would agree with the experimental values over the whole range of wavelengths (p. 78).

There are other attempts to produce a formula (see Whittaker 1989, p. 28) empirically which was of the form $E = CT^{5-\mu}\lambda^{-\mu}e^{-bl(\lambda T)^{v}}$. Which for μ = 5, ν = 1, gives Wien's law, and for μ = 4, ν = 1, *b* = 0, gives Rayleigh's. The correct law was first given by Planck in a communication, which was read on 19 October 19th, 1900 before the German Physical Society (Planck, 1900a, p. 202-204).

All subsequent investigations for determining the spectral distribution in radiation employs Planck's (1900) formula, thus it behooves one to elaborate on some of its intricate details. The notation of the following equations use the form from Siegel & Howell (1992), henceforth designated as S/H since many of the figures to be shown will be using their representation. Planck's spectral distribution is given in Eq. 34.

$$e_{\lambda b}(\lambda T) = \pi i_{\lambda b}(\lambda, T) = \frac{2\pi c_1}{\lambda^5(e^{c_2/\lambda T}-1)} \tag{34}$$

(From Eq. 2.11 in S/H (1992))

The constants to be employed are shown in Table 24.

Symbol	Definition	Value
C_1	Constant in Planck's spectral energy (or intensity) distribution	$0.59552197x10^{8}W\cdot\frac{\mu m^4}{m^2.sr}$ $0.59551297x10^{-16}W\cdot\frac{m^2}{sr}$
C_2	Constant in Planck's spectral energy (or intensity) distribution	$14{,}387.69\ \mu m\cdot k$ $0.01438769\ m\cdot K$
C_3	Constant in Wien's displacement law	$2897.756\ \mu m\cdot K$ $0.002897756\ m\cdot K$

Table 24
Radiation Constants

The mks system will be used in the ensuing calculations, where:
C_1 is defined as $2\pi hc^2{}_0$
$C_2 = hc_0/k$
where *h* is Planck's constant
$h = 6.6260755x10^{-34}J\cdot s$
k is the Boltzmann constant
$k = 1.30658x10^{-23}J/K$

Depending on the type of investigation Eq. 34 may also be represented in terms of frequency as shown as Eq. 35

$$e_{\lambda b}(\lambda)d\lambda = \frac{2\pi C_1 d\lambda}{\lambda^5\left(e^{\frac{C_2}{\lambda T}}-1\right)} = \frac{-2\pi C_1 v^3 dv}{c_0^4\left(e^{\frac{C_{2v}}{C_0 T}}-1\right)} = -e_{vb}(v)dv \tag{35}$$

(From Eq. 2.12 in S/H (1992))

The quantity $e_{vb}(v)$ is the emissive power in vacuum *per unit frequency interval* about *v*. The intensity is

$$i'_{vb}(v) = e_{vb}(v)/\pi$$

so that

$$i'_{vb}(v) = \frac{2C_1 v^3}{c_0^4(e^{c\frac{2v}{CoT}}-1)} = \frac{2hv^3}{c_0^2(e^{h\frac{v}{kT}}-1)} \tag{36}$$

(From Eq. 2.13 in S/H (1992))

Most modern day analyses use the wavenumber, which eliminates the need for using the speed of light, c_0. The wavenumber η = 1/λ is the number of waves per unit length. Then and $d\lambda = -\ (1/\eta\hat{}2)\ d\eta$ and

$$e_{\lambda b}(\lambda)d\lambda = -\frac{2\pi C_1\eta^3 d\eta}{e^{\frac{c_2\eta}{T}}-1} = -e_{\eta b}(\eta)d\eta \tag{37}$$

(From Eq. 2.14 in S/H (1992))

The quantity $e_{\eta b}(\eta)$ is the emissive power *per unit wavenumber interval* about η. The intensity is

$$i'_{\eta b}(\eta) = \frac{e_{\eta b}(\eta)}{\pi} = \frac{2C_1\eta^3}{e^{\frac{C_2\eta}{T}}-1} \quad (38)$$

(From Eq. 2.15 in S/H (1992))

As shown in the figure from Richtmyer and Kennard, Planck's equation can be put into a form that eliminates the need for a separate curve for each Temperature, *T*. Dividing by the fifth power of *T* yields

$$\frac{e_{\lambda b}(\lambda,T)}{T^5} = \frac{\pi i'_{\lambda b}(\lambda,T)}{T^5} = \frac{2\pi C_1}{(\lambda T)^5(e^{\frac{C_2}{\lambda T}}-1)} \quad (39)$$

(From Eq. 2.16 in S/H (1992))

Eq. 39 can also be placed in a more universal form in terms of the variable $\eta/T = (1/\lambda T)$,

$$\frac{i'_{\eta b}(\eta,T)}{T^3} = \frac{2C_1\left(\frac{\eta}{T}\right)^3}{e^{C_2(\frac{\eta}{T})}-1} \quad (40)$$

(From Eq. 2.17 in S/H (1992))

The foregoing has been a brief review of the various forms used in analyzing blackbody radiation. It now remains to carry out an analysis wherein Boscovich's (1922) ideas will be enlisted to produce empirical results that compare with the acceptable results using Planck as the standard.

When we observe a heated piece of metal, it will begin to glow dull red, then orange, brilliant yellow and finally white. This constitutes what is referred to as a continuous emission spectrum, which is governed by Kirchhoff's law of radiation (Kirchhoff, 1882, p. 572-573), which states that the ratio of emissivity absorptivity is the same for all bodies at the same temperature. If we state Kirchhoff's law in terms of absorptivity, *A*, and emissivity, *E*, then from Richtmyer & Kennard (1947)

> *Absorptivity* – In general, radiation falling upon a surface is partly absorbed, partly reflected, and, unless the body is very thick or very opaque, partly transmitted. We shall define the absorptivity of a surface, symbol *A*, as the fraction of the radiant energy, incident on the surface, which is absorbed.
> Absorptivity is (1) a pure numeric, (2) for any actual body, less than unity, and (3) varies greatly with wavelength of the incident radiation and, to a lesser extent, with the temperature of the absorber.
> A surface whose absorptivity is unity for all wavelengths is called an "ideal" black surface. No such surface actually occurs in nature, but some bodies, such as black velvet or lampblack, reflect only a very small fraction of the incident radiation. It will be seen presently that in the theory of radiation a special interest attaches to the ideal black surface or body.
> A very simple relation exists between the absorptivity of a surface and its total emissive power, *E*. Suppose that two surfaces have total emissive powers E_1 and E_2 and absorptivities A_1 and A_2, respectively. By considering the thermal equilibrium of such surfaces when present in an isothermal enclosure, as described in the next section, it can be shown that necessarily
>
> $$\frac{E_2}{E_1} = \frac{A_2}{A_1}$$
>
> If, in particular, we make A_1=1 that the first surface is black, E_1 has obviously the maximum value that is possible at a given temperature; for A_1 in the last equation cannot exceed unity. Thus, no surface can emit more strongly than a blackbody. If E_0 is the total emissive power of a blackbody and *E* the total emissive power of any other body whose absorptivity is *A,* we find from the last equation that $E = AE_0$
> These conclusions are known as "Kirchhoff's Law" and have all been confirmed by experiment. The same relations have been shown to hold for each wavelength separately (p. 142-143).

In essence, if the absorbance is high, the emittance is also high. At this point one might ask how do Boscovich's (1922) ideas play a role in analyzing this thermal spectrum. It is well known that Kirchhoff assumed that the radiation spectrum is independent at the internal of surface structure of a body and depends only on the temperature.

On searching the literature, one finds that most applications of Kirchhoff's law refers to his cavity interpretation where a body that absorbs all incident radiation, i.e. *A* = 1 is called "Black" since such a body shows high absorptivity.

This concept of blackbody radiation described by Kirchhoff is the result of his experiment in which he used a cavity whose walls had been heated to a uniform temperature. The resulting radiation field inside the cavity consisted of reflected energy as well as the original emission from the walls. A small wafer having a perfect black surface introduced into the cavity is allowed to come to thermal equilibrium with the walls. Thus, it is assumed that using a small hole in the enclosure, any radiation escaping would be indicative to that emitted from a "blackbody".

In effect, this might be called a "simulation". This concept is addressed by d'Abro (1932), Kirchhoff's law establishes several important points. It shows that, for a given temperature of the enclosure, the composition of the imprisoned equilibrium radiation is exactly the same regardless of the nature of the matter present. The only restriction imposed is the one previously stated; namely, the matter must be susceptible of admitting at least some radiation of each conceivable frequency. It can also be shown that the shape and size of the enclosure does not affect the results. To submit to experimental measurement, the intensities of the various monochromatic radiations, we perforate one of the walls with a pin. Some of the radiation streams out and may be analyzed by suitable instruments. We assume that the loss of radiation through the pinhole is too small to affect the conditions within the enclosure, and hence that the sample analyzed gives the correct composition of the equilibrium radiation.

As we have mentioned earlier, the equilibrium radiation for any given temperature of the enclosure is exactly the same as the blackbody radiation that would be emitted by a perfect black body at the same temperature. The reason for the equivalence is easily understood. Any radiation, which falls on the opening in the wall, passes into the enclosure, is reflected from wall to wall and does not emerge again. To all intents and purposes the radiation is totally absorbed, just as it would be to fall on a perfect blackbody. The advantages of substituting the heated enclosure for a blackbody are numerous. In the first place, we have said that no perfectly black body can be found, whereas the heated enclosure simulates this ideal existent. In the second place, the enclosure is more easily maintained at a stated temperature than is a piece of soot. Finally, since the radiation in the enclosure is a manifestation of an equilibrium condition rather than of an individual process, we may to a larger extent ignore the mechanism by which the radiation is emitted from the matter and yet submit the problem of its composition to theoretical treatment (p. 449-450).

Experimental Results

Before we consider the derivation of the correct law of equilibrium radiation by means of theoretical arguments, let us examine the general results established by experiment. An enclosure was heated to one temperature or another, and the radiation streaming from the aperture was analyzed. Experimenters found that the intensity, i_v, of the radiation of frequency, v, was not affected by the shape of the enclosure or by the material of which the enclosure was made; the intensity was found to depend solely on the frequency, v, and on the temperature, T, of the enclosure. This dependency is expressed mathematically by the equation

(1) $i_v = F(v, T)$,

Where $F(v,T)$ is some unknown function of the frequency and of the temperature. To obtain the empirical law of equilibrium radiation we should have to determine the exact form of this function from direct measurements of intensity, frequency, and temperature. However, for reasons, which will now be explained, the law of radiation was not discovered in this way. Human measurements being necessarily imperfect, the measurements performed by different experimenters (or by the same experimenter at different times) do not usually agree: slight discrepancies may be expected. As a result, slightly different forms are suggested for the same empirical law; and we cannot be certain that any one of the laws suggested is rigorously correct. As a result, the different experimenters suggested different more or less complicated radiation laws and were unable to agree on a correct form of the function $F(v,T)$ in (1).

Chronologically, Eq. (1) should read $i_\lambda = F(\lambda_2 T)$. It was Planck who was the first to use the form given by Eq. (1). Garber pointed this out by stating, "Planck was the first theorist to develop his expressions in functions of the frequency, v, rather than the wavelength. However, in his derivation of Wien's law, he worked in Wien's terms and used the wavelength" (1976, p. 97).

Brush (1999) also speaks of a simulation, stating:

> It is recognized that it is necessary to do experiments with perfect "blackbodies" simulated by a cavity (Hohlraum) maintained at a definite temperature, from which radiation was allowed to emerge through a small hole. The derivation from "blackness" increases with the size of the hole relative to the size of the cavity (p. 521).

Ackermann (1989) addressed substantiation for the idea of simulation.

> An experimentalist may wish to measure a certain phenomenon, so that progress involves turning the first phenomenon into the second so it can be measured. It may be that one piece of apparatus designed to produce the phenomenon being measured can only be placed where one would like to place the only apparatus that can apparently measure the phenomenon. In a dizzying variety of such variations, experimentalists must permute and

> adjust what is available in order to simulate what is desired (p. 188).

The idea of simulating the radiation from a solid body was very successful in the predictions of Planck whose mathematical development led to the modern concept of Quantum Mechanics. Since such experiments as those used by Kirchhoff, did not exist in Boscovich's time, one is tempted to ask, how can his ideas be used to describe this type of radiation.

We can be assured that Boscovich and those of his time did observe a solid when heated to become incandescent and display the various colors mentioned earlier. An important point to be made here is that the words "solid" and "luminous" are used. When one looks at Kirchhoff's experiments, we see that what is observed is a "surface" phenomenon, which says nothing about the interior of the body that is radiating. This takes us back to the earlier statements of Kangro (1976, p. 28), in which he refers to Lommel's observation in which he discusses the "vis viva" of solid body intermolecular vibrations.

Now, since thermal radiation is emitted normally only by solids and in a few cases liquids, it would behoove us to investigate how the interior of the body contributes to what one observes on the surface. Perhaps an appropriate place to begin is to discuss what the situation was that led up to the mathematical treatment of the radiation distribution laws. Kangro (1976) mentions Tyndall's work where Tyndall considers heat to be made of motion. A brief view of Kangro (1976) states that

> Tyndall talked of "calorific intensity", "calorific power", "effect", or simply of "radiation" or "heat". In 1865, he used the term "energy" for the "potential" and "dynamical" energy when dealing with motion. Only when considering the conversion of mechanical energy into "some other form", he said, "that energy, we shall afterward learn, is heat" (p. 8).

Kangro (1976) continues his remarks on Tyndall with, "There appears to be a definite rate of vibration for all solid bodies having the same temperature, at which the *vis viva* of their atoms is a maximum" (p. 9). Following Tyndall, Kangro (1976) selected the works of Lommel along with the work of Michelson. Lommel's idea of heating a solid body where its "vis viva" is increased has been mentioned earlier in this work.

We then go to some of the ideas generated by Michelson (1888). Michelson, in his mathematical treatment hypothesizes as follows; "Absolute continuity of the spectra emitted by solid bodies can only be explained by the complete irregularity of the vibrations of their atoms" (1888, p. 426). Hence the distribution of radiation energy with respect to individual vibrations must be undertaken by means of probability calculations. He disregards the grouping of atoms as molecules in a solid body. Each atom vibrates about an equilibrium position, which is controlled by the surrounding atoms. In this region he supposes "that each atom moves freely in the interior of a spherical elastic shell of infinitely small radius p" Michelson (1888, p. 426).

The two most significant features of Lommel (1881) and Michelson (1888) is that they both used solids and their resulting equations used the wavelength, λ, which having the dimension of length will prove to be important later. While Planck used the frequency, v, in his interpretation, he nevertheless developed his ideas from Wien in conjunction with Michelson. Kangro (1976) spells this out by stating that Planck's quantum theory was due to the work of Michelson. He concludes that,

> The work of Wien, as shown above, is revealed only as a late development of Michelson's original ideas, cannot be doubted. The work of Planck in its turn appears as a direct continuation and extension of the work of Wien and Michelson. When we consider the researches of Planck, we cannot but conclude that the theory of light quanta is a child of the statistical method of molecular optics, a method, the general idea of which was first explicitly applied by Michelson in this field. Planck's merit consequently consists in the further elaboration and realization of this idea.
>
> In fact, Planck quotes the work of Wilhelm Wien in connection with the development of his radiation theory, and the latter quotes Michelson's memoir. Indeed, Michelson, in deriving his law of energy distribution invokes in addition an article by Lommel. These facts provide a critical problem in the history of science. No matter how we trace backwards from the work of Planck or of Wien and consider the pertinent investigations on which subsequent advance were made, Michelson's ideas also are to be connected with the development, the results of which Michelson himself encountered (p. 35).

At this point it is deemed feasible to now return to Boscovich and determine how his ideas may be employed in another classical approach to explain blackbody radiation.

Before attempting this, another viewpoint regarding the theoretical aspects of Kirchhoff's (1901) research in the interpretation of blackbody radiation has appeared and is discussed in several published papers. As mentioned or implied earlier, when the absorption A=1, Kirchhoff (1901) assumed that the radiation emitted by a body did not depend on its internal structure, but only on temperature. Recent investigations have shown that this is not really true.

According to Robitaille (2006),

> Through the formulation of his law of thermal emission, Kirchhoff conferred upon blackbody radiation the quality of universality. Consequently, modern physics holds that such radiation is independent of the nature and shape of emitting object. Recently, Kirchhoff's experimental work and theoretical conclusions have been reconsidered. In this work, Einstein's derivation of the Planckian relation is reexamined. It is demonstrated that claims of universality in blackbody radiation are invalid (p. 22).

This work and subsequent publications by Robitaille (2008a) arose from a publication by Schirrmacher (2001), in which he discussed the question regarding the legitimacy of Kirchhoff's experiment and it's resulting justification for Planck's radiation formula. Since Planck's analysis and subsequent equation for blackbody radiation is linked to the assumed universality of Kirchhoff's formulation and if Kirchhoff's proof of universality is invalid, then this carries over to Planck's analysis.

Schirrmacher (2001) declares,

> That Kirchhoff's law was a necessary prerequisite for Max Planck's finding of the proper radiation formulas widely accepted, although not much attention was paid to the relation of their respective histories in particular of justification. Simply speaking, it is the relation between the proof of the existence of a solution and the specification of the correct formula (p. 2).

Robitaille (2003 & 2008a) sums it up by stating,

> Since the days of Kirchhoff, blackbody radiation has been considered to be a universal process, independent of the nature and shape of the emitter. Nonetheless, in promoting this concept, Kirchhoff did require, at the minimum, thermal equilibrium with an enclosure. Recently, the author stated that blackbody radiation is not universal and has called for a return to Stewart's law. In this work, a historical analysis of thermal radiation is presented. It is demonstrated that soot, or lampblack, was the standard for blackbody experiments throughout the 1800's. Furthermore, graphite and carbon black continue to play a central role in the construction of blackbody cavities.
>
> Finally, Planck's treatment of Kirchhoff's law is examined in detail and the shortcomings of his derivation are outlined. It is shown, once again, that universality does not exist. Only Stewart's law of thermal emission, not Kirchhoff's, is fully valid (p. 36).

Robitaille (2008a) follows this up with a statement that Planck's equation is not being disputed in any way. The accuracy of this equation along with its merit has been established beyond question. Stewart's (1858) law states that when an object is analyzed in thermal equilibrium, its absorption is equal to its emission. This leads to the idea that the emissive power of an object depends on its temperature, its nature, and on the frequency of the observation. According to Stewart (1861), radiation is not a surface phenomenon, but takes place throughout the interior of the radiating body leading to the fact that the radiative and absorptive powers of that body must be equal.

Stewart (1863) states,

> I first endeavored to show, not only as a simple deduction from the theory of exchanges, but also as a result of experiments, that in a field of uniform temperature the absorption of a plate or particle is equal to its radiation. Now, since a thick plate absorbs more heat than a thin one, it will also radiate more, so that here we are once led to acknowledge a radiation proceeding from the interior of bodies as well as one of their surfaces.
>
> Assuming it therefore as proved that the radiation of a particle or plate is independent of its distance from the surface, the proof of the law which asserts "that absorption is equal to radiation, and that for every description of heat," may for convenience sake be carried into the interior of the body, by which means we are able to rid ourselves of surface reflexion. Let us therefore suppose that in the interior, a stream of radiant heat is constantly flowing past a particle *A* in the direction of the next particle *B*. Now, since radiation is independent of distance from the surface, the radiation of *A* is equal to that of *B*; and since absorption is equal to radiation, the absorption of *A* is therefore equal to that of *B*. Again, as the stream of radiant heat passes *A*, part of it will be absorbed by *A*; but since the radiation of *A* is equal to its absorption, this stream will be as much recruited by the one as it is diminished by the other, so that when it has passed *A* it will be found unaltered by its passage with regard to quantity.

> Of this heat it has already been shown that *B* absorbs as much as *A*; and in order that this may be the case, the *quality* as well as the *quantity* of the heat which impinges upon *B* must be the same as those of the heat which impinged upon *A*. For, suppose that the heat, by passing *A*, had changed its quality, though not its quantity, and that it had been transformed into a description of heat scarcely absorbed at all by the substance in question; then the absorption of *B* would manifestly be less than that of *A*, and this we have already shown cannot be the case. We conclude therefore that the stream of heat, in passing *A*, has neither altered its quantity nor its quality, and hence we argue that radiation is equal to absorption, and that for every description of heat.
> This is the whole proof; and I am quite at a loss to know in what respect it is deficient, especially since Kirchhoff has not definitely stated his objections (p. 354-356).

This quote from Stewart, while rather lengthy, is deemed necessary since it serves as a prelude to how such an idea may have significance in a Boscovichian approach to "blackbody" or more inclusive "thermal radiation". Stewart's law in plain terms may be expressed as what occurs in the inside (interior) of a body is what is observed on the outside (surface) of that body. Of course it is assumed that this is a solid body.

Returning to Lommel's comment on the increase at vis viva (energy) upon heating of a solid body (as cited in Kangro, 1976, p. 28), and Michelson's (1888) experimental results for the spectra of a solid seems like an appropriate place to start using Boscovich's ideas coupled with Stewart's claim of radiation from both the interior and exterior of a body.

First, one should consider what happens to the physical characteristics of a body when heated. The most general effect upon being heated is a change in the bulk of a solid. In most cases there is an increase in the size, with both an area and volume expansion. The surface to volume ratio is not linear and each has its own thermal expansion coefficient.

We now proceed to Boscovich (1922) who, in the *Theoria*, mentions the relationship between the surface, which gives the shape of a body, and the volume subsequently depending upon the shape.

> 376. For there are an infinite number of continuous curved surfaces, in which nevertheless all the points of any mass lie; nay, further, there are an infinite number of curved lines passing through all the points. Therefore, we can only mentally conceive a certain surface which shall include all the points or exclude a few of them which are more remote by gathering the rest together; this can be done by a kind of moral assessment, but not by an accurate geometrical construction. This surface gives the shape of the body; and with that idea, all that relates to the different kinds of shapes is in agreement in my Theory with the usual theory of the continual extension of matter.
> 377. Volume depends upon shape; and volume is nothing else but the whole of the space, extended in length, breadth, and depth, which is included by the external surface. Further, unless we picture that surface which I mentioned as determining the shape, there can be no definite idea of volume. Nay indeed, if we think of the tortuous surface in which all the points lie, we shall never have a volume possessed of a third dimension; whilst if we think of a curved line passing through all the points, no volume will be obtained that has even two dimensions. But in that the usual idea is also wanting, as regards indefinite assessment, owing to those empty interstices that are present in all bodies, and the roughness, as we have said, which arises from the indeterminateness of figure. Here again, if an outside surface is conceived as bounding the figure, all those things that are usually enunciated about volume in relation to figure agree in my theory with those of all others; for instance, that the same volume as regards magnitude can be bound by surfaces that are quite different, both in shape and size, and that the least surface of all having the same volume is that of a sphere. Also, that in similar figures, the volumes are in the triplicate ratio of homologous sides, the surfaces in the duplicate ration; and upon these depend a truly great number of phenomena, and especially those, which are connected with the resistance of both fluids and of solids.
> 378. The mass of a body is the total quantity of matter pertaining to that body; and in my Theory, this is precisely the same thing as the number of points that go to form the body. Here now we have certain indefiniteness, or at least the greatest difficulty, in forming a definite idea of mass; and that, not only in my theory, but in the usual theory as well, on account of the addition of words *points that go to form the body;* this excludes heterogeneous substances (notes 376-378).

Here Boscovich (1922) has outlined his curved lines of limit points and the areas they contain may be extended to the curved surfaces and the contents of the solids, which can be imagined to be his points. These points, subsequently when heat (vis viva) is applied may oscillate about their respective limit points.

We now go to another interpretation of Planck's formula for blackbody radiation. Stachel (1998) discuss Einstein's dilemma regarding Planck's laws.

Einstein (as cited in Stachel, 1998) mentions two possible objections to his proposed theory of a quantum gas. As applied to blackbody radiation, Planck's formula for the density of blackbody radiation, is given below as Eq. 41

$$e(v,T) = \frac{8\pi h v^3}{c^3[\exp(hv/kT)-1]} \tag{41}$$

may be split into two factors, each of which is related to one of the two objections:

(1) The first objection is related to the already-mentioned matter-radiation analogy, which Einstein notes is not universally accepted. (He may well have had Bohr in mind, which refused to countenance the light quantum hypothesis. It is related to the factor $8\pi v^2/c^2$, which Bose showed can be interpreted as the number of cells in the phase space of a gas of light quanta, treated as particles.

(2) The second objection is to the method of counting equiprobably cases for a quantum gas, massless or massive (1998, p. 232-233).

"The statistical method applied by Bose and myself is by no means indubitable, but on the contrary only appears to be justified *a posteriori* by its success in the case of radiation" (Einstein 1925, p. 18 as cited in Stachel, 1998, p. 232-233).

It is related to the factor $hv/[\exp\left(\frac{hv}{kT}\right)-1]$, which Bose interprets as the average energy per cell when a light quantum gas is in thermal equilibrium. Its value depends on the method of counting equiprobable distributions of light quanta among the cells. From this count, one computes the probability, W, and hence (using Boltzmann's principle) the entropy, S, of the state of a gas, which is then maximized to determine the thermal equilibrium state.

By examining the role of these two issues in Einstein's work between 1901-1909, we may hope to understand why he did not develop the idea of a quantum gas; his ready acceptance and quick application of the idea of massive particles after Bose developed it for light quanta; and why he felt much still remained obscure about the reasons for the idea's success.

"$8\pi v^2/c^3 V dv$ can be interpreted as the number of elementary cells of the six-dimensional phase space for the [light] quanta" (Bose, 1924, p. 384 as cited in Stachel, 1998, p. 232-233). Here, V is the volume of the cavity.

Letting $p(v) = \frac{8\pi v^2 dv}{c^3}$

Converting frequency into wavelengths (since $v = c/\lambda$), the number becomes $8\pi/\lambda^4$ per unit volume.

Then, $$p(\lambda) = 8\pi \frac{d\lambda}{\lambda^4}\frac{hv}{e^{hv/kT}-1} \tag{42}$$

(From Richtmyer & Kennard, 1947, p. 178).

This is the value of $\psi\lambda d\lambda$, the energy density belonging to the range $d\lambda$. Let us substitute in it $v = \frac{c}{\lambda}$, c being the speed of light in vacuum. Thus, we obtain, as Planck's new radiation law, in terms of λ.

$$\psi_\lambda = \frac{8\pi ch}{\lambda^5}\frac{1}{e^{ch/\lambda kT}-1} \tag{43}$$

Returning to the Siegel & Howell representation of this equation, it may be rewritten as,

$$e_{\lambda b}(\lambda T) = \pi i'_{\lambda b}(\lambda, T) = \frac{2\pi C_1}{\lambda^5(e^{\frac{C_2}{\lambda T}}-1)} \tag{34}$$

(From Eq. 2.11 in S/H (1992))

Dividing by the fifth power of the temperature, T, yields Eq. 44 given below:

$$\frac{e_{\lambda b}(\lambda,T)}{T^5} = \frac{\pi i'_{\lambda b}}{T^5} = \frac{2\pi C_1}{(\lambda T)^5\left(e^{\frac{C_2}{\lambda T}}-1\right)} = \frac{2\pi C_1}{(\lambda T)^4}\left[\frac{1}{\lambda T}\left(\frac{1}{e^{\frac{C_2}{\lambda T}}-1}\right)\right] = \frac{2\pi C_1}{(\lambda T)^4}[F(\lambda T)] \tag{44}$$

This equation gives the quantity $e_{\lambda b}(\lambda,T)/T^5$ in terms of the single variable, λT

Plotting $F(\lambda T)$ produced the following graph, Fig. 51.

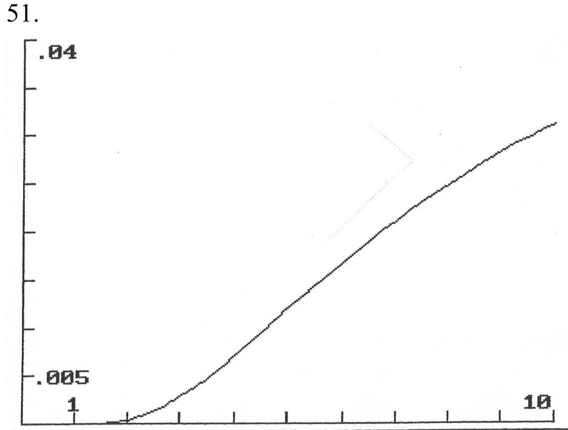

Fig. 51
Horizontal axis: λT (λ in microns)
Vertical axis: $F(\lambda T)$

The function $F(\lambda T)$ as seen in Fig. 51 is now given another interpretation, slightly different from that where Einstein mentions Bose's ideas. Returning to the remarks concerning the change in bulk when a solid is heated, there is both a surface and volume expansion whose change in area and volume may be calculated knowing the coefficient of linear expansion.

This coefficient of expansion need not be considered per se here, but one can think that the size of the body "grows". In other words, one can consider $F(\lambda T)$ as a "growth curve". The concept of such a curve had its beginning in a paper by Gompertz (1825). Winsor (1932) states that in addition to actuaries, various investigators have used the Gompertz curve as a growth curve in such areas as biology, botany and even economics (p. 1). Following Winsor (1932), the curve is generally written in the form,

$$y = ke^{-6a-bx} \tag{45}$$

In which k and b are essentially positive quantities. From Eq. 45, it is clear that as x becomes negatively infinite, y will approach zero, and as becomes positively infinite y will approach k. Differentiating Eq. 45, we have

$$\frac{dy}{dx} = kbe^{a-bx}e^{-e^{a-bx}} = bye^{a-bx} \tag{46}$$

A graphical description of the Gompertz curve is shown in Fig. 52 along with another growth curve called Logistic. We will only be concerned with the Gompertz curve.

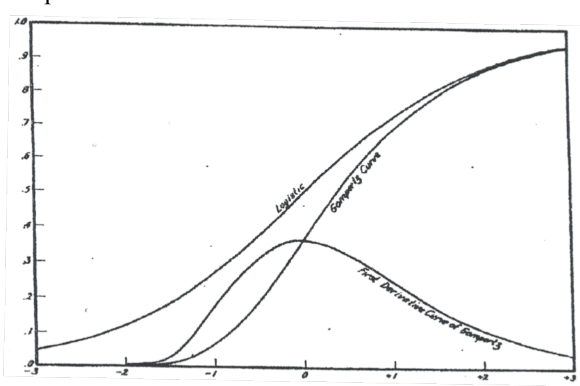

Fig. 52 (Fig. 1 from Winsor, 1932)

Fig. 1 shows the form of the curve for the case $k = 1$, $a = 0$, $b = 1$. There are also shown the logistic and the first derivative of the Gompertz curve.
Equations:
Gompertz: $y = e^{-e^{-x}}$
Logistic: $y = \frac{1}{1+e^{-x}}$

The mathematical properties of the Gompertz Logistic curves are given below,

PROPERTY	GOMPERTZ	LOGISTIC
Equation	$y = ke^{-e^{a-bx}}$	$y = \frac{k}{1+e^{a-bx}}$
Number of constants	3	3
Asymptotes	$\begin{cases} y = 0 \\ y = k \end{cases}$	$\begin{cases} y = 0 \\ y = k \end{cases}$
Inflection	$\begin{cases} x = \frac{a}{b} \\ y = \frac{k}{e} \end{cases}$	$\begin{cases} x = \frac{a}{b} \\ y = \frac{k}{2} \end{cases}$
Straight line form of equation	$\log \log \frac{k}{y} = a - bx$	$\log \frac{k-y}{y} = a - bx$
Symmetry	Assymetrical	Symmetrical about inflection
Growth rate	$\frac{dy}{dx} = bye^{a-bx} = by \log \frac{k}{y}$	$\frac{dy}{dx} = \frac{b}{k} y(k-y)$
Maximum growth rate	$\frac{bk}{e}$	$\frac{bk}{4}$
Relative growth rate as function of time	$\frac{1}{y}\frac{dy}{dx} = be^{a-bx}$	$\frac{1}{y}\frac{dy}{dx} = \frac{b}{1+e^{-a+bx}}$
Relative growth rate as function of size	$\frac{1}{y}\frac{dy}{dx} = b(\log k - \log y)$	$\frac{1}{y}\frac{dy}{dx} = \frac{b}{k}(k-y)$

The following group of graphs represents the various properties of the Gompertz curve and is given below. The curves are from a work given by Medawar (1945b).

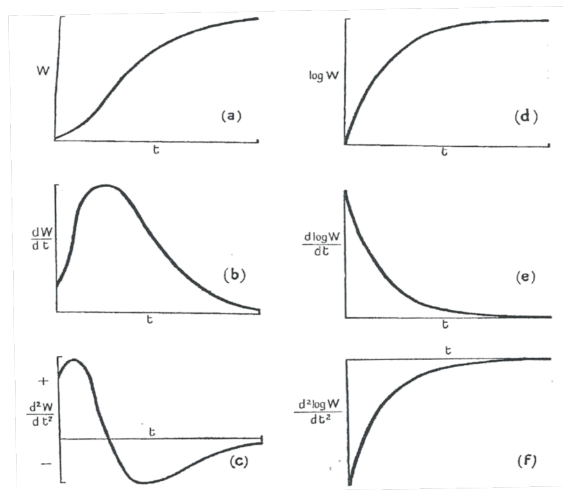

Text-Fig. I. (a) The curve of the growth; (b) of growth-rate; (c) of acceleration; (d) the curve of specific growth; (e) of specific growth-rate; (f) of specific acceleration. The curves have been plotted from an equation for the Gompertz function, but the scales of the ordinates have been so adjusted as to make the height of each graph uniform.

(Fig. I from Medawar, 1945b, p.162).

At this point it is deemed critical to introduce another feature of the Gompertz curve, which involves senescence. This term will be seen to have very important implications later. It was Thornley (1976) who in his book, *Mathematical Models of Plant Physiology,* produced the Gompertz curve shown in Fig. 53 below.

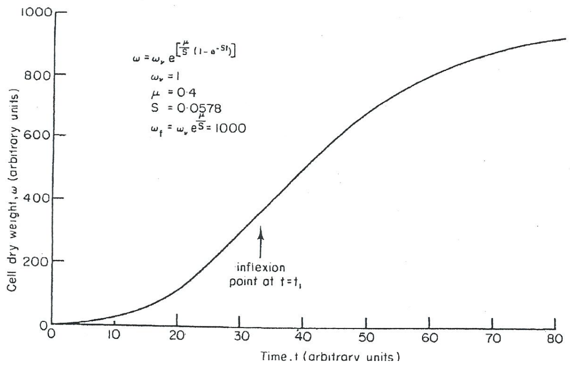

Fig. 53 (From Thornley, 1976, p. 203).

The equation shown on the graph along with the associated parameters can be seen to agree in form with that of Winsor. The interesting feature of these parameters is the term S = 0.578, where *S* is the senescence term. Senescence is defined as the progressive loss of an ability to grow. It can be found that this term may also be applied to biology and even chemistry. Thornley's treatment is not without its peer. It was Richards (1969) who used the Winsor form prescribed as

$W = Ae^{-be-kt}$

Now equation Richards and Thornley:

Richards	**Thornley**
A	$W_0 e^{\mu}/s$
b	μ/s
μ	s

For Thornley, assume:

$W_0 = 1$

$\mu = 0.4$

$s = 0.0578$

Then, for Richards, using Thornley's values, produced the following curve:

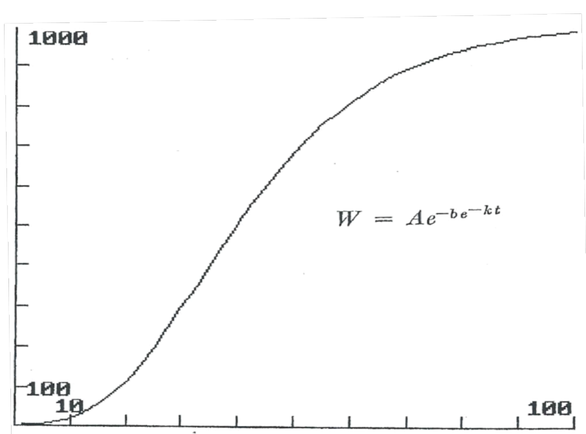

Fig. 54
Time, *t*, arbitrary units

t	W
0	1
10	20.862
20	114.694
30	298.399
40	510.228
50	689.388
60	816.185
70	897.275
80	946.245
90	974.88
100	991.323

Table 25

The curve shown in Fig. 54 is an exact duplicate of Thornley's curve with the tabulated values given in Table 25. We now may return to the assimilated curve for growth depicted in Fig. 51, shown as $F(\lambda T) vs \lambda T$. The numerical values are shown in Table 26.

λT	$F(\lambda T)$
1	.000001
2	.000376
3	.002778
4	.007046
5	.011927
6	.016668
7	.02098
8	.024802
9	.028159
10	.031102

Table 26

Based on Thornley's (1976) concept of a senescence function *S,* senescence "function" was created to produce the same curve values for $F(\lambda T)$.
It is given by:

$$\frac{k_1}{k_2 \cos\left(\frac{k_3}{x+k_4}\right)} \tag{47}$$

Using the senescence "function" in a nonlinear regressive analysis produced the following formula, which produces a curve exactly as $F(\lambda T)$ and is referred to as $F_c(\lambda T)$.

$$F_c(\lambda T) = \frac{k_5 e^{\left(-e^{\left(\frac{k_6}{x}\right)}\right)}}{e^{\left(\frac{k_1}{k_2 cos\left(\frac{k_3}{x+k_4}\right)} x\right)}} \tag{48}$$

Where:
$x = \lambda T$
$k_1 = 0.8490$
$k_2 = 0.1164$
$k_3 = 2.097$
$k_4 = 6.898$
$k_5 = 0.189$
$k_6 = 0.0037$

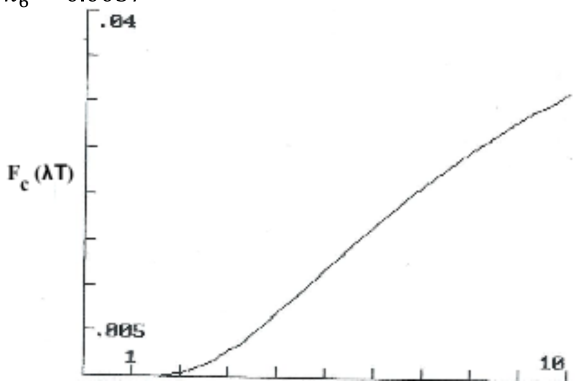

Fig. 55 (calculated using Eq. 48)

The values for $F_c(\lambda T) vs \lambda T$ are shown in Table 27. Note that their values are almost exactly as those shown in Table 26 for $F(\lambda T)$.

λT	$F_c(\lambda T)$
1	.000001
2	.000375
3	.002759
4	.007016
5	.011914
6	.016693
7	.02105
8	.024912
9	.0283
10	.031267

Table 27

Following Medawar's (1945b) representation of his growth curve rate and acceleration in terms of $F(\lambda T)$, $F'(\lambda T)$ (derivative) and $F''(\lambda T)$ (second derivative), similar descriptions are shown in Fig. 56.

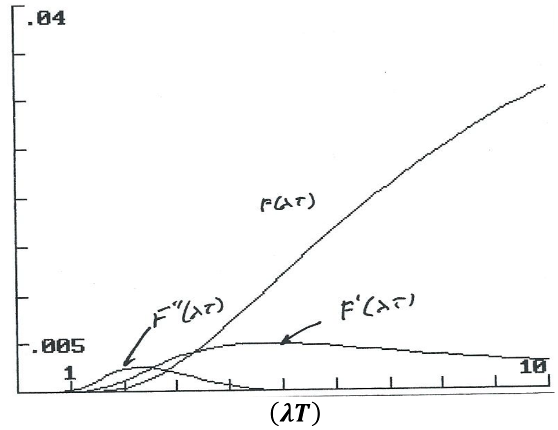

Fig. 56

It should be noted that $F''(\lambda T) = 0.00$ at $\lambda T = 4.66$ and $F'(\lambda T) = 0.25F(\lambda T)$ at $\lambda T = 4.66$ it should be. The reasons for this will be explained later.

At this point we return to the aforementioned situation concerning the asymmetrical growth in the surface area and volume of a solid when it is heated. The senescence function $F(\lambda T)$ will determine its growth. Now we must decide the relationship of growths in the surface area and volume.

Referring to the discussion concerning the spectral series, Fig. 2 from Gill (1941) showed the "allowed" and "forbidden" orbits, which corresponded to the alternate points of cohesion and non-cohesion, produced logarithmic (equilateral) spirals. Now it can be shown that with adjustment at certain parameters, the spiral approaches an ellipse (Andronov et al, 1966). Recalling that the number of intercepts, which correspond to the alternate points of cohesion and non-cohesion, was based on the Fibonacci numbers. From Table 6, the difference of the Fibonacci numbers for $U_{40} - U_{39} = 39{,}088{,}170$ intercepts. Going to $U_{100} - U_{99}$ produce approximately $3.3x10^{21}$ intercepts, which yields a width of approximately $3.3x10^{-20}$ arbitrary units. Such a small interval might be considered to be a solid.

From Fig. 21 (Fig. 6 from (Martinovic, 1988)), the whole surface of a system of confocal spheroids was shown along with limits of cohesion and non-cohesion. This allows one to now consider this as a solid and thereby determine its surface area and volume. As an aside, mention should be made concerning the volume and area in the growth of logarithmic coiled seashells. Raup and Graus (1972) discussed Mosely and his attempts to derive expressions for the volume and surface areas that were applicable to both planispiral and conispiral shells. These ideas were adopted and advanced by

Illert (1982) in which he emphasized the repetitive macroscopic to microscopic shell growth. He states,

> The biological requirement that shelly structures must exist in a three-dimensional space is shown to be a sufficiently powerful mathematical constraint to ensure the existence of geometrical artifacts, which can, perhaps, be likened to the conservation laws, pseudoforces, and fields of classical physics (p. 21).

With these ideas in mind, it is now time to investigate whether or not such ideas can be carried over analogously to the so-called "blackbody" radiation. First, we address the idea of a surface area in a microscopic sense, of a heated solid. Since we are dealing with ellipsoids, then as a first approximation (the surface area of an ellipsoid cannot be calculated in closed form) using an ellipsoid created by revolution about the x-axis as shown in Fig. 57 along with the associated parameters. Eq. 49 gives the area, S_x.

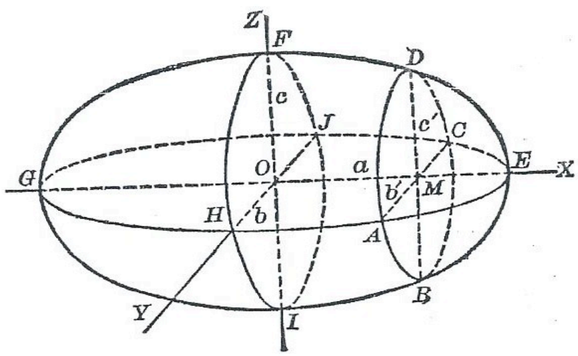

Fig. 57

Ellipsoidal surface $S_x = 2\pi b^2 + \frac{2\pi ab}{e}$ arc sin e,

where e = eccentricity = $a\frac{\sqrt{a^2-b^2}}{a}$ (49)

Ellipse: $\frac{x^2}{\phi^2} + \frac{y^2}{1} = 1, e^2 = -\phi', a = \pm\phi, b = 1,$

$\phi = \frac{1+\sqrt{5}}{2}, \phi = \frac{1-\sqrt{3}}{2}$ e = eccentricity

Given:

$\phi = -0.618$

$e = \sqrt{-\phi} = 0.786131378$

$\sin^{-1} e = 0.904556$ (e in radians)

$a = \phi, b = 1$

Yielding: $s_x = 17.98079743$

We find: $\frac{s_x}{ln\phi} = 37.38057413$

Comparing this with $2\pi C_1 = 3.7417606$, which differs from $\frac{s_x}{ln\phi}$ by a factor of 10. Putting in the units for C_1 from Table 24 yields $2\pi C_1 = 3.7417606x10^8 \frac{W\mu m^4}{m^2.5v}$, which differs from $\frac{s_x}{ln\phi}$ by less than 0.01%.

Continuing the analogy of a solid and hypothetical shell forms, it has been shown by Illert (1983) that it is not easy. The equations by Moseley were modified and general expressions were derived, however due to the fact that in the shell formation the outside grows at a faster rate than the inside. Thus, while the use of an equilateral spiral is deemed necessary in all the calculations, Illert (1983) asserts that,

> …A basic distinction must be made between the biological factors, which control shell form, and the resultant geometrical characteristics of that shell form. Given the relative details of calcium carbonate, the fact that the resultant shell shape closely approaches certain vigorous geometrical models is not an indication that shell growth is governed by the mathematical equations involved; one must strongly emphasize it is merely an inevitable result of the mode of growth of the animal concerned.
>
> To expediently facilitate synthesis of a general theory of spiral shell form, we shall not exclude the possibility that the details of microscopic processes becomes whatever necessity dictates in order for macroscopic principles of form and organization to obtain their appropriate expression.
>
> What is needed is a mathematical demonstration that seashell geometries appear in our physical world merely as variation manifestations of a large-scale organizing principle of nature (p. 25).

The foregoing treatment of shell volume and surface structure was used primarily to show that there have been efforts to construct models to systematically describe growth.

Thus, while the functions developed using the growth form $F(\lambda T)$ and the surface area of an ellipsoid, differed from the conventional Planckian form, it was conjectured that the aforementioned entities might be used to predict the emissive characteristics of a "blackbody".

The following equation, Eq. 50, was employed to compute the spectral distribution of emissive power.

$$\frac{e_{\lambda b}(\lambda,T)}{T^5} = \frac{Bk_5 e^{\left(-e^{\left(\frac{k_6}{x}\right)}\right)}}{x^4 e^{\left(\frac{k_1}{k_2\cos\left(\frac{k_3}{x+k_4}\right)x}\right)}} \quad (50)$$

Where:

$x = \lambda T$
B = 3.73805741 x 10^{18}
k_1 = 849.0
k_2 = 0.1164
k_3 = 7097.0
k_4 = 6898.0
k_5 = 0.189
k_6 = 3.7
These values were used to compare with Planck's calculations shown in Siegel & Howell (1992, p. 26). The Planck calculations used (Siegel and Howell, 1992 p. 25)

$$\frac{e_{\lambda b}(\lambda,T)}{T^5} = \frac{\pi'_{\lambda b}(\lambda,T)}{T^5} = \frac{2\pi C_1}{(\pi T)^5 (e^{\frac{C_2}{\lambda T}}-1)} \qquad (51)$$

(From Eq. 2.16 in S/H (1992))

$2\pi C_1 = 3.74177489x10^{21}$
$C_2 = 14{,}387.69$
$\frac{e_{\lambda b}(\lambda,T)}{T^5}, \frac{W}{(m^2 \cdot K^5 \cdot \mu m)}$ (in units of 10^{-13})

λT	Planck	This work
500	.000038	.000038
1000	2.11146	2.12025
1500	33.6502	33.6828
2000	87.9036	87.5359
2500	121.719	120.871
3000	128.305	127.346
3500	118.75	117.964
4000	102.973	102.443
4500	86.4142	86.1112
5000	71.3974	71.2593
5500	58.6328	58.6013
6000	48.1167	48.148
6500	39.5805	39.6449
7000	32.6927	32.7716
8000	22.6552	22.7346
9000	16.0575	16.1237
10000	11.6367	11.6879
11000	8.60925	8.64776
12000	6.49081	6.5194
13000	4.97787	4.99902
14000	3.87675	3.89242
15000	3.06137	3.07302
16000	2.44797	2.45668
17000	1.97982	1.98637
18000	1.61781	1.62276
19000	1.33448	1.33824
20000	1.11027	1.11315

Table 28

In general, the percentage differences in Table 28 ranges from 0.0 to less than 1%. A comparison of Eq. 50 and Planck is shown in Fig. 58 below: (Open circles represent this work)

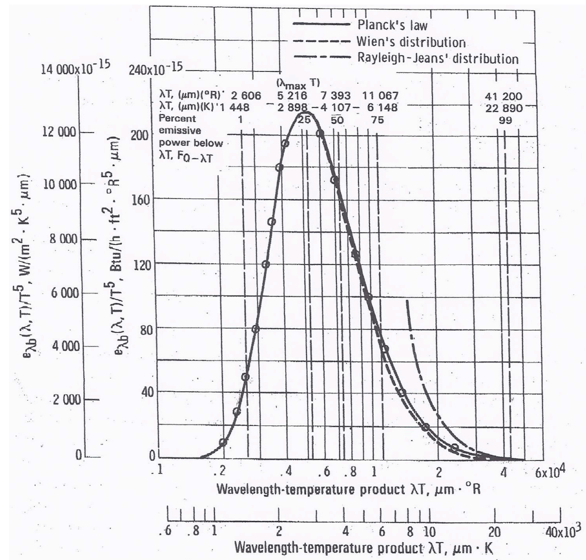

Fig. 58 (Fig. 5 from (S/H, 1992))
Spectral distribution of blackbody hemispherical emissive power as a function of λT.
Calculated using Eq. 50

Using Wein's displacement laws:

Planck = $\frac{e_{\lambda b}(\lambda,T)}{T^5}$ max = 128.67 x 10^{-13}
This work = 127.71 x 10^{-13}
% Difference = 0.75%

A calculation was also made of the wave number divided by the temperature given in the universal form for Planck's equation by variable η/T ($=1/\lambda T$)

$$\frac{i'_{\eta b}(\eta,T)}{T^3} = \frac{2C_1(\frac{\eta}{T})}{e^{C_2(\frac{\eta}{T})}-1} \qquad (52)$$

Where C_1 from Table 24 was used. Eq. 53, shown below gives, the equation used to duplicate this quality.

$$\frac{i'_{\eta b}(\eta,T)}{T^3} = \frac{G x^2 e^{-e^{(m_4 x)}}}{e^{\left(\frac{m_1 x}{\cos\left(\frac{m_2}{\frac{1}{x}+m_3}\right)}\right)}} \qquad (53)$$

Where:
G = 2.248837 x 10^9
m_1 = 7293.8
m_2 = 7079.0
m_3 = 6898.0
m_4 = 3.7

A comparison of Eq. 53 with Planck is shown in Table 29

$\frac{\eta}{T}$	$\frac{i'_{\eta b}(\eta,T)}{T^3}$ Eq. 53	$\frac{i'_{\eta b}(\eta,T)}{T^3}$ Planck
.00001	.076896	.07697
.00002	.285655	.285769
.00003	.596115	.59578
.00004	.98132	.979738
.00005	1.4173	1.41364
.00006	1.88301	1.87664
.00007	2.36024	2.3509
.00008	2.83362	2.82139
.00009	3.2904	3.27575
.0001	3.72038	3.70407
.0002	5.67063	5.68163
.0003	4.32044	4.35091
.0004	2.40465	2.42152
.0005	1.11454	1.11922
.0006	.45811	.458524
.0007	.173003	.172701
.0008	.061362	.061151
.0009	.020741	.020654
.001	.006749	.006721

Table 29

$$\frac{i'_{\eta b}(n,T)}{T^3} = \frac{2C_1(\frac{\eta}{T})}{e^{C_2(\frac{\eta}{T})} - 1}$$

A comparison of the calculated values of Intensity $\frac{i'_{\eta b}(\eta,T)}{T^3}, \frac{W \cdot \mu m}{(m^2 \cdot K^3 \cdot sr)}$. For this work and that of Planck is displayed graphically on Fig. 54

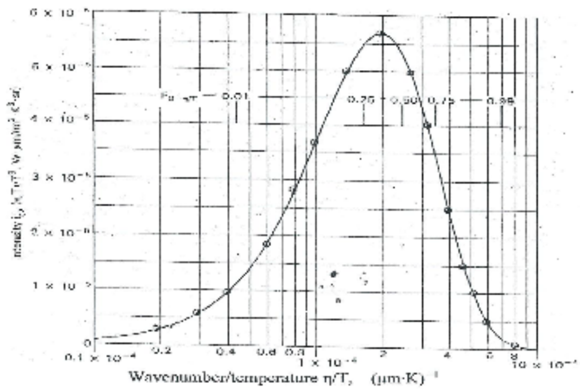

Fig. 54 Spectral distribution of blackbody intensity as a function of η/T

○ Calculated using Eq. 53
− Calculated using Planck's Eq. 52

Returning to Eq. 53 and Planck's Eq. 52, it should be pointed out that Eq. 53 resulted from analyzing the spectra resulting not only from the exterior surface, but also from the interior volume of a solid, while Planck's Eq. 52 was determined from Kirchhoff's surface interpretation of "blackbody" radiation.

Using the two relationships to determine the energy curves commonly referred to as "spectral distribution of emissive power", we have Planck and this work Eq. 54 below:

$$e_{\lambda b}(\lambda, T) = \pi i'_{\lambda b}(\lambda, T) = \frac{2\pi C_1}{\lambda^5(e^{\frac{C_2}{\lambda T}}-1)} \qquad \text{(34) Planck}$$

(From Eq. 2.11 in S/H (1992))

$$e_{\lambda b}(\lambda, T) = \frac{GTn_5 e^{\left(-e^{\left(\frac{n_6}{xT}\right)}\right)}}{x^4 e^{\left(\frac{n_1}{n_2 \cos\left(\frac{n_3}{xT+n_4}\right)xT}\right)}}$$

This work:
G = 3.26900 x 105
T = degrees Kelvin/1000
$n_1 = 0.8490$
$n_2 = 0.1164$
$n_3 = 7.097$
$n_4 = 6.898$
$n_5 = 0.189$
$n_6 = 0.0037$
$x = \lambda$

Note that the parameters for this growth function differ in magnitude from the original growth function. This is due to the fact that the spectral distribution is directly proportional to the temperature, *T*. In effect this may be stated as using Eq. 54

$$e_{\lambda b}(\lambda, T) = \frac{T}{\lambda^4} F(\lambda T) \quad (54)$$

Eq. 54 agrees with Rayleigh (1900) and Jean's (1994) formula for long wavelengths, while also agreeing with Planck's formula for shorter wavelengths, which are consistent with Wien's formula. A comparison for the calculated values of the energy curves and experimental data is shown in Fig. 60. The calculated values using Eq. 54 are shown in dark circles.

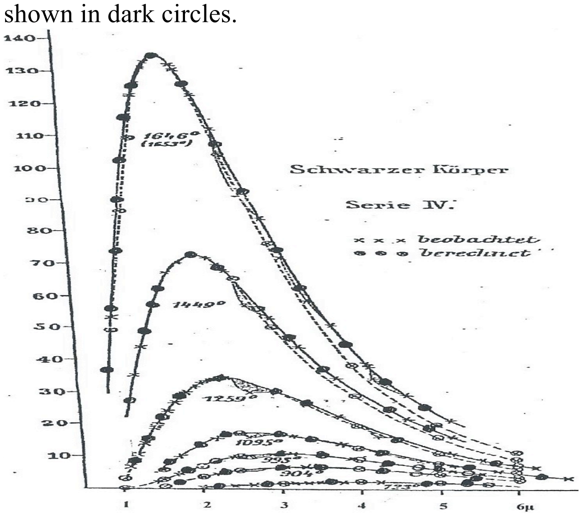

Fig. 60 (Fig. 27 from Kangro, 1976)
Energy curves (Lummer & Pringsheim, 1899, p. 217 (as cited in Kangro, 1976). The hatched depressions originate from absorption by water vapor and carbon dioxide in the air.
Calculated using Eq. 54

A comparison of the experimental data of Coblentz (1916) observations and calculated values using Eq. 54 is shown in Fig. 61 below:

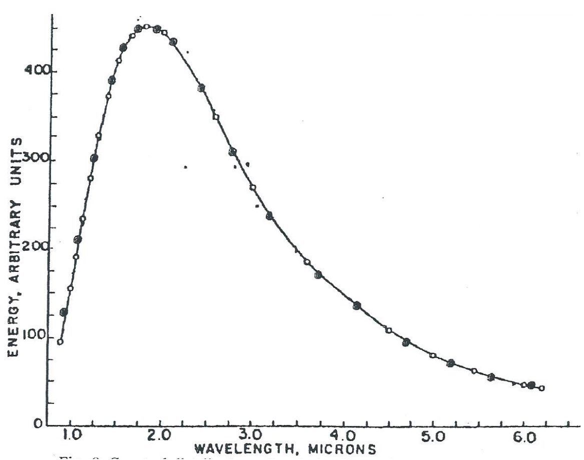

Fig. 61 Spectral distribution of radiation from a blackbody at 1596°K
Coblentz's (1916) observations
Calculated from Eq. 54

To continue further into the classical approach to "blackbody" radiation, it is very important to mention the work of Rubens & Kurlbaum (1901), whose experiments in the long-wave isochromatics served as the beginning of the quantum theory. It was this work that was instrumental in Planck's *Guess* (Pais, 1982). Planck subsequently developed a scientific theory, which was the precursor of Einstein's further development concerning his heuristic approach to his light quantum hypothesis (Pais, 1982).

The following figures from Rubens and Kurlbaum's (1901) work is taken from Kangro (1976), "These curves represent the residual ray isochromatics for fluorspar (24μ with consideration of 31.6μ), rock-salt (51.2μ) and quartz (8.5μ) which Rubens and Kurlbaum published on 10 February 1901" (p. 204 & 206).

The graphs represent Intensity vs. Degrees Centigrade (°C). Indicated in these curves are calculations using formulae from Wien, Lord Raleigh, Planck and Thiesen where Thiesen:

$$E = C \cdot \frac{1}{\lambda^5} \cdot \sqrt{\lambda T} \cdot e^{\frac{c}{\lambda T}}$$

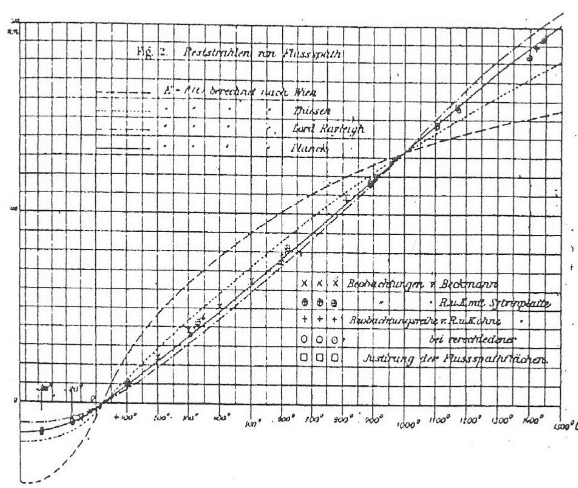

λ = 24.0μ and 31.6μ
Fig. 62 Isochromatics (for p. 203) (Fig. 2 from (Rubens & Kurlbaum, 1901, p. 659-660))

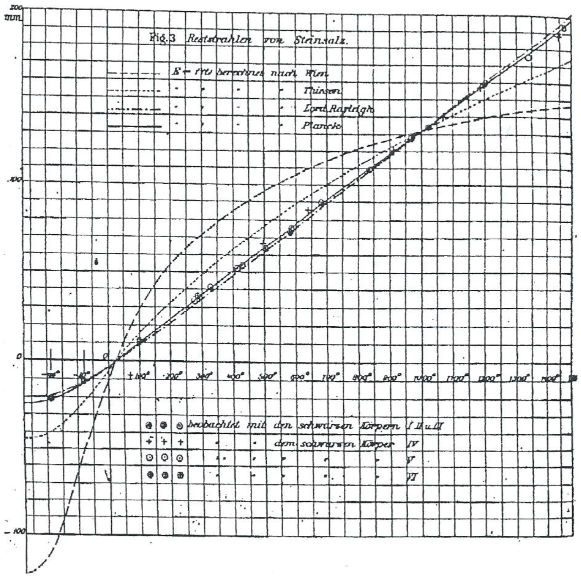

λ = 51.2*μ*
Fig. 63 Isochromatics (for p. 203) (Fig. 3 from (Rubens & Kurlbaum, 1901, p. 659-660))

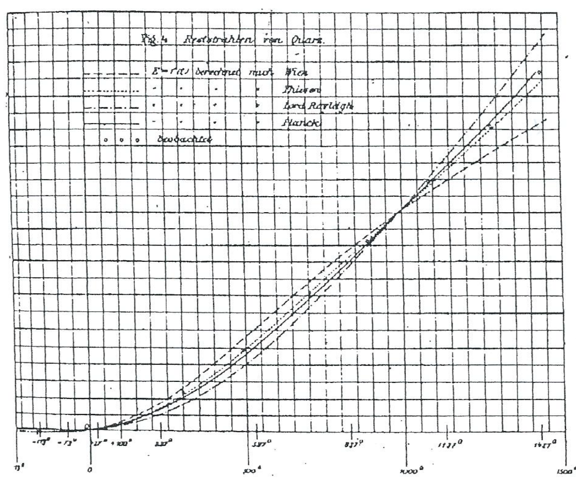

λ = 8.85*μ*
Fig. 64 Isochromatics (for p. 203) (Fig. 4 from (Rubens & Kurlbaum, 1901, p. 661))

A comparison of the Rubens and Kurlbaum (1901) experimental results and calculated spectral distributions using Eq. 54 are shown in Figs. 62-64.

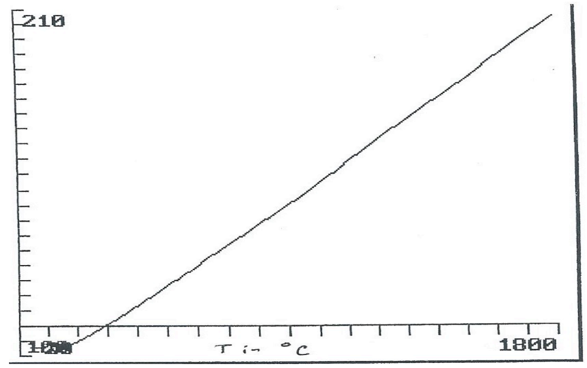

λ = 24.0*μ* and 31.6*μ*
Fig. 62 Calculated Isochromatics

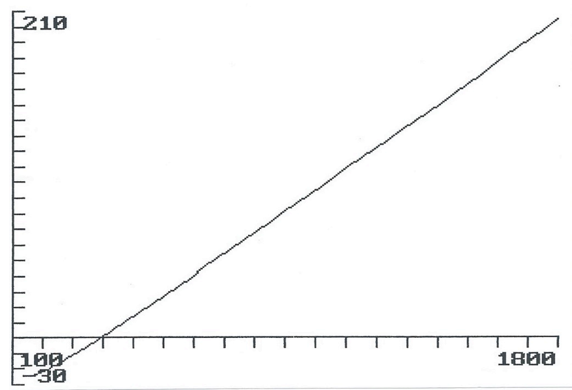

T in °C
λ = 51.2*μ*
Fig. 63 Calculated Isochromatics

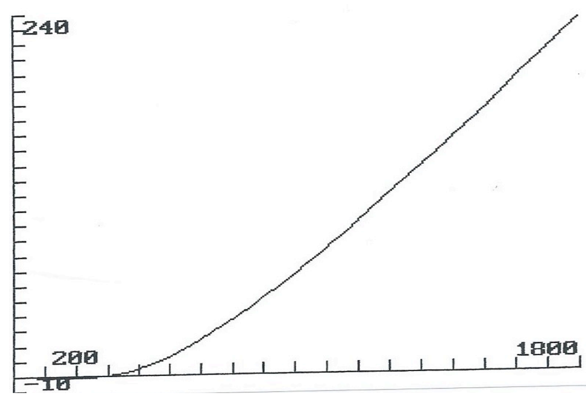

T in °C
λ = 8.85*μ*
Fig. 64 Calculated Isochromatics

The results of the Rubens and Kurlbaum (1899) curves are presented in tabular form in Tables 30-32. Table 30 is given below

Temp in C-Grade n, *t*	Absolute Temperature, *T*	*E* beob	*E* nach Wein	*E* nach Thiesen	*E* nach Rayleigh	*E* nach Lummer n. Jahke	*E* nach Plancke	Galconi	This work
-273	0	---	-42.4	-20.7	-10.7	-17.8	-15.4	-----	-----
-188	85	-15.5	-41.0	-20.2	-10.5	-17.5	-15	-14.4	-14.9
-80	193	-9.4	-26.8	-14.0	-7.4	-11.5	-9.3	-10.0	-9.73
+20	293	0	0	0	0	0	0	0	0
+250	524	+30.3	+50.6	+25.3	+25.3	+30.0	+28.8	+30.2	+28.48
+500	773	+64.	+88.9	+58.3	+58.3	+64.5	+62.5	+64.7	+62.0

		3							
+750	1023	+98.3	+114.5	+94.4	+94.4	+98	+96.7	+98.6	+97.0
+1000	1273	+132	+132	+132	+132	+132	+132	+132	+132.0
+1250	1523	+167	+145	+174.5	+174.5	+167	+167.5	+164.9	+167.3
+1500	1773	+201.5	+155	+209	+209	+201	+202	+147.5	+202.7
+ ∞	∞	-----	+226	+ ∞	+ ∞	+ ∞	+ ∞	+ ∞	+ ∞

λ = 24.0*μ* and 31.6*μ*
Table 30 (Tabelle I from (Rubens & Kurlbaum, 1902)

Temp in C-Graden, *t*	Absolute Temp, *T*	*E* beob	*E* nach Wein	*E* nach Thiesen	*E* nach Rayleigh	*E* nach Lummer n. Jahke	*E* nach Plancke	Galconi	This work
-278	0	-----	-121.5	-44	-20	-27	- 3.8	-----	-----
-188	85	-20.6	-107.5	-40	-19	-24.5	-21.9	-26.5	-22.6
-80	193	-11.8	-48.0	-21.5	-11.5	-13.5	-12.0	- 4.1	-12.3
+20	293	0	0	0	0	0	0	0	0
+250	523	+31.0	+63.5	+40.5	+28.5	+31	+30.4	+32.1	+30.2
+500	773	+64.5	+96	+77	+62.5	+65.5	+63.8	+65.6	+63.9
+750	1023	+98.1	+118	+106	+97	+99	+97.2	+99.1	+97.9
+1000	1273	+132	+132	+132	+132	+132	+132	+132.0	+132.0
+1250	1523	+164.5	+141	+154	+167	+165.5	+166	+164.6	+166.1
+1500	1773	+196.8	+147.5	+175	+202	+198	+200	+197.2	+200.3
+ ∞	∞	-----	+194	+ ∞	+ ∞	+ ∞	+ ∞	+ ∞	+ ∞

λ = 51.2*μ*
Table 31 (Tabelle II from (Rubens & Kurlbaum, 1902)

Temp in C-Graden, *t*	Absolute Temp, *T*	*E* beob	*E* nach Wein	*E* nach Thiesen	*E* nach Rayleigh	*E* nach Lummer n. Jahke	*E* nach Plancke	Galconi	This work
-273	0	----	-1.96	-1.40	-1.00	-1.53	-1.41	----	----
-173	100	-1.6	-1.96	-1.40	-1.00	-1.53	-1.41	-1.2	-1.33
-73	200	-1.5	-1.82	-1.30	-0.92	-1.42	-1.31	-1.1	-1.23
+27	300	----	+0.10	+0.12	+0.10	+0.18	+0.1	----	+0.18
+100	373	+3.4	+4.07	+3.06	+2.21	+3.5	+3.0	+3.0	-----
+227	500	+13.5	+16.5	+12.61	+9.60	+13.5	+12.4	+12.3	+12.44
+527	800	+53.5	+60.5	+53.4	+44.8	+53.2	+50.3	+57.2	+50.57
+827	1100	+102	+107.0	+102.3	+96.7	+102	+99.8	+101.2	+100.6
+1000	1273	+132	+132	+132	+132	+132	+132	+132.0	+132.0
+1127	1400	+154	+147.7	+154.6	+160	+154	+154.6	+154.9	+155.8
+1427	1700	+212.5	+182.3	+206.5	+229	+210	+213.5	+209.4	+213.7

Reststrahlen von Quarz. λ = 8.85*μ*
Table 32 (Tabelle III from (Rubens & Kurlbaum, 1902)

The preceding tables of Rubens & Kurlbaum (1902) also show the results from Lummer & Jahnke (1900) using their formula given by:

$$E = C.\lambda^{-\mu}T^{0-\mu}.e^{-\frac{c}{\lambda T'}}$$

Another set of calculations in the table is from Galgani (1982) using his formula for the energy density given by:

$$g(v,T) = \frac{8\pi}{c^3}v^2\frac{hv + kT}{e^x}$$

where

$$x = \frac{hv}{kT}$$

as a classical analog to Planck's law

$$f(v,T) = \frac{8\pi}{c^3}v^2\frac{hv}{e^x - 1}$$

As can be seen in the forgoing tables, the calculations of this work, in which a classical approach based on Boscovich's ideas, compared rather favorably with the experimental data of Rubens & Kurlbaum (1902). Before we leave the discussion of "blackbody" radiation, mention should be made about Kangro (1976) in which he comments on

Lummer & Pringsheim's *Non-validity of Wien-Planck spectral equation*.

Not only the trend of the c_2 values, in respect of which the authors originally noticed deviation from the radiation law, but also even the curvature produced by the isochromatics gave evidence of the new statement. It is seen that "the quantity $c[= c_2]$ in the Wien-Planck equation should not be treated as a natural constant" (Lummer and Pringsheim, 1900, p. 172 as cited in Kangro, 1976). The correctness of this statement, which is forged on Planck's emphasis on natural constants, cannot be gainsaid!

The numerical values for the derivations in the "constant" c_2 are depicted in Kangro (1901, p. 166-168) and Rubens & Kurlbaum (1901, p. 650) who, in order to reproduce their observations, were forced to assign variable values for this "constant" in their equations.

The aforementioned comment by Kangro concerning c_2 as not being a "natural constant" leads one to consider whether or not it is worthwhile to carry out an analysis using the growth form generated by using the senescence function which was used in both the discrete spectra of thermal radiation. There is a possibility that such use might play a role in resolving this paradox. Such an investigation remains to be seen and might be undertaken in the near future.

We now come to another set of microscopic phenomena that presently requires quantum theoretical treatment. These are namely, Einstein's theory of the photoelectric effect and the specific heats of solids (p. 194-196)

It is well known that these theoretic treatments along with Planck's concepts of "blackbody" radiation were the three most important ideas in the first decade of the twentieth century. In Fig. 65, we see the experimental data along with the calculations by Einstein (1906b, 180-190) and Debye (1912).

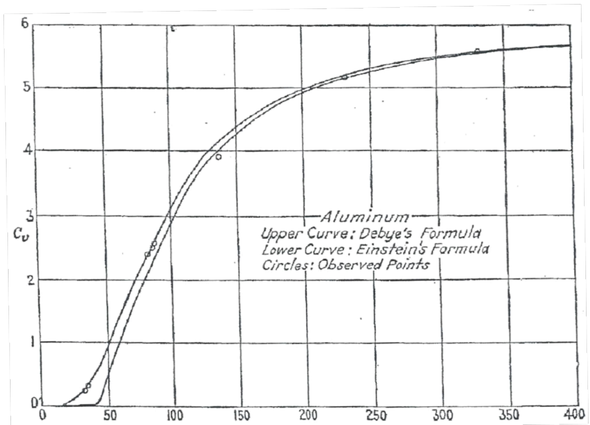

Fig. 65 (Fig. 133 from Richtmyer & Kennard, 1947, p. 437)
Comparison of Specific Heat Formulas with Experiment

It should be noted that these curves have the same asymmetrical shape as the Gompertz curve. Now, since both Einstein (1906b) and Debye (1912) used the analysis from Planck and his radiation formula in their theoretical analysis, it is possible that a similar type investigation using the growth form technique might be applicable in predicting specific heat.

Looking at the experimental data and calculated curve for the photoelectric effect, it is somewhat amazing how much of it resembles the first derivative of the Gompertz growth curve shown in Fig. 1b from Medawar (1945a).

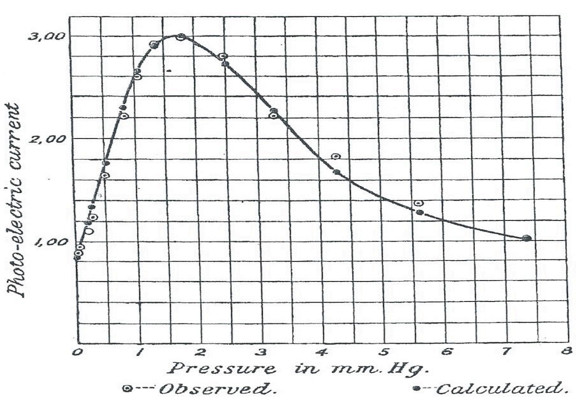

Fig. 66 (Fig. 27 from Allen, 1925, p. 67)

It is also astonishing how its shape is almost identical to the spectral radiation distribution of Coblentz (1913). The similarities depicted by the specific heat and photoelectric effect stipulates that an analysis using the results of this work create an incentive to engage in a future study. Thus far, the emphasis on the use of Boscovich's curve has been to analyze and calculate microscopic phenomena. It is now time to investigate phenomena in the macroscopic region.

While it is tempting to explore the physical states of matter, it would be very cumbersome at this time to consider the other states of matter, such as liquids and gases. The molecular structure of solids such as metals, ionic crystals, etc., would take us too far afield at this point. The possibility is that such an investigation will be left for the future.

It should be mentioned that Stoiljkovic (2011) touched upon this concept, where he discussed the chemical and physical interactions of molecules, charged colloidal particles, clay particles, macromolecules, and nano-particles. To some extent, the foregoing can be considered as macroscopic, however, in keeping with the empirical interpretation of the Boscovich curve, another extended curve of Boscovich is now analyzed to predict gravitational forces within the solar system and beyond to the cosmos.

In Fig. 14 of the *Theoria*, Boscovich (1922), shown in Fig. 67 below, discusses his curve thusly,

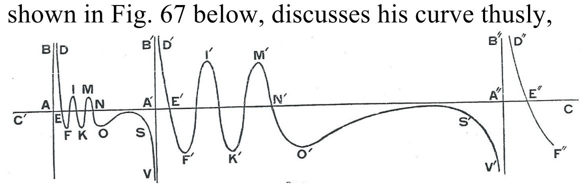

Fig. 67

> 171. If, in Fig. 14, there are any number of segments AA′, A′, A′A′′, of which each that follows is great with regard to the one that precedes it; & if through each point there passes an asymptote, such as AB, A′B′, A″B″, perpendicular to the axis; then between any two of these asymptotes there may be curves of the form given in Fig. 1. These are represented in Fig. 14 by DEFI &c., D′E′F′I′ &c.; and in these the first arm E would be asymptotic and repulsive, and the last SV attractive. In each the interval EN, where the arc of the curve is winding, is exceedingly small compared with the interval near S, where the arc for a very long time continues closely approximating to the form of the hyperbola having its ordinates in the inverse ratio of the squares of the distances; and then, either goes off straightway into an asymptotic and attractive arm, or once more winds about the axis until it becomes an asymptotic attractive arc of this kind, the area corresponding to either asymptotic arc being infinite. In such a case, if a number of points are assembled between any pair of asymptotes, or between any number of pairs you please, and correctly arranged, there can,

so to speak, arise from them any number of universes, each of them being similar to the other, or dissimilar, according as the arcs EF…. N, E´F´…. N´ are similar to one another, or dissimilar; and this too in such a way that no one of them has any communication with any other, since indeed no point can possibly move out of the space included between these two arcs, one repulsive and the other attractive; and such that all the universes of smaller dimensions taken together would act merely as a single point compared with the next greater universe, which would consist of little point-masses, so to speak, of the same kind compared with itself, that is to say, every dimension of each of them, compared with that universe and with respect to the distances to which each can attain within it, would be practically nothing. From this it would also follow that any one of these universes would not be appreciably influenced in any way by the motions and forces of that greater universe; but in any given time, however great, the whole inferior universe would experience forces, from any point of matter placed without itself, that approach as near as possible to equal and parallel forces; these therefore would have no influence on its relative internal state (note 171).

From Boscovich's Fig. 14 curve, we can observe Newton's inverse squares representation flowing into portions of the regions SV and S´V´. It is this region of interest that will be discussed. Graves (1971) made an interesting comment concerning Boscovich and the possibility of a unified field interpretation, where he speaks of Boscovich's field of force.

> It is this "substantialization of force", which is one essential requirement for the notion of a field. In field theory, a particle interacts directly (i.e. by spatio-temporal contiguity) with the field at the point where it is located, and only indirectly with any possible sources of that field. For Boscovich seems, in fact, to be creating a trichotomy of space, matter (identified with the point inertial masses), and force. While it is true that mass and force appear to be proportional, they are different sorts of entities, and Boscovich would certainly want to keep inertial and gravitational masses as separate concepts only accidentally related. Inertial mass is localized at the center of force, but gravitational mass really extends throughout space. But most important of all, insofar as Boscovich may be said to have a field of theory, it is a *unified* field theory. There is no multiplicity of forces surrounding the central mass and exerting independent influences on any test particles elsewhere in space, but only one. Although the total force-function may include many terms, they are all functions of r, which may be simply added together, i.e., $F = \sum_i f_i(r)r$. This force, F, will then affect all bodies in the same way, depending (presumably only) on their respective inertial masses. Boscovich's vision is certainly admirable. Its main weakness is that he never gave analytic (algebraic) expression for the total force; the most he achieved was a graphical representation of it. A reasonable expression might be a sum of increasing negative powers of r, so that $f_i(r) = \alpha_i r^{-i}$, where the first term would be $I = 2$, $\alpha_2 = -Gm$ (the gravitational term). The terms would alternate in sign, with the last term being opposite to that of the gravitational. (We will see that general relativity introduces correction terms of just this sort into the law for the gravitational field of a single mass-particle.) But there is no indication of what the magnitude of these other terms might be, what physical interpretation could be given to each of them, or whether the α's would require introducing any new parameters which might have to refer to other essential properties of matter (p. 123).

In a footnote, Graves (1971) continues,

> Boscovich might, in fact, have been able to resolve Olbers' paradox that the night sky would be infinitely bright in an infinite universe with uniform average density of matter under Newton's law; he could simply have introduced an additional term (proportional to $1/r$, say) effective at great distances (p. 113).

It is this footnote that draws one's interest. Throughout the scientific literature regarding the quantum science of galactic structure, many theorists have commented on the Now Newtonian aspects of the universe on the large scale. Following the hint of the $1/r$ term, a search of the literature finds several investigations. One of the many findings is how many cosmologists modify Newton's gravitational law using a Yukawa functional form for the potential given by: $V_{Yukawa}(r) = -g^2 \frac{e^{-kmr}}{r}$

where g is a magnitude scaling constant, m is the mass of the affected particle, r is the radial distance to the particle, and k is another scaling constant. The potential is monotone increasing, implying that the force is always attractive.

There have been many efforts to modify Newton's law. Seeliger (1895) felt that Newton's inverse square law was not exact and stated that it was only an empirical formula. In his modification he made the assumption that an attenuation factor be used to express the gravitational force F between bodies m and m' be given as:

$$F = -Gmm'\frac{e^{-\lambda r}}{r^2} \quad (56)$$

Seeliger's effort was followed by another modification of Newton's law given by Neumann (1896) who felt that the problem could be resolved by using a potential of the form

$$\phi(r) = \frac{Aa^{-\alpha r}}{r} \quad (57)$$

which led to a generalized force, *F,* given by

$$F = -Gm_1m_2\frac{1+\alpha r}{r^2}e^{-\alpha r} \quad (58)$$

These ideas of Seeliger and Neumann, with a slight adjustment of modification of Newton's inverse square dependence, have recently been address by others. Fischbach et al., (1991) is one of these, whose modification of The Newtonian effects is described using a modified expression for the potential energy *V(r)* is given by:

$$V(r) = -\frac{G_\infty m_1m_2}{r}\left(1+\alpha e^{-\frac{r}{\lambda}}\right) = V_N(r) = V'(r) \quad (59)$$

Here G_∞ is the Newtonian constant of gravity, and the parameters λ and α, respectively, give the range of the new force and its strength relative to gravity. Also, $V'(r)$ describes the correction to the effective gravitational potential arising from the particular non-Newtonian interaction we are considering (which in this case is a Yukawa).
This in turn leads to a force $F(r)$ given by:

$$F(r) = \nabla V(r) = \frac{-G_\infty m_1m_2r}{r^2}[1+\alpha\left(1+\frac{r}{\lambda}\right)e^{-\frac{r}{\lambda}} \quad (60)$$

Fischbach et al., (1991) continue their modification by assuming a model which contains two canceling Yukawa potentials which result in an approximate exponential. It is suggested that the reader consult Fischbach et al.'s assumption, since it contains too much detail to be presented here.

The fact to be considered is that in all of the efforts regarding the modification of Newton's law with a Yukawa potential, substantiates Grave's (1971) comment regarding Boscovich's 1/*r* dependence for a field of force, in this case gravitation with this in mind, a modified Yukawa force based on the Boscovich curve in the *S*, *V* and *S′ V′* regions was developed in an ad hoc manner is given by:

$$F(x) = \frac{ne^{(px)}}{x} \quad (61)$$

The curve using Eq. 61 is shown in Fig. 68

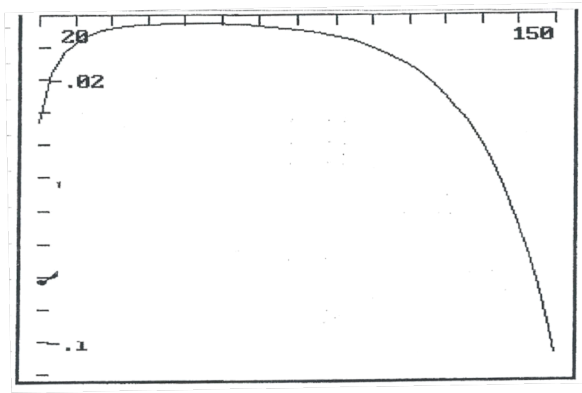

Fig. 68
n = 0.0041215
p = 0.0549

One will note that the exponent is positive instead of the negative exponent that exemplifies the conventional Yukawa force. The reason for this is that in Boscovich's Fig. 14, the curve drops sharply negative in the S′ V′ and S V region.

As an aside, Bertin & Lin in their book, *Spiral Structure in Galaxies, A Density Wave Theory* (1995) produced a curve based on a positive exponent in what appears to be a Yukawa type force which is depicted in Fig. 69 below:

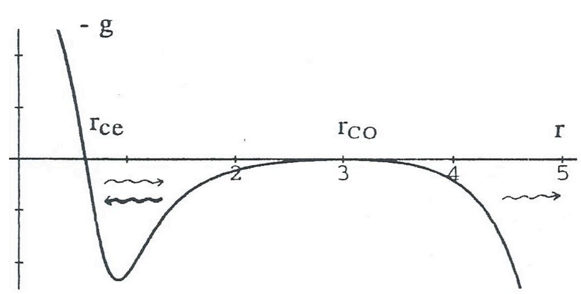

Fig. 69

They mention that there are two turning points (i.e. two zeros of the function g). One is at r_{ce}, simple turning point, and the other at r_{co}, a double turning point. The relation between the Newton inverse square law and the 1/*r* dependence seems obvious and compares to Fig. 68 of this work. This might indicate that Boscovich was ahead of his time again, since an extremely large negative force might imply that this might be due to large masses at extreme distances beyond our observation. Such a situation might explain the so-called "dark matter" that is spoken about in today's cosmology.

Oort (1932) initiated the concept of dark matter and studied stellar motions in the galactic region. Zwicky (1933) closely followed in his study of clusters and galaxies.

Then in the 1960 to 1970 interval, Rubin & Ford Jr. (1970) established a method using more sensitive instruments to analyze velocity curves of distant galaxies with much more precision.

Based on the findings of Oort (1932), Zwicky (1933), and Rubin & Ford Jr. (1970), it can be said that here might be some substantiation of the Boscovich curve. With this information it might be said that this concludes the empirical description of Boscovich's famous curve. Its various regions for the microscopic and possibly solid state range is denoted as Region A. The Newtonian range as Region B and the "dark matter" distance range as Region C.

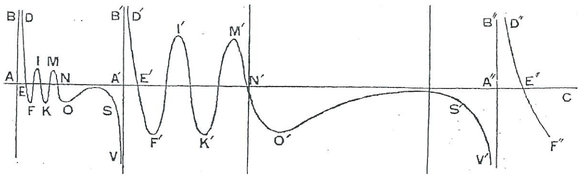

A + B + C| A | B | C

Fig. 70 (From Fig. 14 in Boscovich's (1922) *Theoria*)

$$\text{A: } F(x) = \frac{Be^{(-kx)} sin\frac{1}{5}\pi\left(e^{(kx)} - e^{(-kx)}\cos(\pi x)\right)\sqrt{5}}{x^3} \qquad (62)$$

k = 0.481211825

$$\text{B: } F(2) = -\frac{gk}{x^2} \qquad (63)$$

g = 6.668

$$\text{C: } F(3) = \frac{ne^{(px)}}{x} \qquad (64)$$

n = 0.0041215
P = 0.0549

The numerical values for the constants shown in Fig. 70 have been chosen so as to make the Boscovich curve continuous throughout. One must remember that the curve is a qualitative one and cannot be shown in scale due to the fact that in Region A we measure distances in 10^{-13} or less, while in Regions B and C we measure distances in light years, e.g., in Region C we speak of 46-47 million light years. It goes without saying that much needs to be done especially in defining the various constants used in the curve description. Referring to Seeliger, Kragh (2007) states,

> The modified force law was essentially ad hoc and also arbitrary, since many other modifications might resolve the gravitation paradox in a similar way. The idea of modifying Newton's inverse-square law was not, by itself, very original, as many modifications were proposed in the nineteenth century. The exponential correction factor can be found in 1825 in LaPlace's *Mecanique celeste,* which can hardly have avoided Seeliger's attention. However, what was original in Seeliger's approach was that he used it in a cosmological context and not, as in most other proposals, to solve problems of planetary astronomy (such as Mercury's anomalous revolution around the Sun) (p. 109).

Kragh (2007) also mentions Boscovich and his cosmological ideas:

> Apart from those already mentioned, several other Enlightenment natural philosophers took up cosmological questions. One of them was the Croatian-Italian astronomer and physicist Roger Boscovich, a Jesuit scholar, who in 1758 published his main work *Theoria philosophiae naturalis.* Although best known for its contribution to dynamic atomism and matter theory, the book also included considerations of a cosmological nature. For example, Boscovich imagined that, apart from our space, there might exist other spaces with which we are not causally connected. His conception of the universe was relativistic, such as illustrated by a passage from the end of *Theoria,* which may bring to mind much later cosmological ideas (p. 82).

He continues to quote Boscovich's (1922) ideas about space and time:

> If the whole Universe within our sight were moved by a parallel motion in any direction, and at the same time rotated through any angle, we could never be aware of the motion or of the rotation…Moreover, it might be the case that the whole Universe within our sight should daily contract or expand, while the scale of forces contracted or expanded in the same ratio; if such a thing did happen, there would be no change of ideas in our mind, and so we should have no feeling that such a change was taking place. (p. 82).

Boscovich imagined all matter to consist of point-atoms bound together by Newtonian-like attractive and repulsive forces. If no forces were present, a body might pass freely through another without any collision (after all, points have no extension in space). The possibility led him to a daring cosmological speculation: "There might be a large number of material universes existing in the same space, separated one from the other in such a way that one was perfectly independent of the other, and the one could never acquire any indication of the existence of the other" (1922, note 518).

Boscovich did not elaborate. Here we have, in 1758, a new version of the many universe scenario: not different universes distributed in space and time, but co-existing here and now. It was surely a scenario that harmonized in spirit with ideas that some cosmologists would propose more than two hundred years later. Perhaps we should end this paper here with the hope that some of the ideas herein presented will come to fruition in the future.

References

[1] Ackermann, R. (1989). The New Experimentalism. *The British Journal for the Philosophy of Science*, *40*(2), 185-190.
[2] Allen, H. S. (1925). *Photoelectricity - The Liberation of Electrons by Light* (2nd ed.). London: Longmans, Green and Co.
[3] Andronov, A. A., Vitt, A. A., & Khaikin, S. E. (1966). *Theory of Oscillators*. New York, NY: Dover Publications, Inc.
[4] Balmer, J. J. (1885). Note on the Spectral Lines of Hydrogen. *Annalen der Physik*, *261*(5), 80-87.
[5] Baly, E. C. C. (1927). *Spectroscopy* (3 ed.). New York, NY: Longmans, Green and Co.
[6] Bertin, G., & Lin, C. C. (1994). *Spiral Structure in Galaxies: A Density Wave Theory*. Cambridge, MA: The MIT Press.
[7] Bohr, N. (1913, July). On the Constitution of Atoms and Molecules. *Philosophical Magazine*, *6*(26), 1-25.
[8] Boscovich, R. J. (1922). *A Theory of Natural Philosophy (Latin-English edition: Translated by J. M. Child)*. London: The MIT Press.
[9] Brush, S. G. (1999). *The Kind of Motion we call Heat: A History of the Kinetic Theory of Gases in the 19th Century. Book 2: Statistical Physics and Irreversible Processes*. Netherlands: North-Holland Publishing Co.
[10] Church, A. H. (1904). *On the Relation of Phyllotaxis to Mechanical Laws*. London: Williams & Norgate.
[11] Coblentz, W. W. (1913, January). Journal of the Washington Academy of Sciences. *Constants of Spectral Radiation of a Uniformly Heated Enclosure or so-called Blackbody. II*, *13*(3), 459-477.
[12] Cotton, A. (1899). The Present Status of Kirchhoff's Law. *Astrophysical Journal*, *9*, 237-268.
[12] D'Abro, A. (1952). *The Rise of the New Physics: Its Mathematical and Physical Theories formerly titled 'Decline of Mechanism'* (2nd ed.). New York, NY: Dover Publications, Inc.
[13] Debye, A. (1912). Zur Theorie der spezifischen Wärmen. *Annalen der Physik*, *344*(14), 789-839.
[14] Einstein, A. (1905). Über einen die Erzeugung und Verwandlung des Lichtes betreffenden heuristischen Gesichtspunkt. *Annalen der Physik*, *322*(6), 132-148.
[15] Einstein, A. (1906). Zur Theorie der Lichterzeugung und Lichtabsorption. *Annalen der Physik*, *325*(6), 199-206.
[16] Einstein, A. (1907). Die Plancksche Theorie der Strahlung und die Theorie der spezifischen Wärme. *Annalen der Physik*, *327*(1), 180-190.
[17] Einstein, A. (1917) Phys. Zs. 18, p. 121; English translation: "On the Quantum Theory of Radiation", by D. ter Haar, The Old Quantum Theory, Pergamon Press, New York (1967), p. 167.
[18] Fischbach, E., Talmadge, C., & Krause, D. (1991). Exponential models of non-Newtonian gravity. *Physical Review D*, *43*(2), 460-463.
[19] Fowler, A. (1922). *Report on Series In Line Spectra*. Fleetway Press, Ltd.
[20] Galgani, L. (1982). Modern and Old Views in the Dynamical Foundations of Classical Statistical Mechanics. *Applications of Modern Dynamics to Celestial Mechanics and Astrodynamics*, 173-184.
[21] Garber, E. (1976). Some Reactions to Planck's Law, 1900–1914. *Studies in History and Philosophy of Science Part A*, *7*(2), 89-126.
[22] Gill, H. V. (1941). *Roger Boscovich, S.J. (1711-1787) Forerunner of Modern Physical Theories*. M.H. Gill and Son.
[23] Gompertz, B. (1825). On the Nature of the Function Expressive of the Law of Human Mortality, and on a New Mode of Determining the Value of Life Contingencies. *Philosophical Transactions of the Royal Society of London*, *115*, 513-583.
[24] Graves, J. C. (1971). *The Conceptual Foundations of Contemporary Relativity Theory*. Cambridge, MA: M.I.T. Press.
[25] Heilbron, J. L., & Kuhn, T. S. (1969). The Genesis of the Bohr Atom. *Historical Studies in the Natural Sciences*, *1*, vi-290.
[26] Heilbron, J. L. (1982). *Elements of Early Modern Physics*. Oakland, CA: University of California Press.
[27] Horadam, A. F., & Shannon, A. G. (1988). Fibonacci and Lucas Curves. *The Fibonnaci Quarterly*, *26*(1), 3-13.
[28] Illert, C. R. (1982). *The Mathematics of Gnomonic Seashells*. Semaphore Park, South Australia.
[29] Ivanovic, D.M. (1988). On Some Aspects of Boscovich's Curve. *R. J. Boscovich, Vita E Attivita Scientifica, His Life and Scientific Work,* 49.
[30] Jean, R. V. (1994). *Phyllotaxis: A Systemic Study in Plant Morphogenesis*. Cambridge, England: Cambridge University Press.

[31] Kangro, H. (1976). *Early History of Planck's Radiation Law*. London: Taylor & Francis Ltd.
[32] Kelvin, L. (1904). *Baltimore Lectures on Molecular Dynamics and the Wave Theory of Light*. London: C.J. Clay and Sons.
[33] Kirchhoff (1860). On the Relation Between the Radiating and Absorbing Powers of Different Bodies for Light and Heat. *The London, Edinburgh, and Dublin Philosophical Magazine and Journal of Science*, *20*(130), 1-21.
[34] Kirchhoff, G. (1901). *On the Relation Between the Emissive and Absorptive Power of Bodies of Light and Heat*. New York, NY: American Books Company.
[35] Kragh, H. (2007). *Conceptions of Cosmos: From Myths to the Accelerating Universe: A History of Cosmology*. New York, NY: Oxford University Press.
[36] Kramida, A. E. (2010). A Critical Compilation of Experimental Data on Spectral Lines and Energy Levels of Hydrogen, Deuterium, and Tritium. *Atomic Data and Nuclear Data Tables*, *96*(6), 586-644.
[37] Kuhn, H. G. (1962). *Atomic Spectra*. Cambridge, MA: Academic Press.
[38] Lewis, A. C. (1989). The Influence of Roger Boscovich on Bertrand Russell's Early Philosophy of Physics. *Synthesis Philosophica*, *4*, 649-658.
[39] Lummer, O., & Jahnke, E. (1900). Ueber die Spectralgleichung des schwarzen Körpers und des blanken Platins. *Annalen der Physik*, *308*(10), 283-297.
[40] MacAn, I. (Ed.). (1987). *The Philosophy of Science of Ruđer Boškovi'c: Proceedings of the Symposium of the Institute of Philosophy and Theology, S.J.* Zagreb.
[41] Martinovic, I. (1987). "The Fundamental Deductive Chain of Boscovich's Natural Philosophy" in *The Philosophy of Science of Ruđer Boškovi'c: Proceedings of the Symposium of the Institute of Philosophy and Theology, S.J.* Zagreb. 65-99.
[42] Martinovic, I. (1988). *Boscovich's Model of the Atom from 1748* (M. Bossi & P. Tucci, Eds.). Bicentennial Commemoration of Ruggerio Giuseppe Boscovich. Milan.
[43] Medawar, P. B. (1940). The Growth, Growth Energy, and Ageing of the Chicken's Heart. *Proceedings of the Royal Society of London B: Biological Sciences*, *129*(856), 332-355.
[44] Medawar, P. B. (1945a). *Essays on Growth and Form: Presented to D'Arcy Wentworth Thompson*. Oxford, UK: Clarendon Press.
[45] Medawar, P. B. (1945b). Shape, Size, and Age. In W. E. le Gros Clark & P. B. Medawar (Eds.), *Essays on Growth and Form: Presented to D'Arcy Wentworth Thompson* (p. 137-168). Oxford, UK: Clarendon Press.
[46] Michelson, W. (1888). Theoretical Essay on the Distribution of Energy in the Spectra of Solids. *Philosophical Magazine*, *5*(25), 425-435.
[47] Minorsky, N. (1947). *Introduction to Non-Linear Mechanics: Topological Methods, Analytical Methods, Non-Linear Resonance, Relaxation Oscillations*. Ann Arbor, MI: J.W. Edwards.
[48] Minorsky, N. (1962). *Non-Linear Oscillations*. Princeton, NJ: Van Nostrand.
[49] Mohr, P. J., & Taylor, B. N. (2000). CODATA Recommended Values of the Fundamental Physical Constants: 1998. *Reviews of Modern Physics*, *72*(2), 351-496.
[50] Mohr, P. J., & Taylor, B. N. (2005). CODATA Recommended Values of the Fundamental Physical Constants: 2002. *Reviews of Modern Physics*, *77*(1), 1-107.
[51] Mohr, P. J., Taylor, B. N., & Newell, D. B. (2008). CODATA Recommended Values of the Fundamental Physical Constants: 2006. *Reviews of Modern Physics*, *80*(2), 633-730.
[52] Neumann, C. (1896). *Allgemeine Untersuchungen uber das Newton'sche Princip der Fermwirkungen mit besonderer Rucksicht auf die elektrische Wirkungen*. Leipzig: B.G. Teubner.
[53] Oort, J. H. (1932). The Force Exerted by the Stellar System in the Direction Perpendicular to the Galactic Plane and Some Related Problems. *Bulletin of the Astronomical Institutes of the Netherlands*, *6*, 249.
[54] Pais, A. (1982). *Subtle Is the Lord: The Science and the Life of Albert Einstein*. Oxford, UK: Clarendon Press. [55] Planck, M. (1900). Uber eine Verbesserung der Wien'schen Spectralgleichung. *Verhandlungen der Deutschen physikalischen Gesellschaft*, *2*, 202-204.
[56] Planck, M. (1914). *The Theory of Heat Radiation*. Philadelphia, PA: P. Blakiston's Son & Co.
[57] Poincare, H. (1881). Memoire sur les courbes definies par une equation differentielle. *Journal De Mathematiques Pures et Appliquees*, *3*(7), 375-422.
[58] Prince, A. (1989). The Phenomenalism of Newton and Boscovich: A Comparative Study. *Synthesis Philosophica*, *4*(2), 359-768.
[59] Raup, D. M., & Graus, R. R. (1972). General Equations for Volume and Surface Area of a Logarithmically Coiled Shell. *Journal of the International Association for Mathematical Geology*, *4*(4), 307-316.
[60] Rayleigh, J. W. S. (1900). Remarks Upon the Law of Complete Radiation. *The London, Edinburgh, and Dublin Philosophical Magazine and Journal of Science*, *9*(301), 539-540.
[61] Richards, F. J. (1969). The Quantitative Analysis of Growth. In F. C. Steward (Ed.), *Plant Physiology,*

a Treatise. Analysis of Growth: Behavior of Plants and their Organs (Vol. VA). Cambridge, MA: Academic Press.
[62] Richtmyer, F. K., & Kennard, E. H. (1947). *Introduction to Modern Physics* (4th ed.). New York, NY: McGraw-Hill.
[63] Rider, R.E. (1988). In a Foreign Language: Boscovich and Algebra. *R. J. Boscovich, Vita E Attivita Scientifica, His Life and Scientific Work,* 476.
[64] Ritz, W. (1908). On a New Law of Series Spectra. *Astrophysical Journal*, *28*, 237.
[65] Robitaille, P. M. (2003). On the Validity of Kirchhoff's Law of Thermal Emission. *IEEE Transactions on Plasma Science*, *31*(6), 1263-1267.
[66] Robitaille, P. M. (2006). An Analysis of Universality in Blackbody Radiation. *Progress in Physics*, *2*, 22-23.
[67] Robitaille, P. M. (2008a). A Critical Analysis of Universality and Kirchhoff's Law: A Return to Stewart's Law of Thermal Emission. *Progress in Physics*, *3*, 30-35.
[68] Robitaille, P. M. (2008b). Blackbody Radiation and the Carbon Particle. *Progress in Physics*, *3*, 36-55.
[69] Robitaille, P. M. (2009). Kirchhoff's Law of Thermal Emission: 150 Years. *Progress in Physics*, *4*, 3-13.
[70] Rubens, H., & Kurlbaum, F. (1901). Anwendung der Methode der Reststrahlen zur Prüfung des Strahlungsgesetzes. *Annalen der Physik*, *309*(4), 649-666.
[71] Rubin, V. C., & Ford Jr., W. K. (1970). Rotation of the Andromeda Nebula from a Spectroscopic Survey of Emission Regions. *Astrophysical Journal*, *159*, 379.
[72] Russel, B. (1897). Oscillations of Four Particles Under Attraction and Repulsion. In N. Griffin & A. C. Lewis (Eds.), *The Collected Papers of Bertrand Russell: The Philosophical Papers 1896-99* (Vol. 2, p. App. II.1.). London: Routledge.
[73] Rydberg, J. R. (1896). The New Elements of Cleveite Gas. *Astrophysical Journal*, *4*, 91.
[74] Schirrmacher, H. (2003). Experimenting Theory: The Proofs of Kirchhoff's Radiation Law Before and After Planck. *Historical Studies in the Physical and Biological Sciences*, *33*(2), 299-335. doi:10.1525/hsps.2003.33.2.299
[75] Seeliger, H. (1895). Ueber das Newton'sche Gravitationsgesetz. *Astronomisch Nachrichten*, *137*(9), 129-136.
[76] Shpol'skii, E. V. (1969). *Atomic Physics* (S. Chomet, Ed.). London: Iliffe Books.
[77] Siegel, D. M. (1976). Balfour, Stewart and Gustav Robert Kirchhoff: Two Independent Approaches to Kirchhoff's Law. *Isis*, *67*(4), 565-600.
[77] Siegel, R., & Howell, J. R. (1992). *Thermal Radiation Heat Transfer* (3rd ed.). New York, NY: Hemisphere.
[78] Smith, P. F., & Longley, W. R. (1910). *Theoretical Mechanics*. Boston, MA: Ginn & Co.
[79] Stachel, J. (1998). Einstein's Light-Quantum Hypothesis, or Why Didn't Einstein Propose a Quantum Gas a Decade-and-a-Half Earlier? In D. Howard (Ed.), *Einstein: The Formative Years, 1879-1909* (pp. 231-251.). Boston, MA: Birkhauser.
[80] Stewart, B. (1861). An Account of Some Experiments on Radiant Heat: Involving an Extension of Prevost's Theory of Exchanges. *Earth and Environmental Science Transactions of the Royal Society of Edinburgh*, *22*(1), 1-20.
[81] Stewart, B. (1863). Reply to Some Remarks by G. Kirchhoff in his Paper "On the History of Spectrum Analysis". *Philosophical Magazine*, *25*(4), 354-360.
[82] Stewart, B. (1888). *An Elementary Treatise on Heat*. Oxford, UK: Clarendon Press.
[83] Stoiljkovic, D. (2011). Contemporary Verifications and Applications of Boscovich's Theory of Natural Philosophy. *International Conference for the Tercentenary of the Birth of Ruggiero Giuseppe Boscovich (Ragusa 1711 – Milano 1787).* University of Pavia: Pavia, Italy.
[84] Thomas, R. L., & Cannell, M. G. R. (1980). The Generative Spiral in Phyllotaxis Theory. *Annals of Botany*, *45*(3), 237-249.
[85] Thomson, J. J. (1907). *The Corpuscular Theory of Matter* (2nd ed.). New York, NY: Charles Scribner's Sons.
[86] Thomson, J. J. (1913). On the Structure of the Atom. *Philosophical Magazine*, *26*, 794.
[87] Thornley, J. H. M. (1975). Phyllotaxis. II. A Description in Terms of Intersecting Logarithmic Spirals . *Annals of Botany*, *39*(161), 509-524.
[88] Thornley, J. H. M. (1976). *Mathematical Models in Plant Physiology*. Cambridge, MA: Academic Press.
[89] Tyndall, J. (1865). Uber Leuchtende und dunkle Strahlung. *Annalen der Physik*, *200*(1), 36-53.
[90] Whyte, L. L. (1961). *Roger Joseph Boscovich: Studies of His Life and Work on the 250th Anniversary of His Birth*. London: Allen & Unwin.
[91] Wien, W. (1896). Ueber die Energievertheilung im Emissionsspectrum eines schwarzen Körpers. *Annalen der Physik*, *294*(8), 662-669.
[92] Winsor, C. P. (1932). The Gompertz Curve as a Growth Curve. *Proceedings of the National Academy of Sciences of the United States of America*, *18*(1), 1-8.
[93] Whittaker, E. T. (1989). *A History of the Theories of Aether and Electricity* (2nd ed.). London: Longmans, Green and Co.

[94] Zwicky, F. (1933). Die Rotverschiebung von extragalaktischen Nebeln. *Helvetica Physica Acta*, *6*, 110-127.